Title

Understanding the Ecological Challenges in California Protected Areas: Through the Lens of Remote Sensing Technologies

Author

Jia, Shenyue

Publication Date

2016

Peer reviewed|Thesis/dissertation

University of California
Los Angeles

Understanding the Ecological Challenges in California Protected Areas Through the Lens of Remote Sensing Technologies

A dissertation submitted in partial satisfaction
of the requirements for the degree
Doctor of Philosophy in Geography

by

Shenyue Jia

2016

Abstract of the Dissertation

Understanding the Ecological Challenges in California Protected Areas Through the Lens of Remote Sensing Technologies

by

Shenyue Jia

Doctor of Philosophy in Geography

University of California, Los Angeles, 2016

Professor Thomas Welch Gillespie, Chair

Protected area (PA), usually built to address the potential ecological pressure from different sources, aims to sustain, protect, and maintain the wilderness of nature for ecological, economic, and scenic purposes. Establishing, maintaining, and expanding the monitor network of PAs helps to enhance the ecological and biological value of these areas, especially in the light of species decline and habitat degradation. Intensively monitored and regulated through various administrative agencies, California keeps one of the best maintained network of PAs in the world, which supports various studies to address the significant threats to the preservation of wilderness from the projected warming climate and pressure from human development, including water deficit and prolonged drought, abnormality in wildfires, urban sprawl, and light pollution.

With the help of satellite remote sensing technologies and geospatial analysis, we can overcome the limitation of data availability in traditional ecological studies and expand the study of PAs to a continuous gradient both in time and space. This dissertation aims to develop a comprehensive understanding through remote sensing technologies on three significant and linked ecological disturbance in California PAs, including the change of land cover, the dynamic of wildfire, and the extent and intensity of human activity reflected by stable

nighttime light. Exploiting various of remote sensing observation and its derivatives, this study investigated the three topics through trend, seasonality, abnormality, spatial distribution, and hotspot of change to provide a cost-effective and repeatable studying paradigm for PA managers to better understand the past and present situation, as well as the ecological challenges of PAs. In addition, it also supplemented the study of PAs as a case study focusing on a non-tropic ecosystem, which usually involves greater interaction with human thus faces ecological pressure at a higher level.

The analysis on land cover dynamics and change from 2000 to 2015 found that many protected areas in California have experienced an increase of brownness since 2000. PAs with a higher coverage of greenness are associated with a higher temporal variability, mostly because of the more complex life cycle of green vegetation and the sensitivity to the disturbance, possibly due to a drying climate regime. Partly linked to the gradual influence from the drying climate, the change in the regime of wildfire may cause a more drastic change in land cover, through the removal of aboveground biomass and its inuence on the post-wildre regrowth. In the study focusing on California PAs from 2000 to 2013, a shift in wildfire-prone land cover and season was observed starting from 2008, while the wildfires southern California shrubland during the fall season became nearly extinct and the northern California evergreen forest wildfires in the late spring increased, partly explained by the recent loss of available fuel in biomass and the increase of potential of ignition in evergreen forest as a result of prolonged drought. Most burned areas experienced a signicant weakening of the immediate growing season, although the inuence from re on local landscape decayed over time, which became irrelevant after ve years on average. The lower fuel moisture and a more intensive removal of aboveground biomass makes shrubs more sensitive in time, with a shorter period for biomass removal by re and a greater delay in the start and peak of post-re growing season.

The long-enduring and sometimes intensive disturbance from human activity, especially from the development can be even more disastrous than wildre in damaging the aboveground biomass by interrupting the natural nutrient and mass circulation,thus brings more funda-

mental and sometimes irreversible consequences to ecosystems. However, after decades of protection, especially the removal of settlements in side PAs, land management strategies may have bored beneficial fruits to reduce the negative effects from historical human disturbance. As a good proxy of human activity and development, the historical records of stable nighttime light from 1992 to 2012 tracked the temporal change and spatial migration of hotspot of human activity inside California PAs. A decrease of lit area at night inside PAs occurred from 1992 to 2012, with a turning point around 2004 when the relatively sharp decrease started from became more gradual thereafter. Besides, area covered by higher stable nighttime light not only shrank, but also retreated from the area with high wilderness. If solidly conrmed by other socioeconomic variable, the above nding demonstrated the eectiveness of PA establishment and the fruits of multiple conservation strategies kept for decades.

The investigation of three major disturbances to the wilderness of California PAs provided an example of exploiting the cost-eective and continuously available observation of the Earth surface at a regional level to understand the ecological challenges of PAs. The findings can help the National Park Service and other related agencies of PA administration in the review, adjustment, and proposal of regulations and policies regarding to PAs. Future work and analysis can be focused on improving the accuracy of predictive models involved the analysis, either by concentrating on the dierence between categories of protection, or through a better understanding on the related ecological process and mechanisms to identify or develop better explanatory variables. In addition, when conducting analysis on PAs, the buer area adjacent to PAs cannot be ignored, which is an important source of disturbance to PAs as well as an ecological corridor that links nearby PAs into clusters. Considering the great diversity in the landscape of PAs, the analytical results can be aggregated and interpreted by different ecoregions to derive more accessible guidance to local policy makers.

The dissertation of Shenyue Jia is approved.

Yongkang Xue

Michael Edward Shin

Ulrike Seibt

Thomas Welch Gillespie, Committee Chair

University of California, Los Angeles

2016

To my mother and father...

whose amazing and inconditional love supported me

during all the ups and downs

Table of Contents

List of Figures

List of Tables

Acknowledgments

Firstly, I would like to express my sincere gratitude to my advisor Prof.Thomas W. Gillespie for the continuous support of my Ph.D study and related research, for his patience, motivation, and immense knowledge. His guidance helped me in all the time of research and writing of this dissertation. I could not have imagined having a better advisor and mentor for my Ph.D study.

Besides my advisor, I would like to thank the rest of my dissertation committee: Prof.Yongkang Xue, Prof.Michael E.Shin, and Dr.Ulrike Seibt, for their insightful comments and encouragement, but also for the hard question which incented me to widen my research from various perspectives. My sincere thanks goes to Prof.Gregory S.Okin, who advised me during the first several years of my study, helped me oriented to a brand new environment of study, and developed the technical skills for as a foundation of my further study.

I would also like to thank Prof.Dennis Lettenmaier, Prof.Glen MacDonald, Prof.Yongwei Sheng, Dr.Vena Chu, and Dr.Jida Wang, who provided me insightful comments and suggestions on my research. Without they precious support it would not be possible to conduct this research.

I thank my fellow labmates in for the stimulating discussions, for the sleepless nights we were working together before deadlines, and for all the fun we have had in the last five years. Also I thank my friends in the following institution: UCLA Department of Geography, UCLA Department of Atmospheric and Oceanographic Sciences, UCLA Institution of Environment and Sustainability, and UCLA Chinese Students and Scholars Association. In particular, I am grateful to Katherine Glover for enlightening me the first glance of research.

Last but not the least, I would like to thank my family: my parents and to my boyfriend for supporting me spiritually throughout the five years of my study, especially the hard times of my last year, my life in general.

Vita

2004–2008	Department of Geographic Information System, Nanjing Normal University, Nanjing, China.
2008–2011	Research assistant, School of Geographic & Oceanographic Sciences. Nanjing University, Nanjing, China.
2008	B.S. (Cartography & Geographic Information System), Nanjing Normal University University.
2011	M.S. (Cartography & Geographic Information System), Nanjing University.
2011–2015	Teaching Assistant, Geography Department, UCLA. Taught Geospatial technical classes under the supervision of Prof. Yongwei Sheng, Prof. Michael Shin. Taught Physical geographic classes under the supervision of Prof. Gregory Okin, Prof. Laurence Smith.

Publications

Understanding the Fluctuation of Coccidioidomycosis in Response to Environmental Factors in California (2000-2010) based on the Fungal Life Cycle.(Under review)

CHAPTER 1

Introduction

1.1 Protected Areas: Toward an Effective Restoration of Wilderness

Protected area (PA), by the definition of International Union for Conservation Nature (IUCN), is "a clearly defined geographical space, recognized, dedicated and managed, through legal or other effective means, to achieve the long term conservation of nature with associated ecosystem services and cultural value" [Dudley, 2008]. In the light of continued species decline and habitat degradation, the IUCN has built the World Database on Protected Areas (WDPA) to collect and maintain accurate data on the location, size, type, and status of the worlds PAs [Milam et al., 2016]. In this worldwide network of PAs, IUCN categorized PAs by the level and the focus of protection and the magnitude and intensity of human interaction with nature inside or near the boundary. When combined with other data sets and databases, as well as thematic knowledge, this system can help to advance our understanding of the extent of PAs as a conservation strategy [Coad et al., 2013]. By August 2014, PAs recorded in the WDPA covered 15.4% of the worlds terrestrial and inland water area, excluding Antarctica [Juffe-Bignoli et al., 2014], which is a key step to achieve the Aichi Biodiversity Targets of 2020 set by Convention on Biological Diversity (CBD) to extend the coverage to "at least 17% of coastal and marine areas" [Woodley et al., 2012].

The target toward the preservation of biodiversity and wilderness in and adjacent to PAs can be decomposed into five strategic goals, including 1) address the underlying causes of biodiversity loss across government and society, 2) reduce the direct pressures on biodiver-

sity and promote sustainable use, 3) to improve the status of biodiversity by safeguarding ecosystems, species, and genetic diversity, 4) enhance the benefits to all from biodiversity and ecosystem services, 5) enhance implementation through participatory planning, knowledge management and capacity building [Leadley et al., 2010]. Recent evaluation of the progress to achieve the Aichi Targets indicated that on current trajectory, despite accelerating policy and management response to the biodiversity crisis, the impacts of these efforts are unlikely to be reflected in improved trends in the state of biodiversity by 2020 [Tittensor et al., 2014, Leadley et al., 2010]. Under this background, this dissertation focuses on California, a region was considered a biodiversity hotspot on the earth because of its high number of at-risk endemics (species found only there) [Carle, 2010] and a place dealing with the consequences of two centuries of land development and population growth that had been accelerating ever since the Gold Rush and remained at a high level in recent years because of technological revolution and immigration. By focusing on a typical region of Mediterranean ecosystem, this dissertation also tries to extend the study of PAs beyond tropics and subtropics in South America, Southeast Asia, and Africa to supplement the geographical scope of the study of PAs.

1.2 Why California?

1.2.1 Filling the Gap: Research of Protected Areas at a Regional Level

Most studies of PAs are focused on either the global level or a local level (e.g. selected representative PAs, often national parks). Although the global level studies are crucial as an evaluation and analysis toward the achievement of biodiversity targets worldwide, ecologically speaking, they are not focused on providing guidance and support for PA managers and policy makers on how to address the ecological challenges locally or in the similar landscape. On the other hand, findings from local level studies on representative PAs may not always be compatible for other PAs of the similar landscape. There is a need to address this gap and develop a solid foundation to support the policy making regarding to biodiversity and

maintenance of PAs at a regional level, where the environmental conditions and ecological challenges are similar and the budget and resource allocation is mostly controlled by the same government.

The regional level study of PAs aims to understand the past and present ecological conditions, identify the major challenge to maintain the biodiversity or the protective eectiveness of PAs, and provide scientic supporting information for policy makers and related agencies to evaluate, modify, and develop policies regarding to PAs. Researchers focusing on a regional level of study can assimilate the useful knowledge developed from global and local level studies at macro and micro-scale to build a bridge in between to better facilitate studies at the regional scale. In this case, the analysis of spatial patterns and temporal dynamics can be conducted at a level that is more accessible to stakeholders and policy makers. It also serves as a test ground of general patterns detected by global level studies and mechanisms discovered at the local scale.

1.2.2 Hotspot of Biodiversity under Threaten

California is an ideal place for the regional level study mentioned above. Containing over 1000 PAs at different IUCN protecting levels and under the administration of a multi-stakeholder system, California has over 18.5% of area under protection at different levels, though partly due to the unevenly distributed population. Shaped by the mountain ranges and the oceanic influence from Pacific Ocean, the state with an area of 423971 km^2 on the west coast of the United States is divided into 13 ecoregions by the difference biogeographic characteristics. Besides its famous Mediterranean section, California also contains a large area of warm desert in the southeast inner land and a small section of evergreen forest to the north, where the humidity is higher. It has a high number of endemics and many of them are at-risk. Chapter 2 gives a more detailed description of physical environmental conditions and biodiversity in California.

As a legacy of two centuries of human exploitation and land development, California not

only enjoys the fruit of land reclamation and construction of infrastructure, such as irrigation system to support the largest agricultural production of the United States. Meanwhile, it faces consequences of accelerating ecological pressure from development. Urbanization, habitat encroachment, pollution, mining and oil extraction, invasive species, logging, increasingly severe wildfires driven by both the pressure from population growth and the human-induced climate change in recent years are the establishment of PAs to fight against [Carle, 2010]. All the threats mentioned above has made California a representative region for studies focusing on PAs under the pressure of human development and projected change in climate.

Compared with many other countries worldwide, the United States has a better developed and maintained network of PAs and California is an intensively monitored region. It has 148 designated wilderness areas [Carle, 2010], the greatest number of any state in the U.S. It also has the greatest number of national parks in this country. Besides National Park Service (NPS), USGS, U.S. Bureau of Land Management (BLM), USDA Forest Service, U.S. Fish & Wildlife Service, California Department of Fish & Game, and California Department of Parks and Recreation are also administrative bodies in PAs of California. This well-developed network of monitoring, protecting, and preserving the wilderness and environmental resources has developed detailed data set of PAs and made crucial contribution to protect the ecosystem and outdoor recreational resources, improve management of conservation lands, adapt to and mitigate the effects of climate change, evaluate alternative land-use proposals, and assess vulnerability of the wildlife [Gergely and McKerrow, 2013]. With the support of the effective PA monitoring network, studies focusing on California PAs at the regional level can help the federal, state, and local policy makers to target on the most pressing needs to preserve and maintain the biodiversity and ecological effectiveness of PAs.

1.3 Ecological Challenges of Protected Areas in California

1.3.1 Gradual Change in Land Cover in Response to Climate Change

In most forecast scenarios of projected climate change, the western U.S. is likely to experience an increase of drought, though difference in space exists [Jardine et al., 2013, Parks et al., 2016]. In recent years, California has experienced a prolonged drought in most areas and it is believed to be the new normal [Guarin and Taylor, 2005, Pincetl and Hogue, 2015]. Such fundamental change in the climate regime imposes radical influence on the vegetation coverage in California, mainly by cutting the soil moisture to support the metabolism and nutrient circulation of plants, and accelerating the actual evaportranspiration (AET) [Carle, 2015b, Tanaka et al., 2006, MacDonald, 2010]. Both disturbs the seasonal cycles of plant growth and may lead to fundamental change in vegetation composition of the landscape. Some of the recent studies revealed that a browning trend is gradually taking place, and may continue as the prolonged, more frequent drought becomes normal [Jardine et al., 2013, MacDonald, 2010]. Containing almost half of the natural vegetation in California, protected areas faces a gradual, but fundamental change in land cover type, which brings new challenges for PA managers and policy maker in designing adaptive land management and wilderness restoration strategies in response of such change. Therefore, it is necessary to obtain a detailed analysis of the land cover dynamics, especially the greenness and brownness for recent years to detect the trend and identify the hotspot of change.

1.3.2 Change in Fire Regime and Post-Fire Ecological Response

As a key element to shape the Mediterranean ecosystem in California, wildfire plays an important role to balance the nutrient circulation and the aboveground composition of vegetation. The prolonged drought recently also increased the hazard of wildfires in California though a hike in the fire perimeter and the burn intensity. A number of studies have revealed that there has been a shift in the fire-prone vegetation type and fire-prone season recently, especially for the fires driven by Santa Ana winds in southern California chaparral [Jin et al., 2014,

Faivre et al., 2014, Jin et al., 2015]. Such shift or change should be discussed in a time series with enough length to avoid the overestimation of a normal fluctuation. But it is important to investigate the possible ecological influence from recent dynamics of fire regime in terms of seasonality, location, and intensity. One of the most fundamental influence from fire on PAs in California is the response from natural vegetation, which was usually discussed on a case-by-case basis [Bond and Keeley, 2005, Moritz et al., 2004, Urbieta et al., 2015] and requires a more systematic investigation with the assistance of remotely sensed data.

1.3.3 Anthropogenic Disturbance

In the last two decades, the population growth and associated ecological pressure in California has been investigated and discussed at different scales focusing on different metropolitan regions. Meanwhile, because of the increasing awareness of natural conservation and protection of wilderness, stricter regulations on or around PAs have been proposed and conducted, not to mention the expansion of PA network in California. The two sides of human-induced influence add to complexity of the anthropogenic influence on PAs [Davis and Hansen, 2011]. Despite the affirmative increase outside PAs, there is a need to investigate if the recent conduction of PA management strategies helps to improve the conservation of wilderness inside PAs [Nagendra, 2008, Jones et al., 2009]. However, the ecological value and effectiveness of protection of PAs should be discussed together with the adjacent area, usually a buffer zone between the boundary of PAs and epicenter of human development [Jones et al., 2009, Mcdonald et al., 2009a].

1.4 Through the Lens of Remote Sensing and Other Geo-Spatial Techniques

Recent development in geo-spatial technologies has advanced the utilization of geo-spatial data to the next level. Examples of such development include the progress in remote sensing observation on biogeographic variables that helps to build bridge between remote sensing

specialists and ecologists, development of spatial analysis and geostatistic methods, as well as construction on cloud computation and data distribution platform to exploit the high volume of geospatial, especially the remotely sensed data more efficiently (e.g. Google Earth Engine, NASA Giovanni). This dissertation aims to utilize some latest development in geospatial technologies to study the ecological challenges in California PAs with continuous time series of observation, addressing on the special characteristics of spatial data such as spatial autocorrelation and heterogeneity.

1.4.1 Remote Sensing and Terrestrial Protected Area Monitoring

Repeatable, cost-effective, and continuous in observation at different scales is the best recognized advantage of satellite-based approaches for studies to identify areas of concern at different scales and support land managers to design and apply adaptive management strategies for PAs [Gillespie et al., 2008, Alcaraz-Segura et al., 2009, Pettorelli et al., 2016]. Recently, remote sensing observation on the earth surface has made great progress in obtaining various biogeographical and biogeochemical measurements instead of raw reflectance of surface. And many related derivatives from reflectance, the best documented earth surface observation, have been developed through modeling and time series analysis focusing on phenology, hydrology, and topography. This helps to fill the knowledge gap between the remote sensing specialists and ecological researchers on PAs by translating the observation of reflectance or emission into the language of ecology and other environmental sciences. Such progress also enables the understanding of biodiversity and other perspectives of PAs through remotely sensed monitoring of land cover and disturbance, primary productivity, pheno-metrics derived from remotely sensed images, and magnitude of human activity detected from space. Besides these established avenues, newly developed research topics include vegetation 3-D structure with LiDAR images, tracking and understanding movement patterns, and monitoring species from space [Pettorelli et al., 2014]. Recent progress in ecology also echoes the wide application of satellite remote sensing methods by proposing the framework of essential biodiversity variables (EBVs) [Pereira et al., 2013], which are mostly developed based on

satellite remote sensing approaches.

1.4.2 Utilizing the Continuity of Time Series

Large volumes of remote sensing products focusing on different topics have been continuously generated at a time step from daily to yearly with coarse to fine spatial resolution. MODIS products collection and Landsat images are both good example of the continuity of observation. The former is produced daily, 16-day, monthly, and yearly depending on the variable since the beginning of 2000 at 250, 500,and 1000 m level that is appropriate for regional level study, while the latter archives multi-decadal observation of earths surface, though the cloud coverage and other atmospheric disturbance sometimes disrupts its continuity [Fry et al., 2011, Homer et al., 2015]. The decadal accumulation of surface observation has created a well-documented time series for different biogeographic variables, which enables the investigation on temporal trend, seasonal cycle, breakpoint in time series with the techniques of time series analysis for macroecology applications [Pfeifer et al., 2012]. A number of tools focusing on time series visualization and analysis utilizing MODIS and other satellite products with continuous time series have been developed, such as TIMESAT (Eklundh and Jnsson 2015) and NASA Giovanni [NASA GES DISC, 2012]. With the assistance of cloud computing platform, researchers can visualize, process, and analyze these data more efficiently, with the implementation of more advanced simulation and analytical techniques [Hansen et al., 2013a, Gorelick, 2012]. Starting from the analysis using NDVI, many recent studies began to adopt more advanced time series analysis methods [Goetz et al., 2005, Verbesselt et al., 2010a] and focus on connecting the results with ecological findings at a finer scale. In addition to satellite remote sensing observation and its derivatives, ecologists also started to combine the satellite observation and products together with them to address the projected climate change [Hansen et al., 2014], although data assimilation is another challenge to utilize the climate reanalysis data or climate model outcomes.

Despite the on-board satellite observation and official basic derivatives (e.g.MODIS prod-

ucts for atmosphere and land), other variables based on a continuous time series have been calculated to address the needs from different fields, for example, the annual pheno-metrics generated from the MODIS NDVI time series by eMODIS team [Jenkerson et al., 2010]. Obtaining a continuous time series from Landsat images involves more technical challenge because of the cloud coverage and other atmospheric factors. But if successful, the details from the smaller cell size can provide valuable opportunities of testing ecological models and theories developed at a local level. The fire occurrence, perimeter, and burn intensity data from MTBS team is a good example of utilizing the spatial resolution and continuity of observation of Landsat [Cochrane et al., 2012, Eidenshink et al., 2007]. Exploitation of the repeating and continuous observation and derivatives of observation from satellites makes remote sensing derived variables more accessible to ecologists and PA managers by converting time series of observation to ecological meaningful measurements, especially considering many of such variables cannot be derived from limited time slices of remote sensing data.

1.4.3 Focusing on the Continuity and Heterogeneity of Space

Satellite-based remotely sensed data also provide observations in the format of spatially continuous surface, and it enables investigation on spatial distribution through different spatial analysis techniques. It is also important to remember the remote sensing observations and derivatives employed in this dissertation may involve three dimensions: two dimensions of space and one dimension of time. In most of the spatial analysis, especially when a regression model is applied, it is important to consider the research question in terms of space, meaning that the spatial autocorrelation and heterogeneity should always be carefully treated in modeling.

Spatial autocorrelation, usually described as "everything depends on everything else, but closer things more so" [Tobler, 1970], can either lead to the overestimation of correlation in regression model or produce great residual because of the incapability of independent variables to explain the spatial aggregation/clustering. In practice, it can be addressed by introducing spatial fixed effect variables to models between variables in the format of continu-

ous time series [Baltagi and Li, 2001, Anselin and Arribas-Bel, 2011] or calculate geographic weight matrix to conduct geographic weight regression (GWR) instead of ordinary linear or nonlinear regression [Anselin, 2013, Anselin, 1988]. Because most modeling analysis involved in studies of this dissertation focuses on an array of measurements based on location, the spatial autocorrelation should be considered in the analysis.

On the other hand, if the purpose of study includes the analysis on spatial distribution or the explanatory capability of spatial heterogeneity on the topic of interest, deriving quantitative measurement of spatial aggregation should be the focus [Getis and Ord, 1992, Tiefelsdorf and Boots, 1995, Assuncao and Reis, 1999]. The hotspot analysis and spatial clustering analysis provides a straightforward and quantitative measurement of spatial heterogeneity, and is widely applied in time slice based analysis to study the spatial distribution of numerous topics [De Smith et al., 2007, Miller and Goodchild, 2014]. Considering the continuity in time series of remote sensing data involved in studies of this dissertation, there is a need to analyze the temporal change of the hotspots and clusters. To better utilize the continuous surface of remote sensing observations, metrics of landscape ecology can also be employed to study the connectivity and isolation detected by the quantitative measurement of spatial distribution [Goetz et al., 2009]

1.5 Organization of Dissertation

This dissertation focuses on California, one of the best maintained PA monitoring system in the world and a region with both richness in biodiversity and intensive interaction between nature and human. It has three research targets. First, investigate the temporal dynamics and spatial distribution of three major ecological challenges to California PAs, including land cover dynamics, change in fire regime and post-fire response, and human activities. Second, provide an example of study focusing on PAs at a regional level and for a non-tropic ecosystem to support the designing of adaptive land management and protection strategies for PA managers and policy makers. Third, explore the effectiveness of utilizing continuous

time series to understand the present and future of PAs. The three purposes are reflected in each research chapter to address one of the three major ecological challenges.

The dissertation is organized as follows: Chapter 2 describes the physical environmental background of California and provides a brief history of recent nature-human interaction in California; Chapter 3 investigates the change and dynamics of land cover in California PAs from 2000 to 2013, and it serves as a baseline of the following discussion of natural and human disturbance; Chapter 4 focuses on wildfire, the major natural disturbance in the landscape of California PAs, and discusses the change in fire regime as well as the post-fire response from vegetation; Chapter 5 studies and evaluates the change of human activities detected by stable nighttime light images in California PAs from 1992 to 2012, and analyzes the possible drivers of such change using demographic data; Chapter 6 concludes the findings from the previous three research chapters and discusses future works and possible improvements in the big picture of studies on PAs and biodiversity.

CHAPTER 2

California: Where wilderness Meets Human

2.1 Physical Environmental Background

California is a large state with great topographic complexity and a wide range of climatic and habitat diversity. According to the Level III ecoregions map from EPA [Omernik, 1987, Hughes and Larsen, 1988], California includes 12 ecoregions divided by major topographic barriers. The diverse landscape of California is shaped by the two major mountain systems that extends in a north-south direction, the Coast Ranges (North and South) on the west side of the state and the Sierra Nevada and Cascade Range on the east. Other major topographic features from North to South include Klamath Mountains, Central Valley, Transverse Ranges, Peninsular Ranges, Colorado Desert and Mojave Desert (Figure 2.1).

The great variation in topography exerts an influence as great as latitude in fixing the regional climate, as well as the vegetation coverage of California. The climate of cismontane region (area to the west of Sierra Nevada Ranges) is Mediterranean, with a dry and cool summer and humid and mild winter. Vegetation types include coastal marsh, coastal sage scrub, chaparral, grassland, and pine forest [Ornduff et al., 2004]. Because of the presence of mountainous masses of land, the zonation of vegetation is significant, with drought-tolerant vegetation at the foothill and types favoring precipitation in the mid elevation. The montane region (high mountain areas) receives higher precipitation and is usually covered by coniferous forest, montane chaparral, and subalpine forest. Located in the rain shadow area of the high Sierra Nevada Ranges, the transmontane region (east of Sierra Nevada and the inner land desert) receive very little precipitation. Plants (scrub and bush scrub) are adapted to

the aridity and tolerant to the prolonged drought. The Central Valley is now mostly occupied by cultivated croplands and grassland, and have very few protected areas. The diversity of landscapes makes California a crucial habitat for many distinct native species. The rapid increase of population in California has introduced great challenges to preserve such diversity in the protected areas. In present, over 1000 protected areas have been established in California at different protective levels of IUCN (Figure 2.2).

2.2 A Brief History of Human Settlement and Interaction with wilderness

Area where is now the state of California used to have the highest population density of Indians found in North America. The successors, Spanish mission builders and rancheros, followed by gold-seeking 49ers and settles then established settlements and cities here. Many of cities in California began as trade center villages serving the surrounding farm and ranch lands. Urban development spread outward from such centers, then covered some of the most productive farm lands in the states alluvial plains, coastal valleys, and upland terraces [Carle, 2010, Carle, 2015a].

Although overgrazing, drought, new tax laws, and federal homestead and other land laws encouraged settlement and development in California since it became a state in 1850, the quest of gold is well recognized as the driving force behind the relationship between residents in California and the land. During the Gold Rush started in 1860s and peaked in the 1880s, the landscape along hillsides was completely altered by removing and sweeping plants downstream by water cannons as a practice of hydraulic mining. Today, the evidence hydraulic mining operations was still observable in field. The intensive mining operations were then regulated by the nations 1872 Mining Law, which is still active in controlling mining activities on public land.

The construction of the Pacific Railway also led to acquisition of public land along the railway. By enticing settlers, the land became real estate, which stimulated the urbanization

and boosted the expansion of farming. After the World War II, the powerful economic growth and the technological revolution made California a magnet to the inter-state and international immigrants. Today, California is the top agricultural producer of the U.S. and supports a population in the size of 37.35 million, according to the U.S. census bureaus 2014 American Community Survey data. The population of California now concentrated on two mega-regions. The southern California mega-region extends from the southern border up through San Lois Obispo and Bakersfield, and sprawls into Mojave Desert along Interstate 5. In northern California, the Bay Area is connected to Sacramento and sprawls along corridors of development southward to Fresno in the San Joaquin Valley and eastward on Interstate 80 through the Sierra Nevada foothills. Area with a population below 10 people per km2 mostly locates in Mojave Desert, mountainous area of Sierra Nevada, and the forest covered area in Klamath Mountains California. The environmental pressure brought by population growth and the demand from agriculture brings great challenges to the protection of wilderness and nature, which is essential to adapt to the projected warming and change in climate regimes.

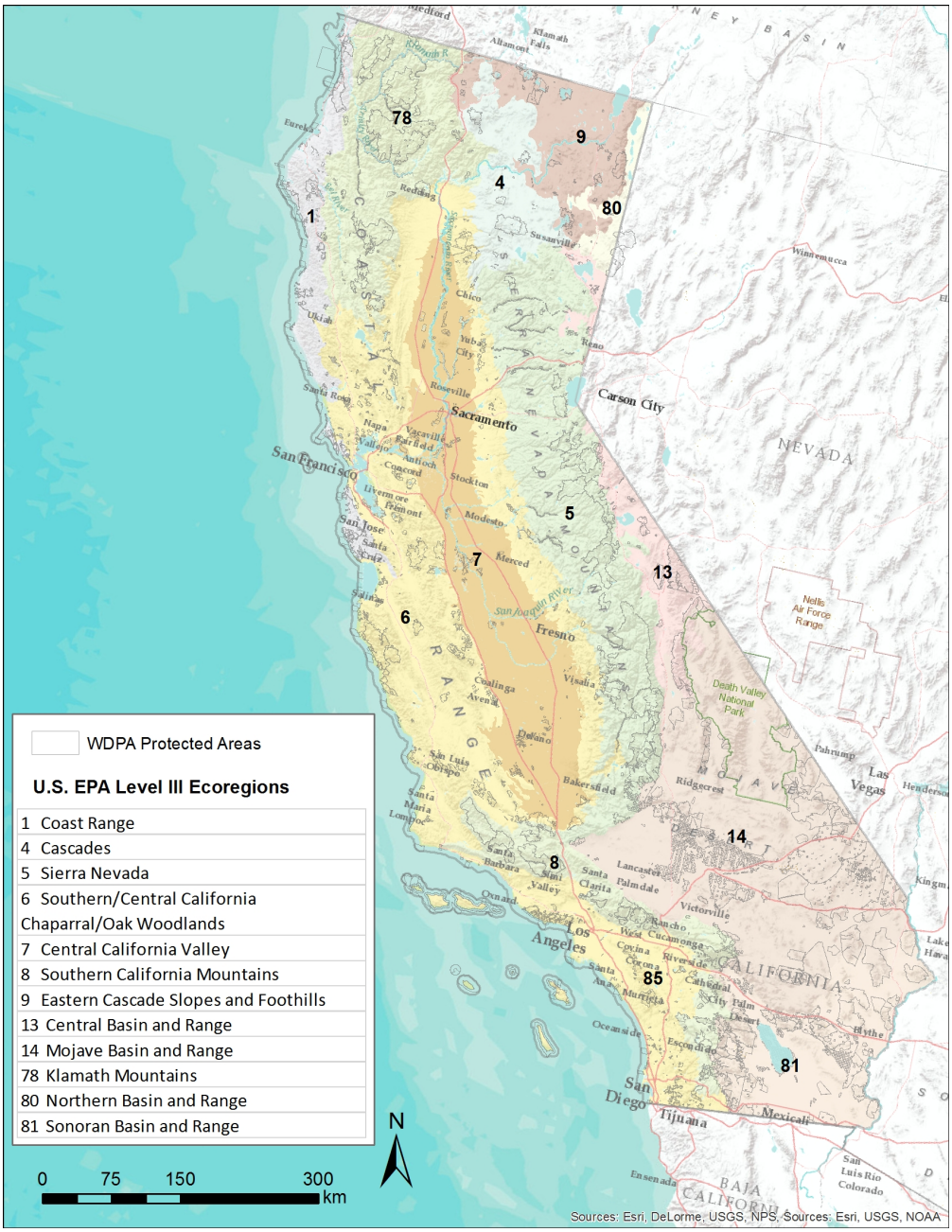

Figure 2.1: Reference map of California. Numeric labels are IDs of EPA Level III Ecoregions; ecoregions are shaded differently; boundaries of WDPA protected areas are colored with light grey; names of major topographic features are also shown on the map.

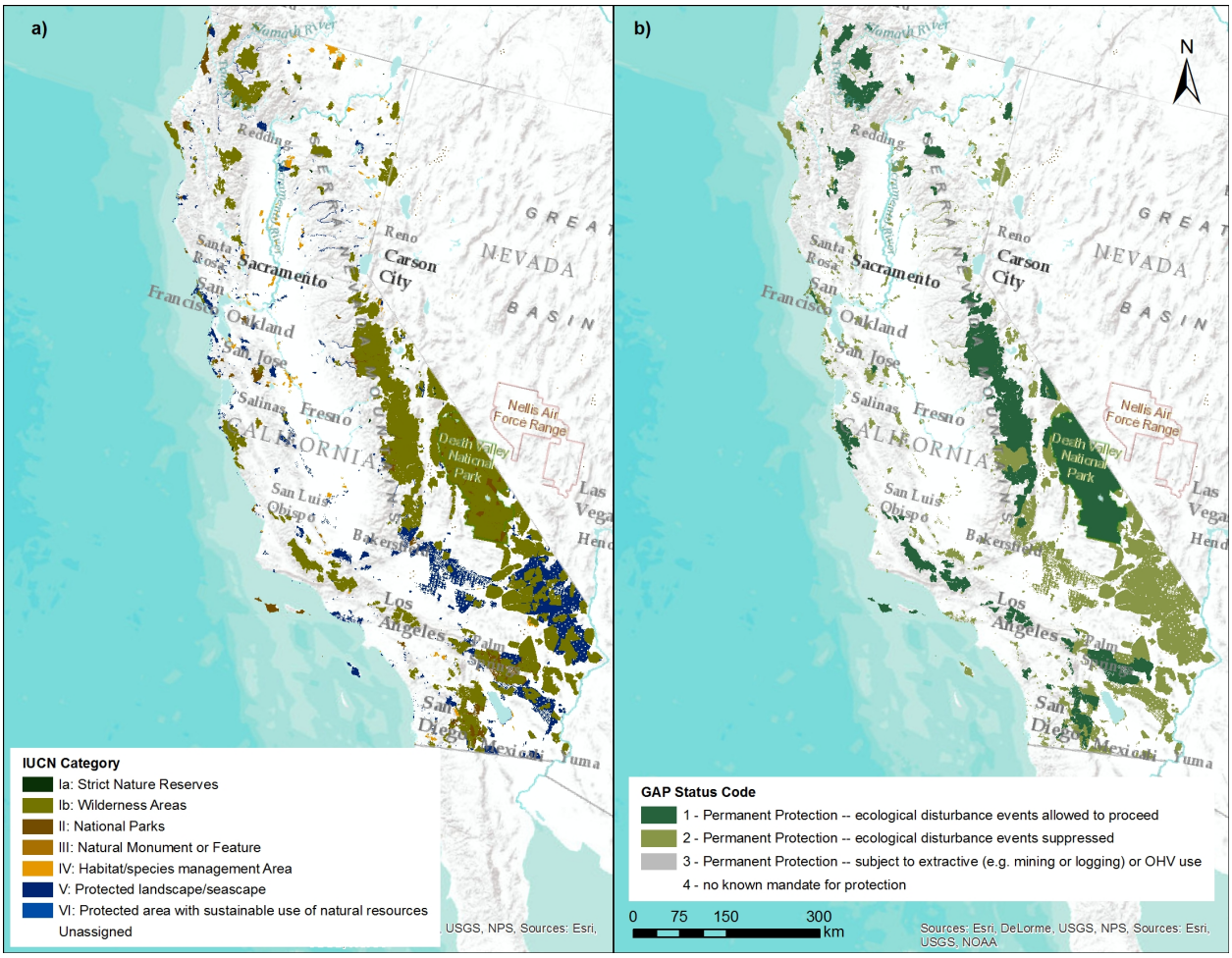

Figure 2.2: PAs in California with IUCN management categories and USGS GAP status code.

CHAPTER 3

Land Cover Change and Dynamics of Protected Areas in California from 2000 to 2015 with Space-borne Remote Sensing

3.1 Introduction

Protected areas (hereafter referred as PAs) have been established in areas with high level of biodiversity and endemism and contain representative examples of natural ecosystems. For authorities maintaining a well designed administrative system of PAs and other conservative areas, such as United States National Park Service (NPS), it is important for policy makers to understand the past, the present, and the projected future of PAs to evaluate, review, and propose management policies and projects [Fancy et al., 2008].

The above purposes are often fulfilled with the assistance of the space-borne remote sensing method recently, combined with field campaigns and observing initiatives. Remote sensing is a low cost and repeatable approach to build inventory, generate baseline, monitor change, and detect disturbance in PAs [Gillespie et al., 2008]. Both discrete (e.g.land cover classification) and continuous (e.g. NDVI, EVI) remote sensing products have been widely applied in this field. The land cover classification products, especially those derived from Landsat at a finer spatial scale (30 meter cell size) with a longer temporal interval provide more detailed information of change and disturbance, such as development and human activities. For example, utilizing the mapping of global forest [Hansen et al., 2013b, Schmidt and Karnieli, 2000] and the assessment on variations in sagebrush habitat of south-

western Wyoming [Xian et al., 2012]. Although provided as snapshots in many cases, the land cover classification products can provide detailed information of conversion in land cover types, which is usually the most straightforward information of land cover change, and often served as a basis of further analysis with quantitative biogeographic measurements.

In additional to the utilization of discrete land cover classification products, many studies focusing on PAs investigated the subtle dynamics that are not drastic enough to alter the land cover type but of a great ecological significance, such as the greening and browning trend of the forest and shrub land. A variety of continuous biogeographic measurements from remotely sensed imageries have been applied, including MODIS and AVHRR vegetation indices and leaf area index (LAI) [Nemani et al., 2009, Alcaraz-Segura et al., 2009], MODIS reflectance [Gross et al., 2013], net primary productivity (NPP) [Crabtree et al., 2009]. In these examples, utilizing the continuous time series of biogeographic indicators instead of focusing on snapshots of land cover classification products helps to extract the temporal and spatial patterns of dynamics and usually generates a more comprehensive understanding of change. The methodologies implemented in the above studies aimed to maximize the merit of the short temporal interval between observations and the large collection of imagery.

Most studies of PAs have focused on tropical or alpine ecosystems because of the high value of conservation and biodiversity [Curran et al., 2004, Kramer et al., 1997]. However, some drier areas also maintain a high level of biodiversity, such as the Mediterranean ecosystem in California. The highly diverse environmental conditions have generated many subtle factors that affect plants distribution in California, such as slope direction, soil depth, history of disturbance, intensity of shade, and availability of moisture[Ornduff et al., 2004, Barbour et al., 2007]. As one of the five Mediterranean ecosystems on the earth, California contains a high number of native and endemic plant species (5862 taxa) [Hickman, 1993, Ornduff et al., 2004, Natural Resources Conservation Service, 2015]. Though receiving less attention than tropical area, semi-arid and arid ecosystems in the southwest U.S. have attracted increasing address recently because of the prolonged drought and increased wild fire activities [Carle, 2015a]. Studies focusing on PAs in California, which not only serve

as a crucial bank of biodiversity but also an important economic source through tourism and recreation, should step beyond case analysis focusing on a few major PAs with land cover snapshots [Gillespie et al., 2015]. Analysis should involve a comprehensive investigation of the recent decade with space-borne remote sensing products on the dynamics of land cover, fluctuation of important land cover components, and spatial distribution of change[GEO BON Office, 2011]. Utilizing both the categorized land cover and continuous time series of land cover with a complete spatial extent would be the most effective method to fulfill these expectations. As a major authority that manages a large proportion of PAs in the country, the U.S. National Park Service is celebrating the centennial anniversary in 2016 and there is a need to review and evaluate the status and trends of protected areas in California, the home of 27 national parks, to establish a solid foundation in terms of research and protection for the next chapter of NPS.

We focueds on applying the combination of both categorized land cover classification and the continuous land cover components to detect and investigate the dynamics of land cover in all PAs of California comprehensively. This research has three primary objectives. First, we investigated if there has been significant change in land cover change and types in PAs of California. Second, we analyzed if significant changes in greenness, brownness, and barren areas have occurred from 2000 to 2015 in protected areas in California. In particular, we predicted an increase in brownness, considering the four continuing years of drought starting from 2011 in California. Third, we identified positive and negative metrics of change in greenness, brownness, and bareness and evaluate the sensitivity of change, which can be used by natural resource managers to assess trends in PAs of California.

3.2 Materials and Method

We conducted the analysis based on the boundaries of protected areas (PAs) from World Database on Protected Areas (WDPA) [IUCN and UNEP-WCMC, 2015]. WDPA covers all recorded PAs in the world. It also contains the IUCN management categories of PAs as a

record of status of management (Figure 2.2a). A similar categorizing system (GAP status code)of the United States provided by USGS National Gap Analysis Program (GAP) is also associated to PAs in California (Figure 2.2b). The following analysis will be focused on these areas, utilizing categorized land cover type and continuous land cover time series.

3.2.1 Land Cover Types and Transition Matrices for PAs in California

The National Land Cover Database (NLCD) from Multi-Resolution Land Characteristics Consortium (MRLC) provides detailed land cover classification mosaics using the Anderson Land Cover Classification System [Anderson, 1976] at a spatial resolution of 30 meters [Homer et al., 2007, Fry et al., 2011, Homer et al., 2015]. This land cover product is derived from Landsat TM and ETM+ imagery collection. The dataset is available at a 5-year interval, including 2001, 2006, and 2011. NLCD not only provides a snapshot of the land cover but also illustrates the changes since the previous time slice. With these data, we can obtain an overview of the land cover status and the changes in landscape of PAs in California at a fine scale.

We first extracted the land cover types of all PAs in California (1441 PAs in total) from NLCD 2001, 2006, and 2011. PAs with multi-parts were broken into separate polygons (9953 in total) for a more accurate calculation of zonal statistics, such as majority, minority, and variety of land cover types inside each PA. We also calculated transition matrices of land cover types for the period 2001-2006, 2006-2011, and 2001-2011 for all PAs.

3.2.2 Extract the Quantitative Proportion of Land Cover Types from MODIS Imagery

Although most PAs are free of conversion in land cover types because of the high level of protection and management, change of greenness and brownness still is still active on a decade basis inside PAs and is of great ecological significance. In order to identify such

change, there is a need to obtain a series of continuous land cover signatures to generate the trend of change, the magnitude of change, and the temporal and spatial sensitivity of change. This cannot be achieved without utilizing the continuous and complete time series of surface reflectance. Moderate Resolution Imaging Spectroradiometer (MODIS) generates complete time series of land cover reflectance at a 16-day interval or less and a coarser spatial scale (250 m, 500 m, or 1000 m). Its continuity in time and short revisiting interval is crucial to the analysis on temporal dynamics. A key challenge of utilizing the MODIS reflectance products in studies on land cover dynamics is to translate the raw reflectance into the land cover components[Coppin et al., 2004, Somers et al., 2011, Rocchini et al., 2010]. Spectral analysis techniques can be applied to generate complete quantitative proportion of given land cover types at a much finer temporal resolution than the snapshots of land cover classification datasets such as NLCD [Yin et al., 2013]. As one of these techniques, spectral mixture analysis (SMA) has been widely applied in deriving land cover signatures from MODIS reflectance products and other space-borne sensor imageries with high temporal resolution[Somers et al., 2011, Li et al., 2005, Gillespie, 1992, Okin et al., 2001]. Compared with available MODIS products such as NDVI, EVI, and vegetation continuous field (VCF), SMA provides more flexibility with a user-defined spectral library for endmembers, meaning that the time series derived from the reflectance products are not limited to green vegetation.

Non-photosynthetic vegetation (NPV), sometime recognized as brown vegetation, would be an example of the advantage of applying SMA on reflectance products. It is a crucial element of semi-arid and arid ecosystems, whether it is senescent material that contributes organic carbon to soils, standing dead vegetation that can serve as fire fuel, leaves that have yellowed in response to stress, or living structural tissue[Okin, 2010]. Because of the missing of the "red-edge" characteristics in the spectrum, NPV is much less addressed in the study of vegetation using space-borne remote sensing observations. SMA can directly extract the fraction of NPV, as well as the green, or photosynthetic active part of vegetation[Guerschman et al., 2009, Guerschman et al., 2015, Okin, 2007, Serbin et al., 2013]. This technique would be helpful to understand the ecology of Mediterranean landscapes, such

as many PAs in California.

In this study, we applied the multiple endmember spectral mixture analysis (MESMA) from relative spectral mixture analysis (RSMA) derived by Okin (2007) on MODIS nadir BRDF adjusted reflectance (NBAR) products (product MCD43A4, tile h08v04 and h08v05) at the 500-meter cell size. Dates with only one tile of the two available were dropped out to obtain mosaics of h08v04 and h08v05 to cover the entire California. PAs with area less than one MODIS pixel (500500m) were screened for further analysis (264 out of 1441 PAs). According to the theory of spectral mixture analysis, we assume that the reflectance detected by space-borne sensors of a pixel is a linear mixture of different land cover types. The purest or the most representative spectra of these land cover types are referred as endmembers [Gillespie et al., 1990, Gillespie, 1992]. The contribution of each type is equivalent to the proportion it occupies in the pixel. As the soil is always a contributor to the reflectance, the above assumption can be translated to the following equation if m types of soil and n types of non-soil land cover types are considered as endmembers (Equation 3.1)

$$\rho_{pixel}^{t_i} = \sum_{j=1}^{m} f_j^{t_i} \rho_j + \sum_{k=1}^{t_i} \rho_k + \varepsilon \tag{3.1}$$

where $\rho_{pixel}^{t_i}$ is the reflectance of the pixel at time t_i, ρ_j is the reflectance of the different types of soil, $f_j^{t_i}$ is the fractional area covered by soil at time t_i, and $f_k^{t_i}$ is the fractional area of each non-soil component at time t_i with reflectance ρ_k. All ρ_j and ρ_k are endmembers. The last term, ε, is the residual after best-fit coefficients have been determined, which should be minimized. Equation 3.1 is also subjected to the constraints that

$$\sum_{j=1}^{t_i} f + j^{t_i} + \sum_{k=1}^{n} f_k^{t_i} = 1 \tag{3.2}$$

Fractions of four land cover types are calculated in this study, including green vegetation (GV), non-photosynthetic vegetation (NPV), bare soil (BS), and snow. In the following results and discussion sections, we will focus on the first three components.

The first step to implement MESMA is to obtain the contribution from soil as the first item in Equation 3.1. It is also a baseline of all the changes from other non-soil types. After looping over all possible combinations of endmembers from different spectra of GV, NPV, BS, and snow on the selected snow-free date (DOY 137 in the year 2000) to calculate the linear mixture model, we can obtain a pseudo-soil baseline endmember, whose reflectance is the spectrum of the best fitted BS. This baseline endmember was then embedded into Equation 3.1 to calculate the fraction of GV, NPV, BS, and snow for the other dates to generate a complete time series of land cover fractions from 2000 to 2015.

After getting the time series of fractions, we calculated the annual average for 2001 and 2015 as a comparison between the start and the end of the entire time series. We also generated the difference between the anual average of the two years. In addition to the original time series, we calculated several statistics and derivatives for a better understanding of the trend and pattern of time series, such as the slope of linear trend for GV, NPV and BS, as well as the standard deviation of time series. The large sample size of the time series leads to very significant results in the linear fit models at most pixels, even if the magnitude of slope is still low. So we set the threshold of significance at a lower level ($p < 0.0001$) and mapped out only the significant time series. Mean, median and standard deviation of the slope were generated for all pixels in each PA as well to address the spatial distribution and heterogeneity of change. Table 3.1 summarizes the calculations derived from MESMA generated land cover signatures.

3.3 Results

3.3.1 Land Cover Change in PAs of California

From the three snapshots of land cover in 2001, 2006, and 2011 obtained from NLCD, we found that most land cover types, especially the four major types (shrub/scrub, evergreen forest, barren land, and grassland/herbaceous) are relatively stable for PAs in California (Figure 3.1a). Among the major land cover types, evergreen forest and open water expe-

Table 3.1: List of results and the derivatives for land cover component time series generated by MESMA.

Category	Name	Dimension
MESMA Original	GV, NPV, BS, and snow time series	2400 (column) × 4800 (2400*2 row) × 648 (days feasible for mosaic)
	Mean of DOY for GV, NPV, BS	2400 (column) × 4800 (row) × 23 (days of year)
	Annual average of GV, NPV, and BS	2400 (column) × 4800 (row) for one years
	Difference in annual average of GV, NPV, and BS for selected years	2400 (column) × 4800 (row) for one year
	Seasonal average of GV, NPV, and BS for selected years	2400 (column) × 4800 (row) × 4 (seasons) for one year
Linear Trend of Time Series	Slope of linear trend for GV, NPV, and BS time series	2400 (column) × 4800 (row) × 1
	Standard deviation of GV, NPV, and BS time series	2400 (column) × 4800 (row) × 1
Basic statistics at the single PA level	Mean/median/stdev of slope calculated for GV, NPV, and BS pixels	One value for each PA
	Average Stdev of GV, NPV, and BS time series	One value for each PA

rienced a decreased of area in 0.93% and 3.06% from 2001 to 2011, while other drier land cover types slightly expanded, including barren land (0.99%), shrub/scrub (0.13%), and grassland/herbaceous (0.60%) (Figure 3.1b). The emergent herbaceous wetlands also increased (4.93%), mostly converted from the adjacent open water areas. Although developed area occupies a very limited amount of area in PAs (0.66%, all intensity levels), there was a significant increase in developed areas at medium and high intensity (11.48% and 38.74%, respectively).

The most frequent "change-to" from 2001 to 2006 type is shrub/scrub. Greatest change-to value is found in the transition from evergreen forest to shrub/scrub. The shrub/scrub is also the most frequently change-from type (Table 3.2), mostly to the wetter types (except for barren land). However, it did not offset the increase generated by the conversion from other wetter types. Thus the shrub/scrub still received a great increase from 2001 to 2006. The barren land is the type with greatest increase from 2001 to 2006, mostly from shrub/scrub. The above facts indicated a significant transition from wetter to drier types from 2001 to

2006.

Compared with the previous time period, the land cover change from 2006 to 2011 in California PAs was more concentrated on a few types (Table 3.3). The most striking transition was still the conversion from evergreen forest to the shrub/scrub. And there was a decrease in open water, mostly converted to much drier types, including barren land or shrub/scrub. With most of other conversion types composing very small proportion from the total changed pixels, the wetter to drier converting trend was consistent as before.

Converting from wetter to drier types was the major trend from 2001 to 2011. The transitions from open water, evergreen forest, grassland/herbaceous, and emergent herbaceous wetlands to drier types are the mostly recognized (Table 3.4). And the shrub/scrub is the top change-to type from many wetter types. As a summary of three transition matrices, we also examined the continuity of change for different land cover types for 2001 to 2006, 2006 to 2011, and 2001 to 2011. Open water, evergreen forest, and open space developed lands consistently decreased during the above partitions of the time period, and mostly converted to drier types. The continuing increase occurred in the drier or more human-influenced types, including barren land and developed land with medium intensity (Table 3.5).

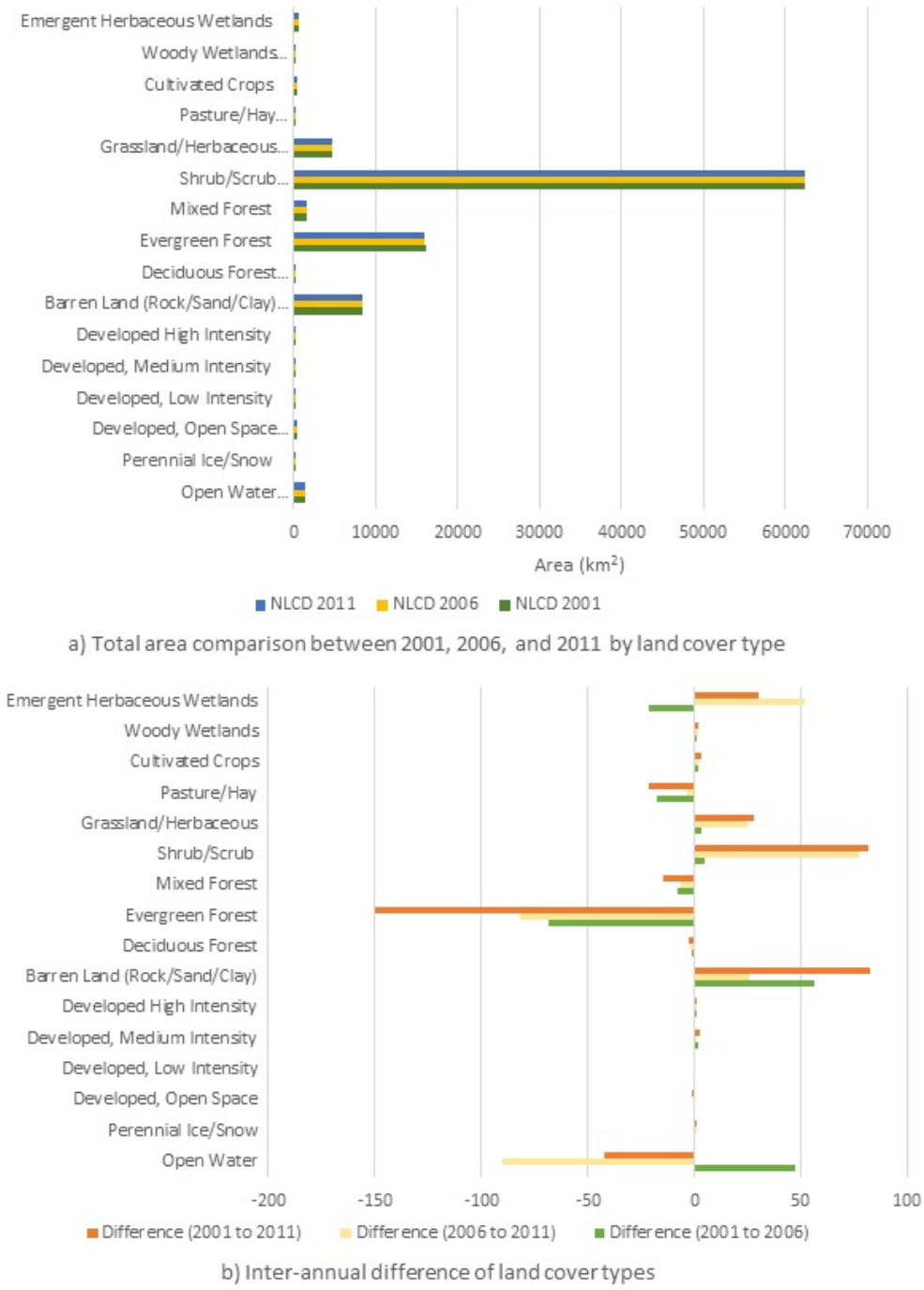

Figure 3.1: Inter-annual change of land cover from NLCD 2001, 2006, and 2011.

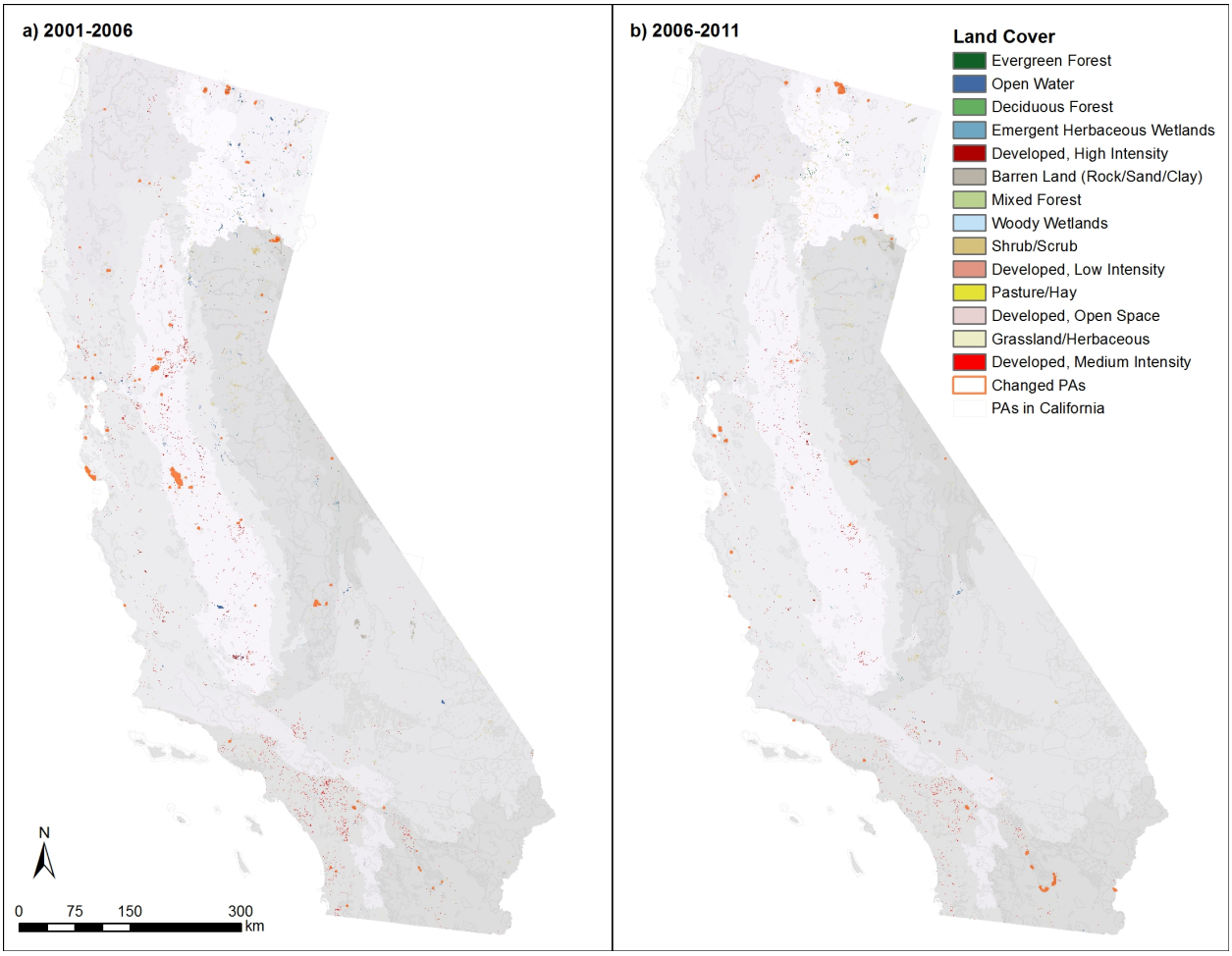

Figure 3.2: PAs with majority land cover changed. Pixels with land cover type conversion are also mapped and shaded with NLCD symbology. Level III ecoregions are included and colored in grey scale.

Table 3.2: Transition matrices of PAs in 2001-2006. Numbers are count of pixels for each class.

			2006 Major Land Cover Type															
			Water	Developed				Barren	Forest			Shrubland	Herbaceous	Planted/Cultivated		Wetlands		
			Open Water	Developed, Open Space	Developed, Low Intensity	Developed, Medium Intensity	Developed, High Intensity	Barren Land (Rock/ Sand/Clay)	Deciduous Forest	Evergreen Forest	Mixed Forest	Shrub /Scrub	Grassland/ Herbaceous	Pasture/ Hay	Cultivated Crops	Woody Wetlands	Emergent Herbaceous Wetlands	2001 Grand Total
2001 Major Land Cover Type	Water	Open Water	1513891	15	2	17	5	14080	77	584	52	1722	2602	2078	5985	399	854	1542363
	Developed	Developed, Open Space	3	558445	2339	6368	1397	3				2	1					568558
		Developed, Low Intensity	2	67	110274	4670	1572	17										116602
		Developed, Medium Intensity		4	89	24392	259											24744
		Developed, High Intensity			5	26	2212											2243
	Barren	Barren Land (Rock/Sand/ Clay)	8958	93	9	6		9286803	132	124	5	10064	311	29	183	381	444	9307542
	Forest	Deciduous Forest	117					214	286599	161	88	1574	1508		11	22	59	290353
		Evergreen Forest	505	3	3	1		1935	339	17805598	594	78276	8118		6	99	428	17895905
		Mixed Forest	74	13				400	12	181	1808548	7087	2540			7	3	1818865
	Shrubland	Shrub/ Scrub	17761	199	49	7		63441	1701	12268	577	69173603	28685	862	1314	1902	4364	69306733
	Herbaceous	Grassland/ Herbaceous	6912	457	67	52		2504	352	1117	101	38267	5186943	234	3688	725	1617	5243036
	Planted/ Cultivated	Pasture/ Hay	24787	164	6	15		211		38		679	40	341528	112	72	267	367919
		Cultivated Crops	9946	38	21	22	5	236		15		598	3525	36	434606	117	1356	450521
	Wetlands	Woody Wetlands	444	3				90	17	21	8	266	1979	13	881	174574	1236	179532
		Emergent Herbaceous Wetlands	12034	106	14	9		536				50	10861	3462	5853	1616	646145	680686
		2006 Grand Total	**1595434**	**559607**	**112878**	**35585**	**5450**	**9370470**	**289229**	**17820107**	**1809973**	**69312188**	**5247113**	**348242**	**452639**	**179914**	**656773**	

Table 3.3: Transition matrices of PAs in 2006-2011. Numbers are count of pixels for each class.

			2011 Major Land Cover Type															
			Water	Developed				Barren	Forest			Shrubland	Herbaceous	Planted/Cultivated		Wetlands		
			Open Water	Developed, Open Space	Developed, Low Intensity	Developed, Medium Intensity	Developed, High Intensity	Barren Land (Rock/ Sand/Clay)	Deciduous Forest	Evergreen Forest	Mixed Forest	Shrub/ Scrub	Grassland/ Herbaceous	Pasture/ Hay	Cultivated Crops	Woody Wetlands	Emergent Herbaceous Wetlands	2006 Grand Total
2006 Major Land Cover Type	Water	Open Water	1487617	7	40	5	2	27182	164	227	35	17925	4217	324	6002	348	51339	1595434
	Developed	Developed, Open Space	1	555899	1254	1836	583	4				8					22	559607
		Developed, Low	3	12	110466	2017	364	15									1	112878
		Developed, Medium		2	110	35283	190											35585
		Developed, High			19	145	5279	5				2						5450
	Barren	Barren Land (Rock/Sand/	1381	28	77	129	70	9365877		29		1469	641		60	20	689	9370470
	Forest	Deciduous Forest	7					12	287077	5	5	1396	591			23	113	289229
		Evergreen Forest	91					857	5	17727567	20	79402	11215	27	39	43	820	17820107
		Mixed Forest	64	1				67		13	1802848	6137	810			22	11	1809973
	Shrubland	Shrub/ Scrub	2244	70	68	4	15	3643	116	1490	20	6.9E+07	15368	15	326	134	1447	69312188
	Herbaceous	Grassland/ Herbaceous	1336	189	113	85	7	310	2	3	1	3439	5239523	351	452	86	1216	5247113
	Planted/ Cultivated	Pasture/ Hay	517					72	11	8		314	1029	343300	26	1246	1719	348242
		Cultivated Crops	1348	37	76	28	10	750	14	3		501	1083	131	444929	143	3586	452639
	Wetlands	Woody Wetlands	75	14	26	5		132			5	28	3	10	16	178952	648	179914
		Emergent Herbaceous	567	8	12			405				56	24		2493	582	652626	656773
		2011 Grand Total	1495251	556267	112261	39537	6520	9399331	287389	17729345	1802934	69397905	5274504	344158	454343	181599	714237	

Table 3.4: Transition matrices of PAs in 2001-2011.Numbers are count of pixels for each class.

			2011 Major Land Cover Type															
			Water	Developed				Barren	Forest			Shrubland	Herbaceous	Planted/Cultivated		Wetlands		
			Open Water	Developed, Open Space	Developed, Low Intensity	Developed, Medium Intensity	Developed, High Intensity	Barren Land (Rock/ Sand/Clay)	Deciduous Forest	Evergreen Forest	Mixed Forest	Shrub/ Scrub	Grassland/ Herbaceous	Pasture/ Hay	Cultivated Crops	Woody Wetlands	Emergent Herbaceous Wetlands	2001 Grand Total
2001 Major Land Cover Type	Water	Open Water	1455709	22	21	19	6	35078	222	473		5509	4874	1856	8139	525	29910	**1542363**
	Developed	Developed, Open Space	5	554762	3310	8450	1992	4				10	1				24	**568558**
		Developed, Low Intensity	7	69	108233	6310	1952	29				2						**116602**
		Developed, Medium		4	125	24323	292											**24744**
		Developed, High Intensity			10	64	2169											**2243**
	Barren	Barren Land (Rock/Sand/	4431	123	87	133	70	9287149	132	145	9	12669	917	19	243	394	1021	**9307542**
	Forest	Deciduous Forest	117					226	284486	151	92	2970	2084		11	45	171	**290353**
		Evergreen Forest	399	3	3	1		2516	438	17713946	606	157619	19115		43	151	1044	**1.8E+07**
		Mixed Forest	24	14				317	25	198	1801508	13422	3314			29	14	**1818865**
	Shrubland	Shrub/ Scrub	6487	265	117	16	16	68142	1694	13301	605	6.9E+07	43010	799	1481	2100	5768	**6.9E+07**
	Herbaceous	Grassland/ Herbaceous	5812	651	192	141	8	2913	350	978	101	40343	5183153	584	3786	834	3190	**5243036**
	Planted/ Cultivated	Pasture/ Hay	6851	158	12	15		241	11	52		783	1183	337261	2368	1318	17666	**367919**
		Cultivated Crops	8178	78	104	55	15	1275	14	79		1166	4364	174	429161	367	5491	**450521**
	Wetlands	Woody Wetlands	345	5	20	1		233	17	22	13	294	2037	21	814	173942	1768	**179532**
		Emergent Herbaceous	6886	113	27	9		1208				186	10452	3444	8297	1894	648170	**680686**
		2011 Grand Total	**1495251**	**556267**	**112261**	**39537**	**6520**	**9399331**	**287389**	**17729345**	**1802934**	**6.9E+07**	**5274504**	**344158**	**454343**	**181599**	**714237**	

Table 3.5: Change of area (number of pixels) for land cover types in 2001, 2006, and 2011.

	Number of Pixels	2001 Grand Total	2006 Grand Total	2011 Grand Total
Water	Open Water	1542363	1595434	1495251
Developed	Developed, Open Space	568558	559607	556267
	Developed, Low Intensity	116602	112878	112261
	Developed, Medium Intensity	24744	35585	39537
	Developed, High Intensity	2243	5450	6520
Barren	Barren Land (Rock/Sand/Clay)	9307542	9370470	9399331
Forest	Deciduous Forest	290353	289229	287389
	Evergreen Forest	17895905	17820107	17729345
	Mixed Forest	1818865	1809973	1802934
Shrubland	Shrub/Scrub	69306733	69312188	69397905
Herbaceous	Grassland/Herbaceous	5243036	5247113	5274504
Planted/ Cultivated	Pasture/Hay	367919	348242	344158
	Cultivated Crops	450521	452639	454343
Wetlands	Woody Wetlands	179532	179914	181599
	Emergent Herbaceous Wetlands	680686	656773	714237

3.3.2 Comparing the Annual and Seasonal Averages between 2001 and 2015

We developed the inter-annual and inter-seasonal comparison between 2001 and 2015 for GV, NPV, and BS fraction derived by MESMA to identify the changes of greenness and brownness. In the snapshot of the composed GV, NPV, and BS fraction for 2001 and 2015 (Figure 3.3), NPV, GV, and BS fractions are colored by Red (R), Green (G), Blue (B) respectively to form a three-band combination to provide a more informative demonstration of the land cover composition. Five regions are highlighted as the most dynamic areas, including (A) Los Padres National Forest (south) and Joshua Tree National Park; (B) Los Padres National Forest (north); (C) Marbel Mountain and Trinity Alps; (D) Stanislaus National Forest, Yosemite National Park, and Sequoia National Forest; (E) Death Valley National Park and Mojave National Preserve.

The five hotspots of dynamics differ from each other in their trend of change. Among the five regions, region C and E feature a bluer trend, meaning a higher BS fraction or bareness (Figure 3.3). Both were resulted from a transition from NPV to BS (from redder to bluer).

In contrast, region A and B had an opposite transition from blue to red or green, indicating an increase of both photosynthetic active (greenness) or non-active vegetation (brownness). The dynamic in D was more heterogenic. We observed an encroachment of greener or redder parts into the previously BS (bluer) occupied areas from west to the east, along ridge of the Sierra Nevada Mountains from 2001 to 2015 (Figure 3.3).

The above trend of change was better reflected in a map of difference in GV, NPV, and BS (Figure 3.4). The most prominent part in the map of difference was a great increase in NPV (indicating the increase of brownness), especially in region A and D. An increase of GV occurred in many coastal PAs, as observed in region A and B. Additionally, the magnitude of change in NPV and BS is greater than GV, which was reflected in the darker shading of NPV/BS than GV in Figure 3.4.

The browning trend, i.e. the increase of NPV, is also observed in the comparison between seasonal average of 2001 and 2015. In the upper panel for 2001, the driest (bluest) period of most inland and southern California (region A, B, D, E) occurred in summer (JJA), while spring (MAM) and fall (SON) were greener (higher greenness) and winter (DJF) was redder (higher brownness). However, the year 2015 had an increased bareness (bluer) during spring and fall in many southern California PAs. On the other hand, although the northern California PAs (region C) had an opposite seasonality compared with the southern ones (green summer and fall, blue or red winter and spring). Similar as the above regions, it had a bluer spring, summer, and fall in 2015. Scattered blue areas also appeared in the region C.

The linear fit of the full time series at each pixel helped to evaluate the trend of change for land cover components during the past 16 years (Figure 3.6. Considering the phenological linkage between the GV, NPV, and BS, we created a composite trend to combine the trend of all three land cover components based on the sign of the average slope inside PAs, and mapped by moisture conditions (Figure 3.7). Average slope of all the pixels inside each PA is mapped as a quantitative illustration of the magnitude of the change (Figure 3.8).

From the above results, we observed an increase of NPV in most PAs of California from

2000 to 2015, regardless of the increase or decrease in GV, which is the bank and source of NPV. Among these PAs, we identified those with both GV and NPV increased as greening PAs (pattern 6 and 7, colored green in Figure 3.7), and those with an expansion of NPV and a decline in GV as browning ones (pattern 3 and 4, colored orange and yellow in Figure 3.7).

The greening PAs, where an increase of greenness occurred, spread along the Coast ranges and Transverse ranges, at the foothill of Sierra Nevada, and in the Mojave Desert (Figure 3.8). Most of the near-coast PAs had a higher coverage of GV, such as Ventana (region B), Marble Mountain, and Trinity Alps (region C). The parallel increase in GV and NPV may not always be the evidence of a solid greening. As revealed in Figure 8 and 11, the expansion of NPV was usually at the same or even a higher magnitude than GV in these PAs. This reflected a browning trend in general rather than greening.

Compared with the greening ones, the browning PAs generally experienced trend reflects an exacerbating browning process from 2000 to 2015, revealed by the decline of GV and the rise of NPV. These PAs are mostly located in the inland desert areas and stretched along the rain shadow side of North and South Coast ranges. An expansion in BS also occurred, especially in the inland desert. If the decrease in GV persists, the increase in NPV may not continue as a result of the loss of its source. Such decrease was worth of further investigation, especially for PAs in the inland desert areas, since the loss of coverage from the drought tolerant vegetation may lead to severe land degradation.

3.3.3 Temporal variability and spatial heterogeneity of PAs

Despite identifying the difference between the start and the end of the time series, we also evaluated the sensitivity of change in both time and space with the standard deviation of time series (Figure 3.9) and the average of standard deviation inside PAs

Temporarily speaking, the greener areas were more dynamic than browner ones. This can be best reflected from the standard deviation of GV time series (Figure 3.9). The foothill of

Sierra Nevada is the boundary of two ecoregions and clearly differentiated the cismontane and the transmontane areas. The standard deviation of GV time series for the generally greener PAs (west of this border) was much higher. In addition, we observed consistency in the magnitude of variability of GV, NPV and BS in the most dynamics PAs. In other words, if a PA has a high temporal variability of GV, this PA was usually more dynamic in NPV and BS as well. PAs along the North Coast Ranges (region C), the Transverse Ranges (region A) and the mid elevation of Sierra Nevada Ranges (region D) were examples of this pattern. In contrast, the inland desert areas (region D) had a much lower fluctuation in time series.

The spatial heterogeneity of change was less correlated with the greenness. The five hotspots of change mostly have a high standard deviation for slope values inside PAs (Figure 3.10). A higher spatial heterogeneity of the slope indicates a great diversity in the landscape inside the same PA. Covered mostly by evergreen forest, Trinity Alps (region C) is the most diverse PA in California, especially for NPV and BS. Such diversity can be attributed to the great difference between east and west part of the PA (Figure 8). The west side has a significant increase in both GV and NPV, while the east side features a less intense decline in both. This can also be found in many PAs with an active change in GV. Drier PAs can have a great spatial heterogeneity as well, such as the Death Valley National Park (region D). Considering the change of NPV and BS, both positive and negative slope patches exist in this region (Figure 3.6), which increases the complexity inside the boundary of PA.

3.4 Discussion

3.4.1 Disturbance from human activity detected from land cover classification

Most PAs in California are under restriction over human activities, such as construction, farming, and logging. The major strategies imposed by management authorities are mostly focused on enforcing the restriction in these areas, for example, removing the livestock to prevent grazing (Channel Islands National Park) and restoring the wilderness by removing

or relocating campgrounds and trails in Los Padres National Forest (USDA Forest Service Pacific Southwest Region 2013). As a result, the number of PAs with the coverage of developed lands and cultivated crop lands is quite small. However, a continuous decrease in the open-spaced developed lands and increase in the medium intensity developed lands occurred from 2001 to 2006, according to NLCD. A clear expansion of the medium to high impervious surface was also detected during this period from NLCD imperviousness map [Fry et al., 2011, Wickham et al., 2013]. These areas stretched along the coastal line and off the major hubs of urbanization, including southern California and the San Francisco Bay area (Figure 3.11). A robust growth in economy made these areas magnets for immigration, introducing more construction of homes and other infrastructure. Such expansion produced increasing fragmentation of natural areas. A good example of this would be the Santa Monica Mountains National Recreation Area (SAMO) in southern California. Adjacent to Los Angeles, there has been report about the significant increase of nightlights intensity in this area, indicating a higher coverage of developed lands [Willis, 2015, Gillespie et al., 2016]. Although the urban sprawl may not directly penetrate into PAs, the direct and indirect ecological influence from the sprawling developed areas cannot be neglected, such as pressure from human activity, light pollution and increase of waste. According to Rundel and Gustafson (2005), many small watersheds or habit islands have become separated from other natural areas by surrounding developments. Although the fragmentation in many PAs of California can be attributed to the increased dryness and the associated land degradation, the managers of PAs adjacent to the rapidly urbanizing areas should pay special attention on minimizing the unnecessary anthropogenic disturbance, especially from construction. Such strategies can help to restore the wilderness in PAs and make the entire ecosystem less prone to the degradation caused by the foreseeing drier climate regime.

3.4.2 Drying trend in PAs of California

The evidence of a drying trend in most of the PAs in California was significant. Both the 5-year interval NLCD products and the 16-day MODIS derived land cover fraction revealed

the similar pattern, according to our inter-annual and inter-seasonal comparison, as well as the calculation of trend for GV, NPV, and BS time series. Most of the browning processes in our study area can be attributed to a drying climate regime and the increase of wild fire occurrence [Carle, 2015a]. From 2000 to 2015, although most PAs have been under management and very few experienced an alternation of the major land cover type, the conversion to shrub/scrub and barren land from other wetter types cannot be ignored. The significant conversion from open water to emergent wetland detected from NLCD products was also another important evidence of drying. Many PAs with no alternation in the major land cover type generally became less green, as seen from the snapshots of land covers in 2001 and 2015. The types with non-interrupted increase and decrease detected in 2001, 2006, and 2011 also reflected the drying trend. Open water and evergreen forest both experienced a consistent decrease from 2001 to 2006 and 2006 to 2011, while the much drier barren land experienced an increase from 2001 to 2011 (Table 3.5). Although most of the PAs are located in the drought tolerate Mediterranean or arid ecosystem, there is a need for policy makers to address the foreseeable risks of land degradation because of the increase of brownness. As the drying exacerbates with the incoming pressure of human activities, the ecosystem needs a prolonged period to bounce back or even has a risk of irreversible degradation, especially for deserts and other semi-arid ecosystems. Considering the vulnerability of these areas, the management authorities of PAs should target on the most change-prone PAs and apply appropriate management on conservation.

3.4.3 Addressing the most dynamic PAs in the strategies of management

The time series of GV/NPV/BS provided statistical measurements on temporal and spatial dynamics, which can help the policy makers to filter the PAs need to be addressed more. As revealed in the standard deviation of time series (Figure 3.9), wetter PAs, or PAs with a higher coverage of GV were usually more dynamic from 2000 to 2015. Compared with PAs with less greenness, the higher GV coverage introduces complexity in seasonality and a higher chance of fluctuation as a response of disturbance. For semi-arid or arid PAs, the

greenness in land cover is extremely valuable to preserve the local climate and keep the PAs from degradation. Because of the ecological significance and the vulnerability of the green part, these PAs should be on the priority list for protection. We provided a list of the twenty most temporarily dynamic PAs, with the IUCN categorized status and management authorities (Table 3.6). From the list we can see many of the most dynamic PAs are at level V of IUCN management category, indicating less intensive restoration strategies have been applied. The management authorities of these PAs should be aware of such fluctuation and analyze the risk of future disturbance, and concentrate on the conservation of the greenness in these PAs with appropriate management strategies.

PAs with a higher magnitude of temporal change usually had a greater spatial heterogeneity (Figure 3.6, Figure 3.7). It indicated that in many PAs with a higher rate of change, the most dynamic part only consists a small proportion of the entire area. In other words, the level and magnitude of change inside one PA can be highly diverse, which is reflected by the high patchiness of PA. A possible scenario can be: several species changed greatly during the time period of this study and such variation has not spread and covered the entire PA, such as the heterogenic change of NPV and BS in Death Valley National Park (Figure 3.6). The change in climate, fire regime, pest invasion, and level of human activities may favor or discriminate certain traits of species and increase the heterogeneity of change in PAs. In addition, the spatial heterogeneity was calculated based on the boundaries of PA, which may not always be consistent with the boundary of the same type of landscape. We provide a list of PAs with the most diverse trend and magnitude of change in Table 3.7. These PAs are worth for a more detailed investigation to distinguish between the different landscapes inside PAs with a finer dataset of landscape units, such as Ecological Land Units (ELUs) by USGS [Sayre et al., 2014], which is a very detailed and systematic division and classification of the biosphere using ecological and physiographic land surface features. With a better defined separation of landscape units, the policy makers can tailor their current conservation strategies to focus on the homogeneous divisions of landscape.

In addition to address the heterogeneity inside PAs, it is also necessary to analyze the

diverse patterns of change in land cover signatures associated with the great difference between landscape in PAs located inside different ecoregions of California, which leaves room for future improvement. California spreads across about ten degrees of latitude. The great variation of landscape because of temperature, moisture, and topographic barriers generated great difference in land cover types and other ecological traits between PAs. Comparing the difference between ecoregions in terms of the change in greenness, brownness, and bare soil of PAs allows aggregation of PAs with similar physical environmental conditions and differentiates the influence from climate conditions between ecoregions. It also makes the results and findings more accessible to policy makers from agencies that are responsible to address the locally specific challenge of ecology.

3.4.4 Understanding the dynamics with continuous land cover components

Considering the life cycle of plants, GV and NPV are indicators of growing season and the non-growing season. These two major land cover components, together with BS, should be combined and form composite measurements to help illustrating and understanding the phenological cycle and the variability of PAs in California. By including NPV as a measurement of the brownness of vegetation, we can interpret the land cover of California PAs with enough address on the unique landscape characteristics of the semi-arid and arid ecosystem. As an explicit description of surface coverage when the vegetation loses the ability of photosynthesis, NPV can provide a more comprehensive picture if combined with the fraction of GV.

In additional to the direction and magnitude of slope of linear fit with time, the composite trend of GV, NPV, and BS mapped provided a good example on utilizing the different land cover components with composite measurements (Figure 3.7). We not only obtained a map of changes in the greenness of PAs but also got the useful information to understand what would be the possible factors to be attributed to. For example, after recognizing a decrease in GV for the Death Valley National Reserve, we can easily find the increase in NPV and BS are the direct explanation of this decrease from the composite trend. Further investigation

can then focus on the analysis about the possible reason of the increase in NPV and BS, such as the prolonged drought and deficit of moisture. With the composite trend of change, the PAs can be mapped and classified by the moisture condition based on all three land cover components.

However, we also found in PAs with a drier landscape, the spectural mixture analysis we applied tended to overestimate either the NPV or the bare soil coverage, and sometimes produced composite trend of GV, NPV, and BS that cannot be explained in terms of physical environment and ecology of the Mediterranean ecosystem, such as areas with all three land cover signatures increasing/decreasing at the same time (Figure3.7). The application of the constaint that forced all land cover signatures added up to one (Equation 3.2) sometimes led to negative fraction of land cover, which also needs improvement. Such discrepancy can be attributed to the quality of endmembers included in the calculation. The large number of soil spectra available from the JHU spectral library applied in our MESMA model as endmembers of bare soils and the inadequate collection of GV and NPV may influence the iteration for identifying the best combination of endmembers, which should be improved for further application. In addition, extra measurements of NPV are necessary to supplement the current limited collection of endmembers focusing on brownness of the landscape. Possible solutions include collecting endmembers directly from the reflectance images for a collection of endmembers that are most suitable for the images for analysis and referring to the observation and knowledge on local ecology and environmental conditions. Utilizing the well developed monitoring network of California PAs is crucial to collect first hand information on the change in land cover, especially the brownness inside PAs. It is also necessary to validate the land cover signatures derived from spectral mixture analysis and evaluate the accuracy of endmembers applied in the analysis. Controlling the number of endmembers for the same land cover component to match with the land cover composition may also be helpful to improve the selection of the best endmember combination.

In addition, the calculation of linear trend and its derivatives in this study has a limitation of not considering the occurrence of wild fire, a major reason of land cover change and even

land cover type alternation. The Mediterranean ecosystem in California is prone to wild fire, and PAs are usually where the influence of wild fires is at the maximum because of the high density of fire fuels. A major fire can remove the aboveground biomass and greatly change the fraction of GV, NPV, and BS, for example, fires occurred in region A (along the Transverse Ranges) and region C (inside the Klamath Mountains). Although the increased occurrence of wild fires in California is also an evidence of the drying climate, it is necessary to exclude the intensively burned area from 2000 to 2015 to avoid the inclusion of abrupt alternation of land cover.

3.5 Conclusion

With the latest published PA boundaries from WDPA by IUCN, we can map out the change of land covers of these PAs and obtain a general picture on the temporal and spatial variability using both categorized land cover types and quantitative land cover components. Going beyond analysis based on several snapshots of land cover, utilizing the MODIS derived quantitative land cover components provided more accurate measurements on the trend of change and the temporal fluctuation. To address the significance of the unique contribution from non-photosynthetic part/phase of vegetation to the semi-arid and arid ecosystem, we derived and focused on the three land cover components derived from MODIS reflection products instead of directly using available vegetation indices. Both of the qualitative and quantitative results are crucial to understand the dynamics of landscape in California PAs over the past 16 years. In this study, we combined the qualitative and quantitative measurements of land cover and obtained three major findings.

First, both the qualitative and quantitative measurements revealed a significant loss of greenness in many PAs. The transition matrices of 2001-2006, 2006-2011, and 2001-2011 recognized the shrub/scrub land as the most frequent change-to type, while the wetter types continued to decrease between time slices. The wide spread expansion of brownness demonstrated by a significant increase of NPV in most PAs was a signal of the exacerbating

dryness during the past 16 years. Policy makers may take the drying trend into account in the development of future management strategies.

Second, anthropogenic disturbance cannot be ignored in PAs, though the number of PAs with medium or high level of human-influenced area is limited. The spread of developments inside PAs along the Pacific coastal line and near the major metropolitans introduced great fragmentation into the surrounding PAs, especially from 2001 to 2006. The increased patchiness may deteriorate the degradation in some PAs with the change of climate and fire regime. Future policies and enforcement should address on restricting human-influenced disturbance in PAs and restoring wilderness in these areas.

Third, PAs with a higher coverage of greenness are more dynamic than drier ones, according to the analysis based on MESMA calculations. Compared with the drier ones, the greener PAs had more complex seasonality and a higher level of temporal fluctuation. It is mostly because the green vegetation is more sensitive to the change in climate regime and other disturbance and the brown vegetation (or NPV). If the management authorities aim to minimize the fluctuation of greenness, these dynamic PAs should receive closer monitoring to track the changes and make corresponding strategies to minimize the possible land degradation.

Further improvement of this study can include addressing on the spatial heterogeneity inside PAs in analysis, improvement on MESMA models, and application of other time series analysis techniques. We also found the spatial heterogeneity inside PAs cannot be ignored when designing the management stategies of PAs. In this study, we found that the spatial heterogeneity exists in PAs and may have a great influence on the strategy of PA management. Considering the complex mosaic of land cover types in many large PAs, an analysis at a finer spatial scale or on splitting the PAs into different ecological units would be necessary to address the internal heteogeneity of PAs. In addition, there is a need to aggregate the results, especially the trend of change by ecoregions to accomondate the diversity between different clusters of PAs. Improvements is also necessary to reduce the overestimation of brownness and the coverage of bare soil in order to better track the dynamics of land cover

signatures. Although the analysis based on GV/NPV/BS derived from MODIS reflectance products recognized important temporal and spatial patterns of change in vegetation, the application of this method requires more validation and comparison with some well recognized vegetation indices such as NDVI. Possible solutions include deriving endmembers from satellite images directly or collecting them from a wider range of locations in field. Taking advantage of the accumulated knowledge from local monitoring system is also an option to better validate the estimation of land cover signatures. The technique of time series analysis applied in this study also needs improvement to obtain more solid seasonality and trend, including decomposing the time series using autogressive model and trend significant tests with the augmented Dicky-Fuller (ADF) statistic [Goetz et al., 2005]. Besides the above validating and pre-processing steps, excluding the intensively burned area from 2000 to 2015 in California is also necessary to minimize the disturbance from abrupt alternation of surface condition on the investigation of trend of dynamics.

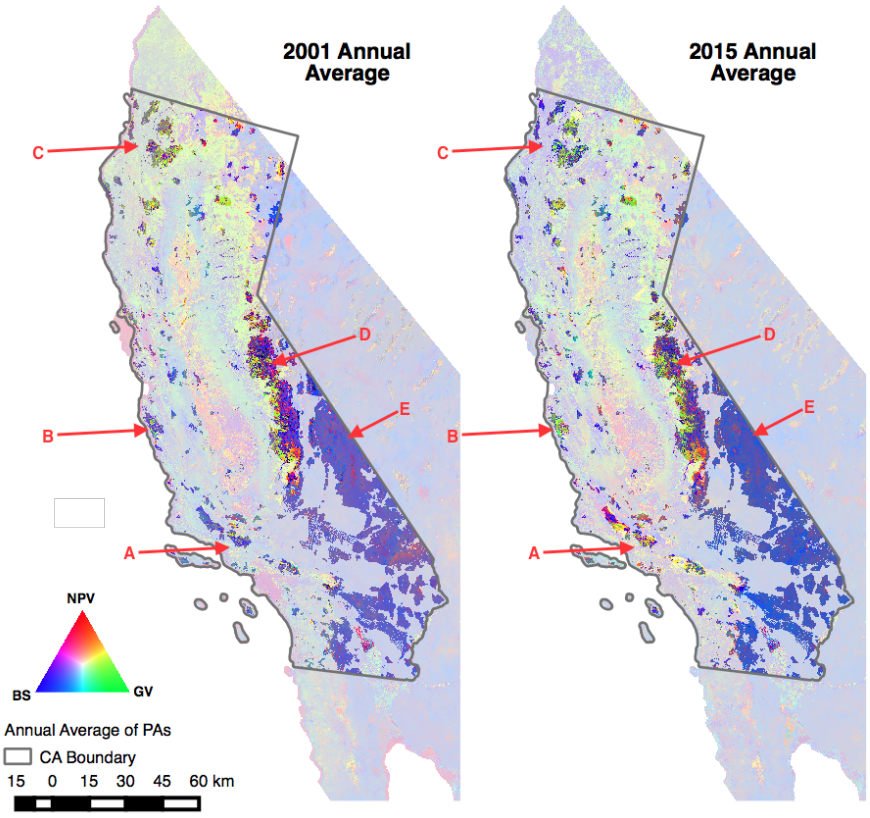

Figure 3.3: Compare the annual average of GV/NPV/BS composition for California between 2001 and 2015 (Figure 3.5. Fractions of land cover components are shaded using RGB band combination (R: NPV, G: GV, B: BS). The lighter shaded background layer in each panel is the annual average of 2001 and 2015, respectively. The brighter foreground layer is the subset from the annual average using PA.

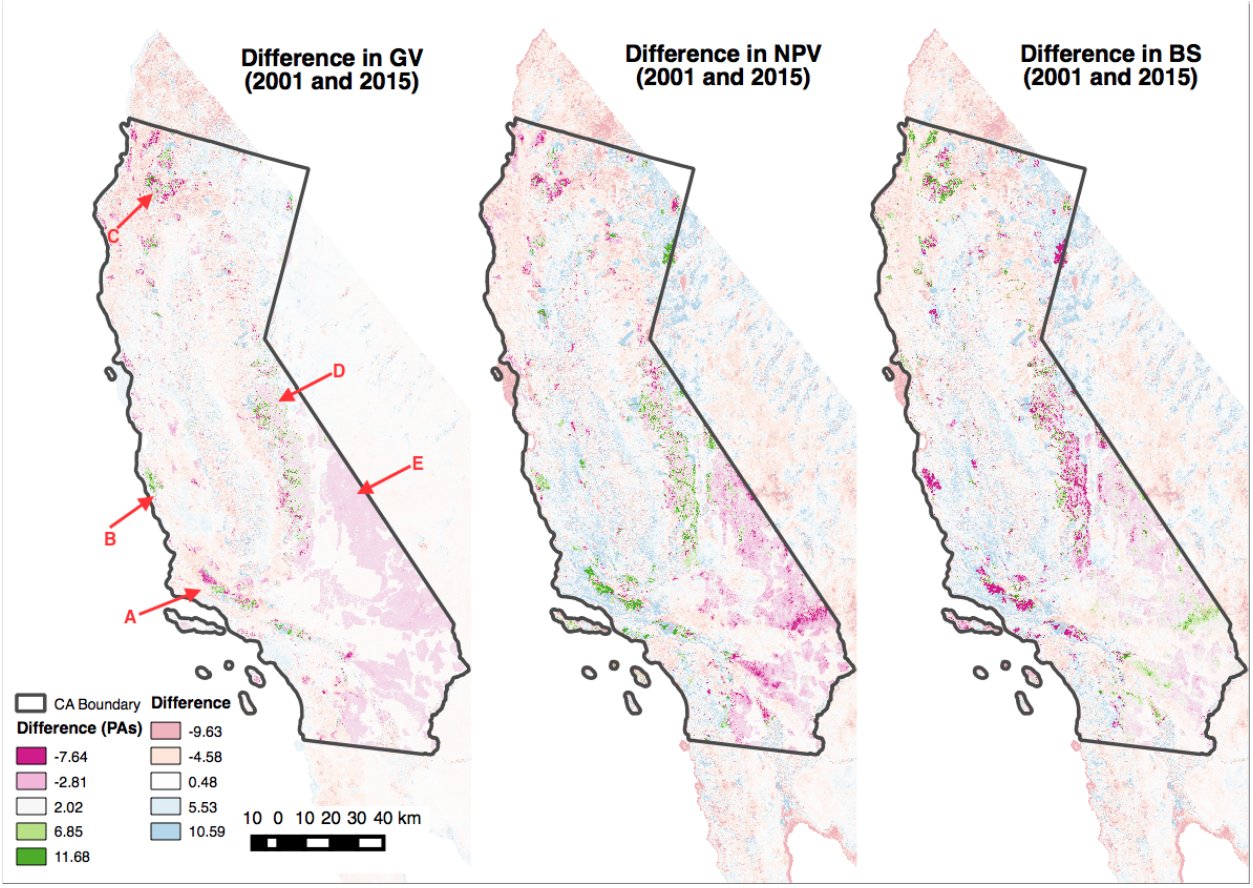

Figure 3.4: Difference of fractions (% of area in one pixel) in annual average between 2015 and 2001. The differences in PAs only and entire California are colored using different color schemes. Difference in California is also shaded with a light color tone as a background, while the PAs are highlighted using a brighter color (magenta to light green).

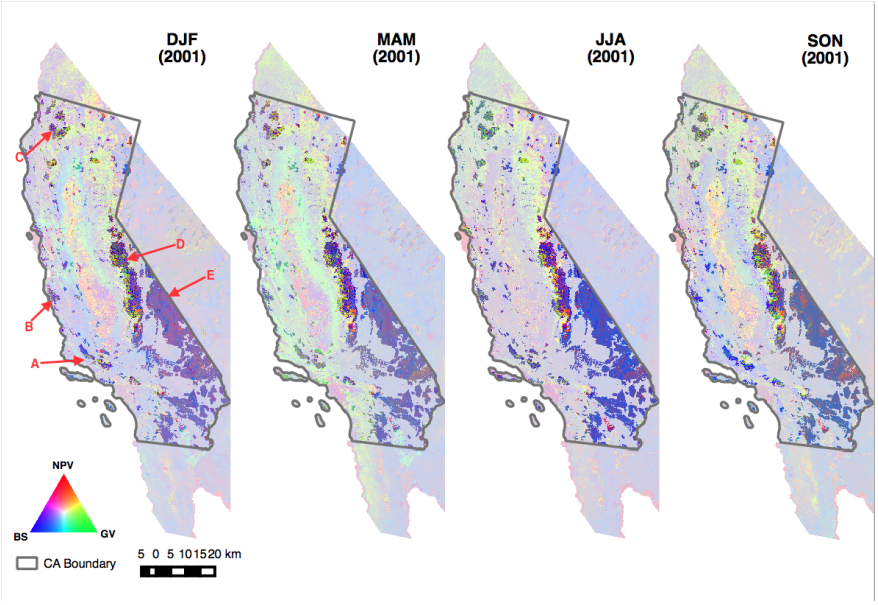

(a) 2001

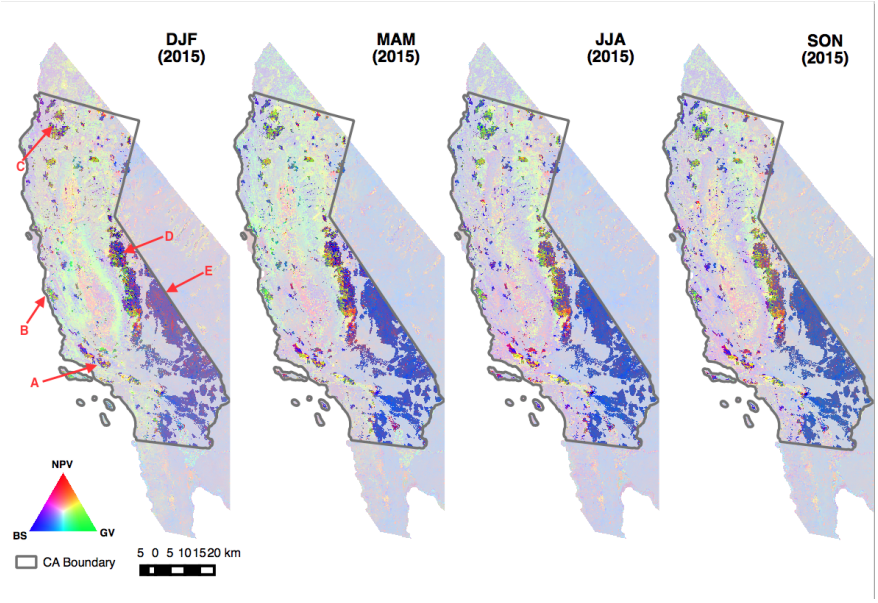

(b) 2015

Figure 3.5: Difference of fractions (Compare the seasonal average of GV/NPV/BS composition for California between 2001 and 2015. Seasonal average was calculated based on the selected DOY (winter: DJF, spring: MAM, summer: JJA, fall: SON). December data for winter average calculation are from the previous year (e.g. in the calculation for winter average 2001, MODIS NBAR products of December 2000 are also used).

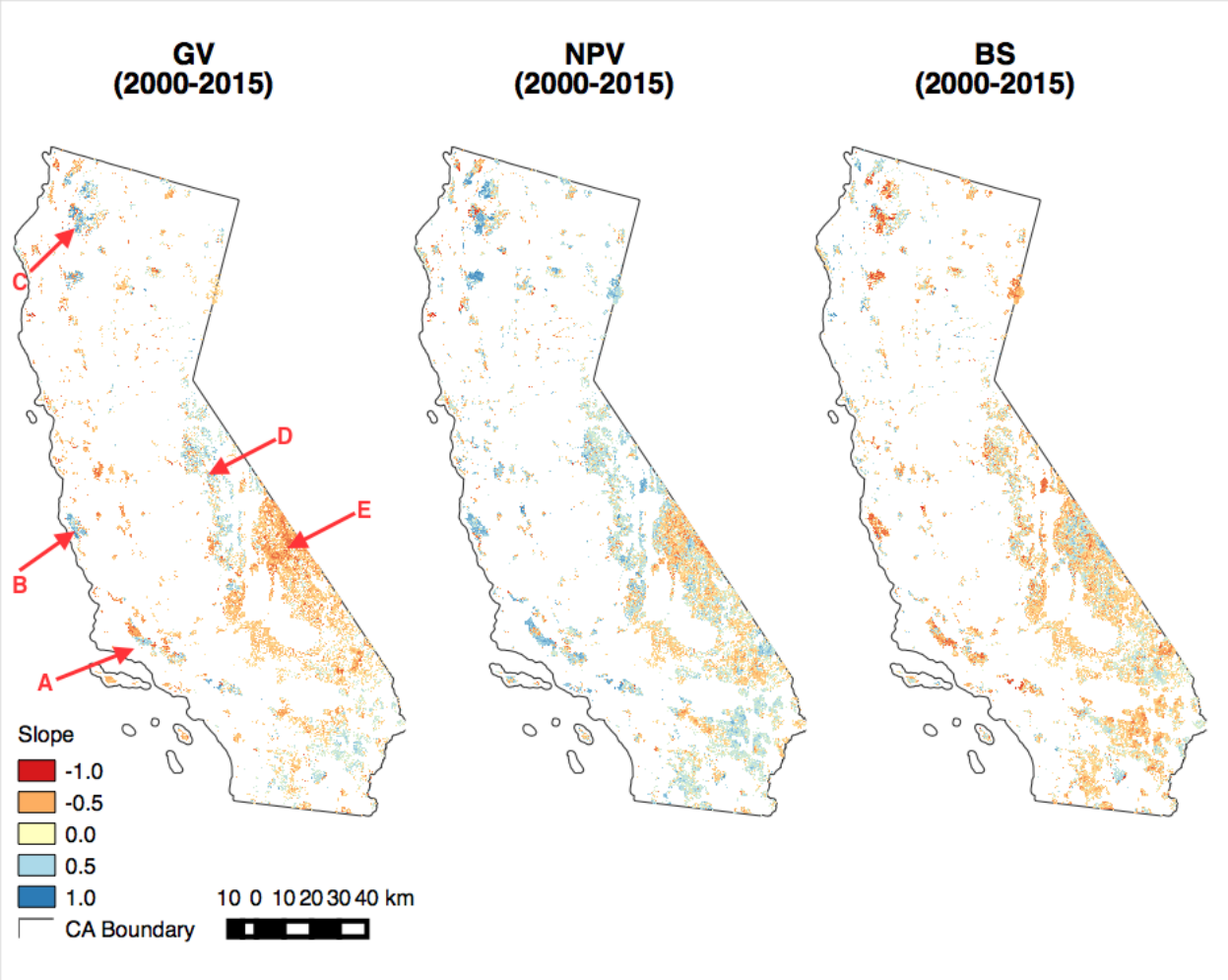

Figure 3.6: Difference of fractions (Significant linear fit for three MESMA time series from 2000 to 2015 ($p < 0.0001$). Cell size equals to 500 m and PAs with an area less than one pixel are dropped out. Deeper blue (red) indicates greater magnitude of increase (decrease) in the linear fit models.

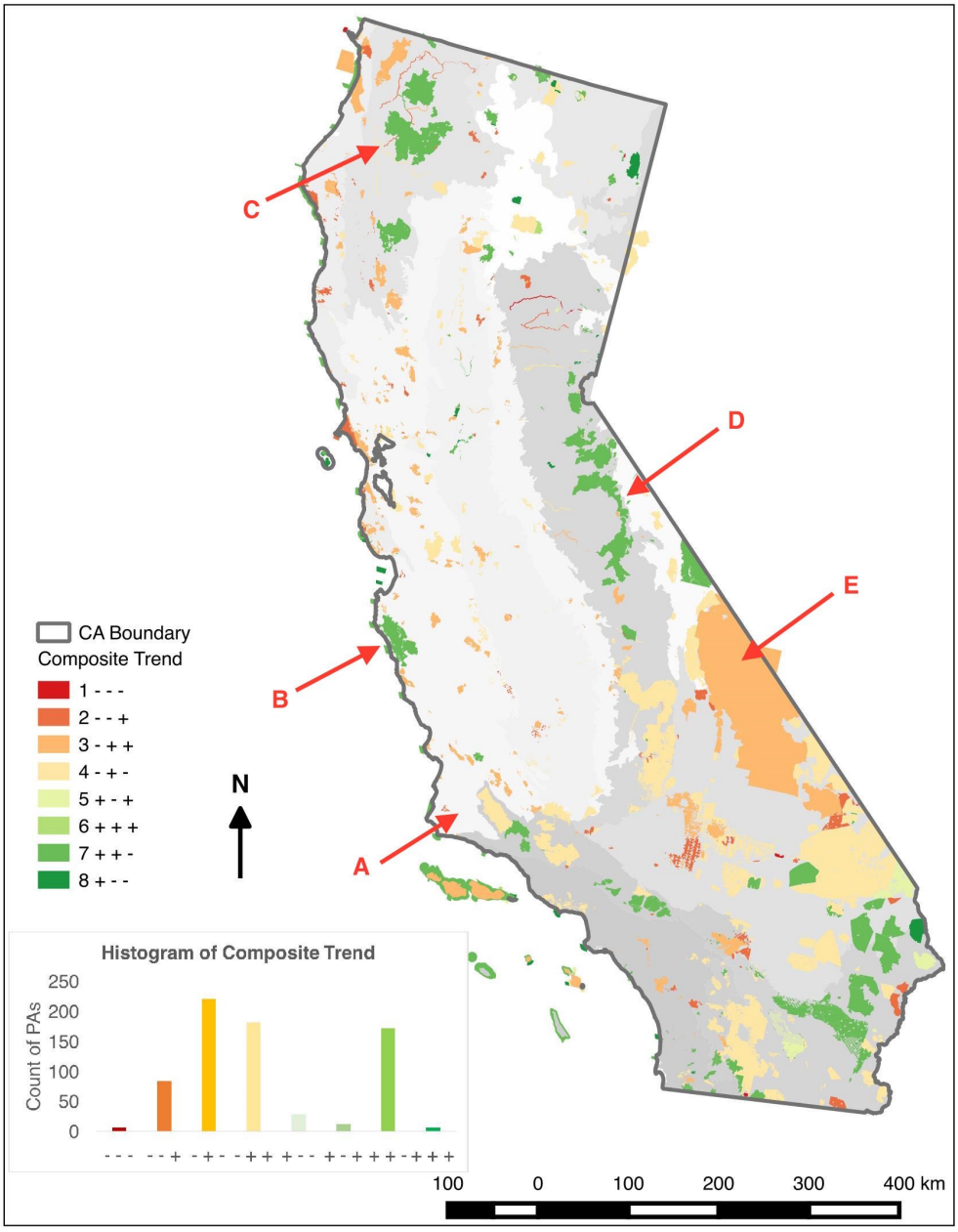

Figure 3.7: Difference of fractions (Composite trend of change for PAs. Positive and negative signs indicate the sign of the average slope in PAs. Sign reads in the order of GV, NPV, and BS. For example, "- + +" means decreased GV, increased NPV and BS. The histogram of composite trend is also included. The shading of PAs indicates the moisture condition from dry (red) to wet (green). Level III ecoregions are colored in grey scale as the background.

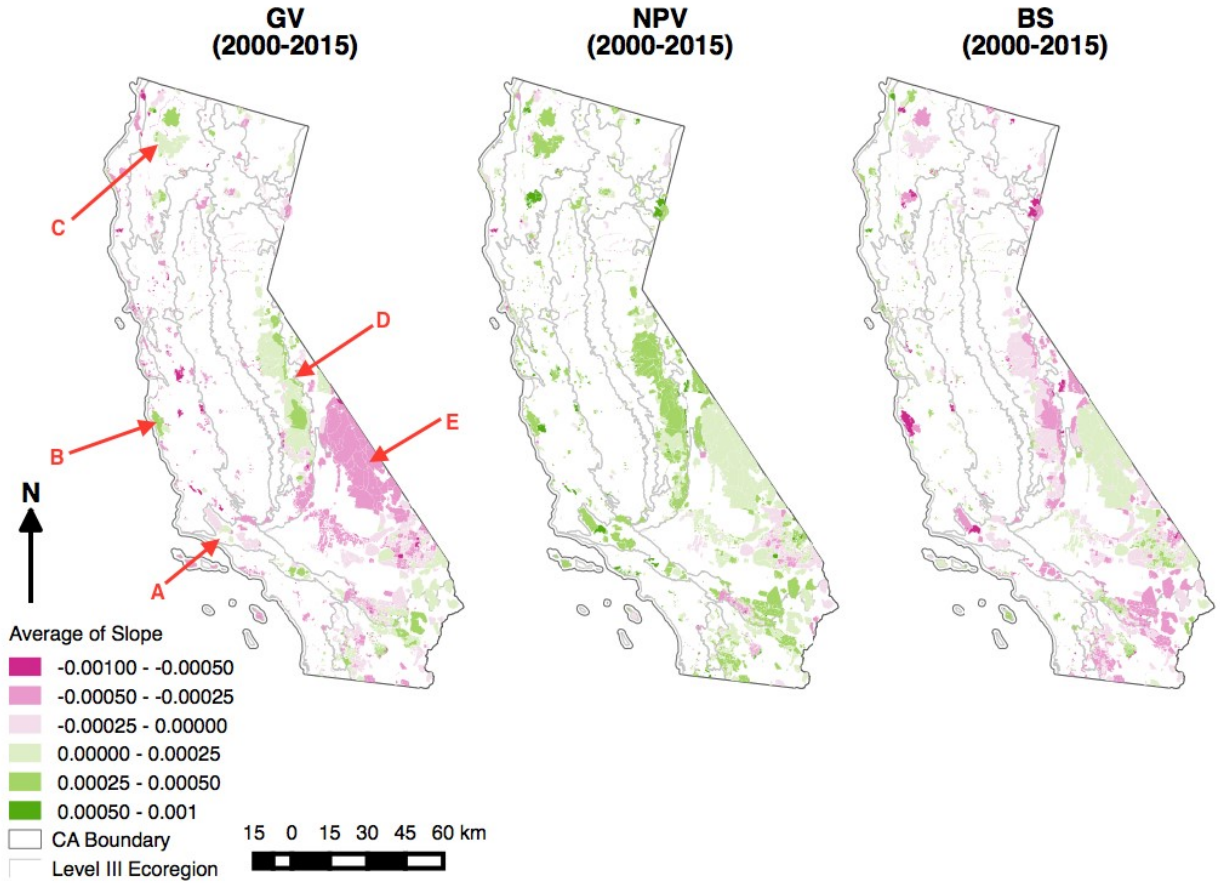

Figure 3.8: Difference of fractions (Average of slope inside each PA. The slope is calculated from the linear fit of MESMA time series at each pixel inside PA. The average is shaded using a red to green color ramp, with red as the negative and green as the positive slope.

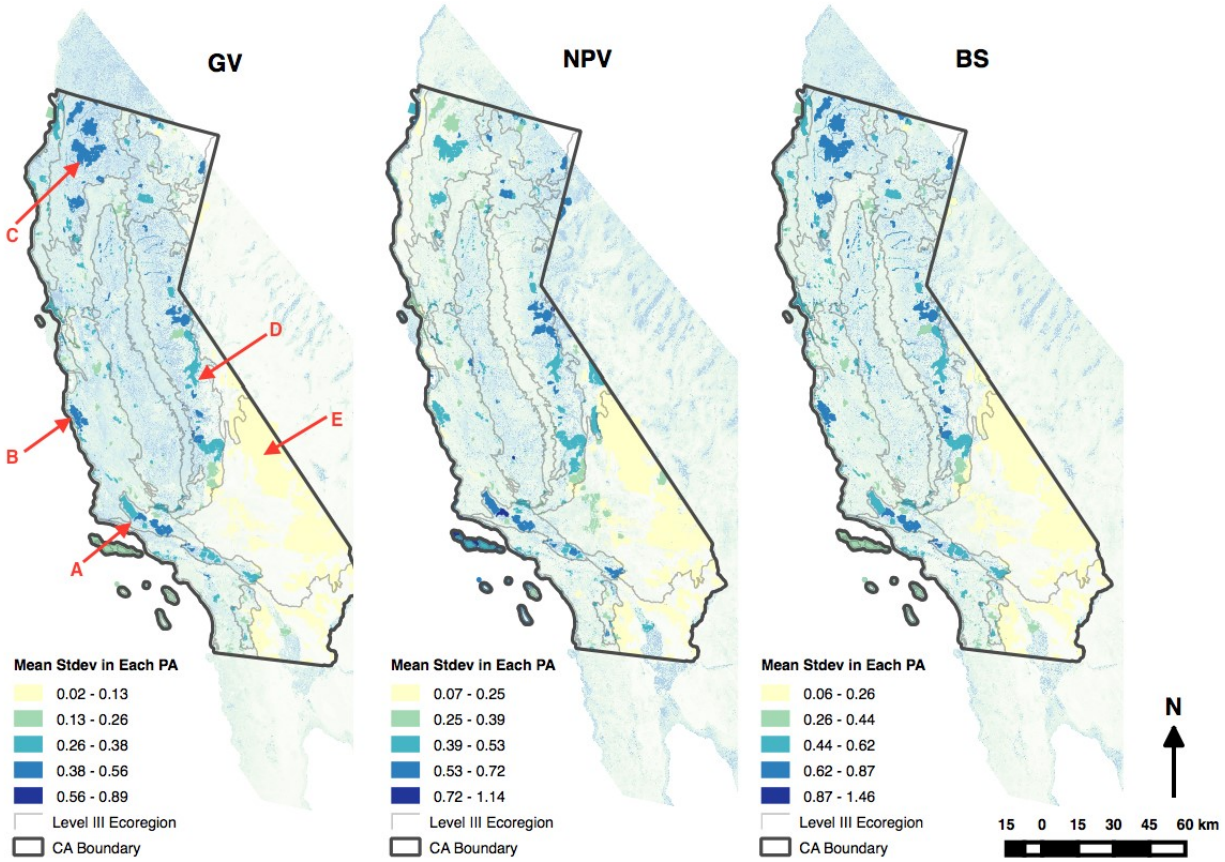

Figure 3.9: Standard deviation of time series (2000 to 2015) at each pixel for GV, NPV, and BS. Note that the three images are in different value ranges. The brigher layer is the subset for PAs. In each PA, the average of standard deviation is mapped. the lighter layer in the back is the standard deviation of the entire study area.

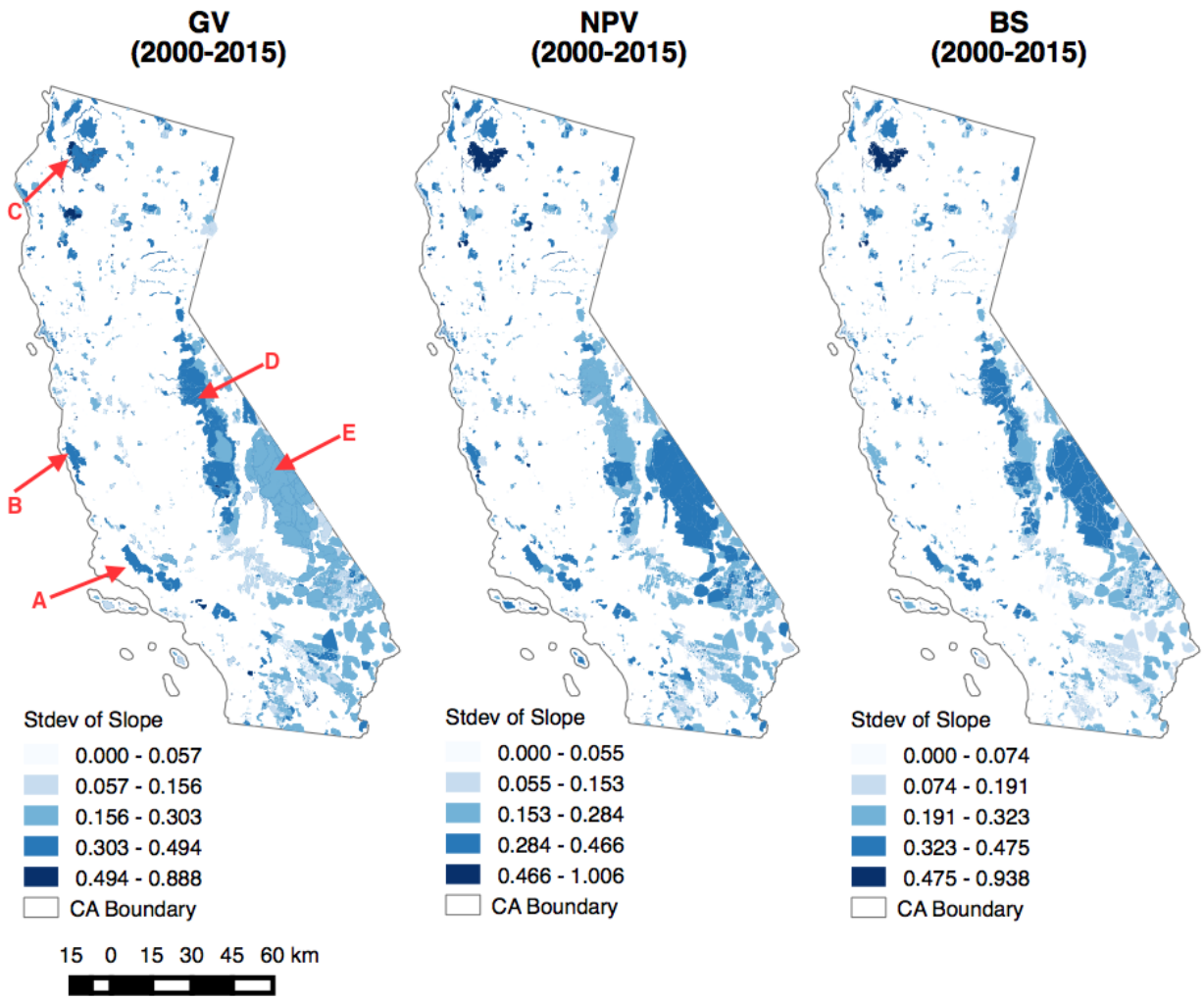

Figure 3.10: Standard deviation (Stdev) of slope inside each PA. Note that the value ranges of each class in the legend for three land cover components are slightly different.

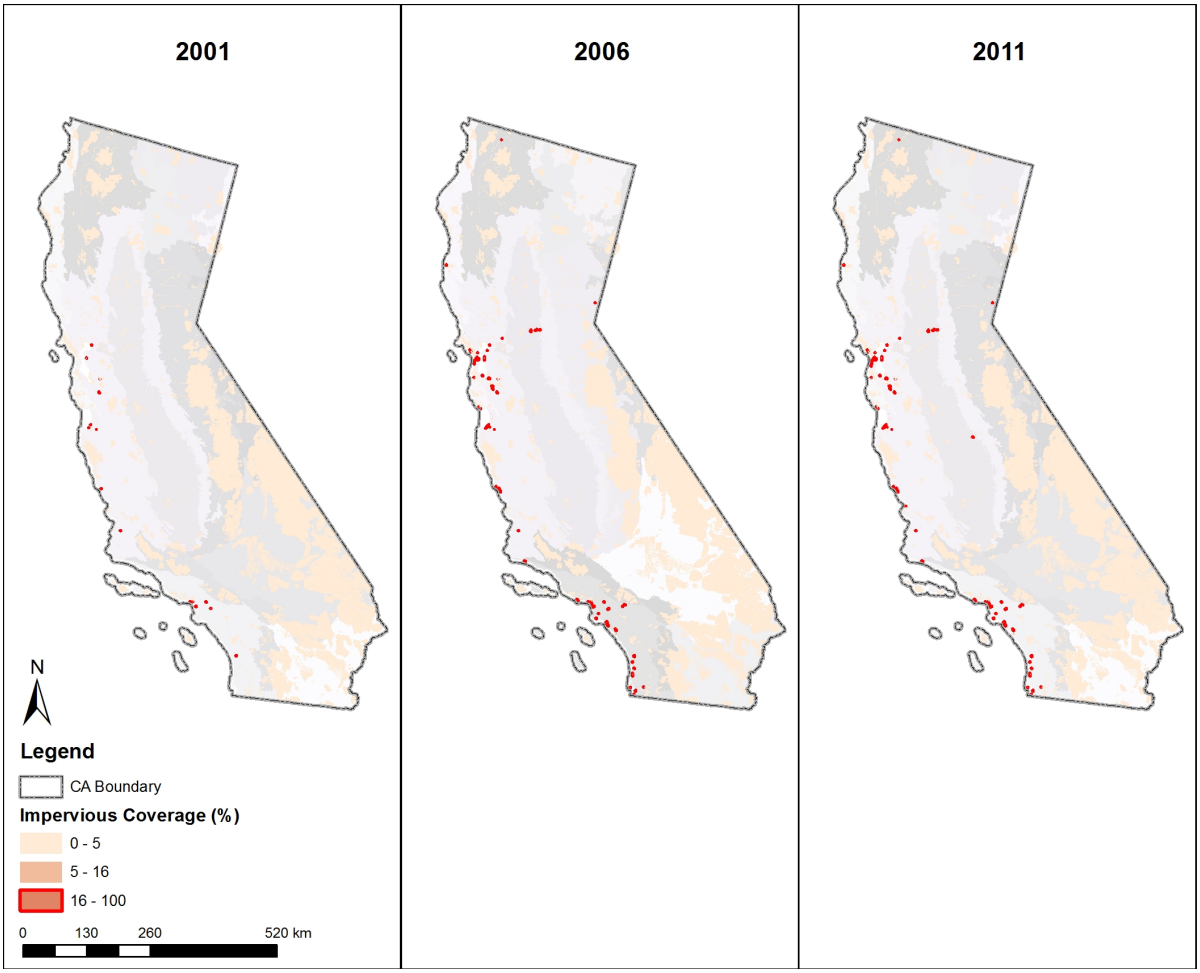

Figure 3.11: Proportion of impervious surface inside PAs of California from NLCD imperviousness map (2001, 2006, 2011). Pixels with imperviousness $>$ 16% are highlighted in red.

Table 3.6: Top twenty PAs with largest standard deviation (stdev) in MESMA time series. Bold and italic areas are above 20 km^2

Name	WDPA ID	Type	Area (sq km)	Average Stdev	IUCN Catgory	Government Management Type	Management Authority
Caples Lake	11115764	Water District Lands	2.0658	0.5176	V	Sub-national ministry or agency	Regional Agency Land
Shiells	11116294	Nature Conservancy	0.5086	0.4850	V	Non-profit organisations	The Nature Conservancy
Big Sycamore Canyon	312357	State Marine Reserve	5.7372	0.4834	V	Sub-national ministry or agency	California Department of Fish
Clear Creek / Sacramento	11115024	Area Of Critical Environmental	0.3636	0.4786	V	Federal or national ministry or agency	Bureau of Land Management
Bell Meadow	11115207	Research Natural Area	2.5902	0.4502	Ia	Federal or national ministry or agency	Forest Service
Devils Postpile	22507	National Monument	3.2362	0.4404	V	Federal or national ministry or agency	National Park Service
Chorro Creek	11115509	Ecological Reserve	2.3594	0.4389	V	Sub-national ministry or agency	State Fish and Wildlife
Point St. George Reef	555586862	State Marine Conservation	***24.6652***	0.4321	V	Sub-national ministry or agency	California Department of Fish
Babbitt Peak	11115205	Research Natural Area	5.7169	0.4234	Ia	Federal or national ministry or agency	Forest Service
Long Point (Catalina	555586849	State Marine Reserve	4.2993	0.4036	V	Sub-national ministry or agency	California Department of Fish
Abalone Cove	555586843	State Marine Conservation	12.3857	0.4028	V	Sub-national ministry or agency	California Department of Fish
Lexington Reservoir	11115800	Water District Lands	3.1797	0.3972	V	Sub-national ministry or agency	Regional Agency Land
Scorpion (Santa Cruz	352749	State Marine Reserve	***24.8629***	0.3855	V	Sub-national ministry or agency	California Department of Fish
Patrick's Point	372971	State Park	2.7786	0.3849	V	Sub-national ministry or agency	State Park & Recreation
Palo Verde	11115540	Ecological Reserve	5.1559	0.3830	V	Sub-national ministry or agency	State Fish and Wildlife
Red Lake	373699	Wildlife Area	3.1594	0.3819	IV	Sub-national ministry or agency	State Fish and Wildlife
Point Vicente	555586842	State Marine Conservation	***38.9395***	0.3799	V	Sub-national ministry or agency	California Department of Fish
Drakes Estero	555586732	State Marine Conservation	6.5994	0.3794	V	Sub-national ministry or agency	California Department of Fish
Long Canyon	11115232	Research Natural Area	8.6271	0.3748	Ia	Federal or national ministry or agency	Forest Service
Jenson River Ranch	11116037	Local Land Trust Preserve	0.7657	0.3621	V	Non-profit organisations	Land Trust

Table 3.7: Top twenty PAs with the largest standard deviation (stdev) of slope inside the boundary. This result indicates the spatial heteogeniety inside PAs. Bold and italic areas are above $20km^2$

Name	WDPA ID	Type	Area (sq km)	Average Stdev	IUCN Catgory	Management Authority
Mendocino Headlands	1111699	State Park	***33.1492***	0.5513	II	State Park & Recreation
Big River Salmon Creek	11115930	Local Land Trust Preserve	***66.7984***	0.5297	V	Land Trust
Headwaters Forest	11115174	Ecological Reserve	1.4465	0.5290	III	Bureau of Land Management
Mill Creek	11115072	Area Of Critical Environmental	***100.3497***	0.4844	V	Bureau of Land Management
New River	11115267	Wild and Scenic River	17.1962	0.4720	V	Forest Service
Smith River	11115278	Wild and Scenic River	5.7716	0.4706	V	Forest Service / State Park &
Sanhedrin	11115315	Wilderness Area	***42.2829***	0.4569	Ib	Forest Service
Elkhorn Slough	368262	National Estuarine	15.7990	0.4558	V	California Department of
Jenson River Ranch	11116037	Local Land Trust Preserve	0.7657	0.4515	V	Land Trust
Owl Creek	11115539	Ecological Reserve	11.2185	0.4432	V	State Fish and Wildlife
Double Point	312093	ASBS State Water Quality	0.3619	0.4195	V	California State Water Resources
Del Mar Landing	312172	State Marine Reserve	0.5544	0.4185	V	California Department of
Lacks Creek	11115063	Area Of Critical Environmental	***27.1550***	0.4149	V	Bureau of Land Management
Yorkville	11115572	Ecological Reserve	0.9167	0.4144	V	State Fish and Wildlife
Agua Tibia	365126	Research Natural Area	***72.7561***	0.3970	Ia	Forest Service
Tolowa Dunes	11115447	State Park	16.1634	0.3956	V	State Park & Recreation
Ione Tertiary Oxisol Soil	11115052	Area Of Critical Environmental	0.3057	0.3892	V	Bureau of Land Management
Limestone Salamander	370956	Ecological Reserve	3.2879	0.3870	V	State Fish and Wildlife
Trinidad Head	312099	ASBS State Water Quality	1.2012	0.3845	V	California State Water Resources
Oroville	372775	Wildlife Area	***47.5015***	0.3827	IV	State Fish and Wildlife / Other

CHAPTER 4

Change in Fire Regime and the Phenological Response in Protected Areas of California

4.1 Introduction

Wildfire is an important ecological factor in Mediterranean ecosystem as it completely or partly removes the aboveground biomass and influences the post-fire nutrient cycling and vegetation composition [Pausas, 2004, Kutiel and Inbar, 1993, Sugihara, 2006]. Previous studies have recognized the wildfire as both an important factor of increase degradation processes and a stimulus of the new cycle of vegetation maturing and densifying [Fox et al., 2008, Capitanio and Carcaillet, 2008]. Thus understanding the fire regime and assessing the post-fire influence on local landscape and the ecosystem is of great significance to interpret how wildfire shapes the Mediterranean landscape. As one of the five Mediterranean ecosystems in the world, the wide spread of fire-prone evergreen forest and shrubland, especially the chaparral makes California an area under a high threat of fire, the large and high-intensity crown fires in particular[Keeley et al., 2008, California Fire Resource Assessment Program, 2003]. Most of the fire-prone areas are inside the protected areas (PAs), where human activity is restricted and the accumulation of fire fuel is generally high [IUCN and UNEP-WCMC, 2015]. In these areas for protecting and restoring natural wilderness, strict and effective fire suppression practices have been applied over decades [Syphard et al., 2007], which has densified the vegetation and increased the chance of getting ignited. Associated with a fire-favoring climate regime, there is a need to investigate the recent change in fire regime and assessed its possible influence on post-fire succession and recovery of the local landscape. PA man-

agement authorities would find this information helpful for the development of future land management strategies, especially on fire suppression and application of prescribed fires. Furthermore, the adjacency from fire-prone areas to major metropolitans makes this kind of study crucial for policy makers to assess the influence and the risk of wild fires.

Recent studies of fire, especially the post-fire response from vegetation usually involve remote sensing techniques at different scales [Moritz et al., 2014, Henry et al., 2005, Hope et al., 2007]. Remote sensing products tailored to address the occurrence, perimeter, and intensity of fire have become available at different spatial scales. The most widely used fire products from remotely sensed imagery include MODIS active fire products (MOD/MCD/MYD14) at the resolution of 250 m, 500 m or 1 km [Giglio, 2010] and the USGS Monitoring Trends in Burn Severity (MTBS) collection for United States territory at the resolution of 30 m, derived from Landsat TM and ETM+ [Eidenshink et al., 2007, Veraverbeke et al., 2011]. There are multiple measurements of fire intensity based on remote sensing images, for example, radiative energy and burn severity. Directly calculated the from infared and shortwave infared reflectance, the normalized burn ratio (NBR) and the differenced NBR between the pre and post-fire images has been widely applied to studies of fire burned in different landscapes, especially analysis focusing on selected major fires [Miller et al., 2009]. The above fire-focused remote sensing data are usually combined with measurement of vegetation coverage (e.g.NDVI) to assess the post-fire influence on landscape and ecosystem at different scales [Harris et al., 2011]. In studies focused on extracting burned areas, the pre and post-fire NDVI is also employed as a measurement for validation [Leon et al., 2012]. Although NDVI is effective in recording the pre and post-fire difference of vegetation coverage as well as the rate of recovery, it does not provide direct measurement on the response in terms of phenology and vegetation composition. Investigating pheno-metrics can provide a more comprehensive understanding of post-fire influence and the response of ecosystem, e.g. start and peak of the growing season, minimum and peak of NDVI. In addition, it also helps to evaluate the long-term influence of fires, especially on the phenological cycle.

Combining the historical record, field observation, and remote sensing techniques, there

have been a number of studies focusing on explaining the post-fire behavior of vegetation from different aspects in California, especially the shrubland. Seasonality, land cover type, and intensity of fire are three basic physical factors that influence the extent of destroy on biomass, the rate and the pattern of post-fire recovery[Keeley, 2002, Carle, 2015a]. A number of studies of several major fires burned in Californian chaparral revealed that the heavily burned area of shrubland usually experiences a short-term increase of vegetation from the exotic grass introduced to the non-vegetated burned area before the re-establishment and regrowth of native shrubs, which usually happens after three to four years of fire[Keeley et al., 2008]. In contrast, the less heavily burned area may have the short-term peak of vegetation growth missing, because of the less intensive removal of standing shrubs, which usually recover within a shorter time period without creating room for invasion of exotic species. In evergreen forest community, the effective removal of leaves by crown fires reduces canopy closure, creates un-vegetated gap, and fertilizes the growth of understory exotic species through the returning of sequestrated nutrition [Stevens et al., 2015]. Other frequently investigated environmental factors include age of fuels and climate regime. Studies have shown that in California shrublandin shrubland of California, the age dependency of fire is not strong [Moritz et al., 2004, Moritz, 2003], while the forest community has an opposite pattern [Odion et al., 2004]. For the climate regime, several recent long-term simulations of fire occurrence in the western U.S. cooperating the climate modeling have found that the recent drying trend in climate may not play an important role as expected (Baker 2015, Baker 2013, Parks et al. 2016), but this conclusion is highly dependent on location of study site [Pausas and Fernandez-Munoz, 2012, Pausas and Keeley, 2014]. It is necessary to extend the investigation of the basic environmental factors shaping the fire regime and the post-fire influence to a broader spatial extent and on various land cover types to obtain a more solid validation of available knowledge from fire ecology.

In this study, we utilized the remote sensing techniques to understand the recent change in fire regime of California and interpret the post-fire vegetation response of fires burned at different intensity, during different seasons, and on different land cover types in California

PAs. There are three major objectives in this study. First, we identified the change in fire regime from 2000 to 2013 in all California PAs and interpret the change based on the knowledge of fire ecology and recent change in environmental factors. Second, we examined the influence on local landscape and phenology of fire from two different aspects. We evaluated the sensitivity of time for response for the biggest twenty-three fires occurred in California from 2000 to 2013. We also quantified the correlation between the response of the post-fire growing season on the basis of time and magnitude of vegetation growth, including the delaying/advancing of key time points of growing season, the length of growing season, and the change of NDVI. Third, we investigated the supporting evidence from remote sensing fire products to the hypothesis on the post-fire recovery pattern of shrubland in California based on case study [Keeley et al., 2008].

4.2 Data and Methods

4.2.1 Fire occurrence and burn severity data

We used fire occurrence, perimeter, and burn severity data from the Monitoring Trends in Burn Severity (MTBS) project (www.mtbs.gov) by USGS and USDA Forest Service. This six-year project has mapped historical fire occurrence locations, perimeter of fire, and burn severity based on differenced Normalized Burn Ration (dNBR) for the entire U.S. territory from 1984 to 2014 (partly) at the 30-meter resolution [Eidenshink et al., 2007]. The Normalized Burn Ratio (NBR) is calculated for each fire from Landsat TM or ETM+ bands 4 (near infared) and 7 (shortwave infared) to enhance the spectral response of fire-affected vegetation [Key and Benson, 1999, Lozano et al., 2007]. The differenced NBR images (dNBR, post-fire NBR subtracted from pre-fire NBR) are referred to as dNBR images. These images were classified and partitioned into six severity classes based on ecological severity thresholding developed from the field validated Composite Burn Index (CBI): 1) Unburned to low severity, 2) low severity, 3) moderate severity, 4) high severity, 5) increased greenness, 6) non-mapping area including major water body and clouds [Eidenshink et al., 2007]. The

increased greenness of the burn severity class means that newly grown vegetation is detected from the post-fire Landsat imagery, usually a sign of immediate recovery for area with a relatively high burn severity. The above thematic classes were included for each fire in the dataset. We used the fire occurrence locations from 2000 to 2013 in California PAs and the above thematic classes to develop a descriptive analysis of the fire regime.

In addition to the thematic classes, dNBR and its Relative version (RdNBR) of each fire can provide quantitative analysis of the relationship between burn severity and the post-fire response of local vegetation. However, a number of validating studies of dNBR and RdNBR focusing on different ecosystems have demonstrated its uncertainty on measuring burn severity [Zhu et al., 2006, Lozano et al., 2007, Miller et al., 2009], which should be considered in the application and the discussion of results.

4.2.2 Measurement of Phenology

We used NDVI and some of its mathematical derivatives to analyze the post-fire vegetation behaviors. NDVI is a standardized and well validated measurement of the vegetation coverage because of its effectiveness in detecting the intensity of photosynthetic activity. It has been widely used to calculate various pheno-metrics and perform time series analysis to detect the trend and seasonality of vegetation. A key requirement of the above calculation is that the NDVI time series are gap-free and continuous. In this study, we used the smoothed and gap-filled MODIS NDVI data produced from the MODIS Terra satellite (MODIS MOD13Q1) and Aqua satellite (MODIS MYD13Q1) by the Oak Ridge National Laboratory in our analysis on pre- and post-fire comparison and post-fire response detection, including identifying the major breakpoints of NDVI and the pre- and post-breakpoint linear trend (Spruce, Gasser and Hargrove 2015). The dataset covers the time period from 2001-01-01 through 2013-12-31 at an 8-day interval, with a spatial resolution of 250 m.

In addition to NDVI, we also incorporated a series of pheno-metrics from the eMODIS Remote Sensing Phenology data collection produced by USGS Earth Resources Obser-

Table 4.1: Pheno-metrics from USGS eMODIS program and the phenological interpretation.

Variable	Acronym	Phenological Interpretation	Description
Start of Season, Time	SOST	Beginning of measurable photosynthesis in the vegetation canopy	Day of year identified as having a consistent upward trend in time series NDVI
Start of Season, NDVI	SOSN	Level of photosynthetic activity at the beginning of measurable photosynthesis	NDVI value (or baseline) identified at the day of year identified as a consistent upward trend in time series NDVI
Time of Maximum	MAXT	Time of maximum photosynthesis in the canopy	Day of year corresponding to the maximum NDVI in an annual time series
Maximum NDVI	MAXN	Maximum level of photosynthetic activity in the canopy	Maximum NDVI in an annual time series
Duration	DUR	Length of photosynthetic activity (the growing season)	Number of days from the SOST to the EOST
Amplitude	AMP	Maximum increase in canopy photosynthetic activity above the baseline	Difference between MAXN and SOSN

vation and Science (EROS) Center based on MODIS level-1B products on a yearly basis [Jenkerson et al., 2010]. The pheno-metrics in eMODIS collection were derived from smoothed NDVI, using a curve derivative method, and were validated with the phenological observations from National Phenology Network (NPN) [Meier and Brown, 2014]. Six pheno-metrics, including Start if Season-Time (SOST), Start of Season-NDVI (SOSN), Time of Maximum (MAXT), Maximum NDVI (MAXN), duration (DUR), and amplitude (AMP) were utilized in this study as indicators of post-fire vegetation response (Table 4.1). The key dates of each year (SOST and MAXT) are stored as day of year (DoY). If the key dates of the current vegetation growing cycle occurred before the first day of the calendar year (i.e.in a previous year), the difference between the first day of current calendar year and the actual key dates of current growing cycle were stored with a negative sign, indicating the key dates occurred how many days before the first day of year.

4.2.3 Detecting breakpoints with B-FAST model

As a major disturbance on the local landscape, wild fires usually remove most photosynthetic active parts of vegetation and can be detected from a significant drop within the NDVI time

series. For most PAs in our study, fire is the greatest disturbance on landscape and is expected to be recorded as the major breakpoint in the NDVI time series. Comparing the time of major NDVI drop with the fire occurrence time is helpful to evaluate the sensitivity of response in the local landscape after fire. It is also important to understand how fast the ecosystem bounces back after fire by comparing the magnitude of trend before and after this time point. The biggest challenge to fulfill the above purposes is to obtain the robust major breakpoint for NDVI time series. A time series analysis method was proposed to detect and characterize the breakpoints (Breaks For Additive Seasonal and trend, BFAST) [Verbesselt et al., 2010a, Verbesselt et al., 2010b]. This model first decomposes the time series into trend, seasonal, and remaining components, then iteratively estimates the time and number of changes, finally characterizes change by its magnitude and direction. It can provide designated number of breaks or only the greatest break of the given time series. Without any pre-defined thresholds from a priori knowledge of the study area, the breaks detected by BFAST purely depends on the nature of time series, including the trend and the seasonality. This method has been applied to a number of studies focusing on NDVI time series analysis at different spatial scales [Verbesselt et al., 2010b, Jong et al., 2012]

We applied the BFAST model on the gap-filled and continuous NDVI time series to obtain the major break point, as well as the before and after slope of linear trend from 2000 to 2013. All of them were calculated to measure the time sensitivity of post-fire response. Considering the high computational cost of BFAST model because of the iteration in the algorithm, we applied the method to the biggest twenty-three fires in California PAs from 2000 to 2013. To evaluate the temporal gap between the drop recorded by NDVI and the fire occurrence, we calculated the difference between the fire occurrence date and the major breakpoint date detected by the BFAST model. Such difference was both mapped and plotted in histograms, shaded by different determinants of fire ecology (land cover, year of fire occurrence, and burn severity classes).

4.2.4 Evaluating the Immediate Post-Fire Behaviors of Vegetation

We calculated the difference between the pheno-metrics listed in Table 1 of the following year after fire and the median of the corresponding pheno-metrics from 2000 to 2013 to quantify the post-fire departure from normal for the immediate post-fire growing season, when the influence of fire is usually at its maximum. The departure results were mapped and compared with burn severity to obtain a qualitative understanding of the post-fire vegetation response from the phenological perspective, including the delay/advance of start (peak) of season, the prolonged/shortened length growing season, and the higher/lower NDVI at the start (peak) of season. These results can provide a basis of the following analysis on the correlation between the quantitative measurement of burn severity (dNBR) and the shift of key phenological time points or the change of NDVI. We later used a series of Generalized Additive Models (GAMs) to fit the dNBR and the departure from median calculated above for SOST, MAXT, SOSN, MAXN, DUR, and AMP. In this model, negative dNBR values, which indicate the occurrence of post-fire increased greenness were excluded to keep the surface condition of burned area consistent. The modeling is calculated separately by the land cover type and season of fire occurrence to evaluate if the above two factors can explain the post-fire behavior of vegetation, especially on how much of the anomality of phenology in the immediate post-fire growing season can be explained by different aspects of fire. We also discussed the modeling results, especially the change of model performance by the length of period after fire to see if they provided evidence to support the pattern of post-fire response in shrubland [Keeley et al., 2008].

4.3 Results

4.3.1 Change in Fire regime of California PAs from 2000 to 2013

Wild fires occurred in PAs consist about one fourth of all wild fires in California from 2000 to 2013 (Figure 4.1). The fluctuation of fire occurrence inside PAs was consistent with the

entire California. Following a year with high fire occurrence (1999), fire counts inside PAs started from a relatively low level from the beginning of the century and climbed to a peak in 2006. The year 2007 was a key time point of the count of fire. There is a significantly high number of fires occurred before and after, leaving this year as a valley of fire occurrence. This year also divided the time series into two sections, a more evenly distributed and generally higher fire occurrence pattern from 2000 to 2006, and a relatively more extreme distribution since 2008. Fire occurrence almost peaked in 2008, followed by a great decrease starting from 2010. However, the pattern of fire perimeters was different. The year 2007 had the second largest area burned since 2000, making itself one of the years with greatest fire perimeters in California PAs (Figure 2). Although most years had a proportional total burned area to their fire occurrences, the year 2004 and 2005 both had a disproportionally smaller burned area with a relatively large fire occurrence. Combining both fire occurrence and perimeters, we can find a four-year cycle in the fire regime of California PAs, especially for fires from 2000 to 2007: starting with few fires at the beginning, the occurrence and perimeters both climbed to a peak after about four years from the previous peak, followed by a new cycle with a small fire occurrence and perimeter again.

Although most fires burned during summer (JJA) and fall (SON) (Figure 4.1-4.2), the spatial distribution of dominant burning season is different before and after 2007. More fires occurred in southern California shrubland with a great burned area from 2000 to 2007 during the fall season, while fires in evergreen forest were generally burned during the summer (Figure 4.3-4.4). However, since 2008, fires burned during the fall in southern California shrubland almost disappeared, with a significant drop in burned area as well. In contrast, there was an increase of fire occurrence in spring (MAM) in northern California evergreen forest (mostly during 2013). The same pattern since 2008 was also found in the perimeter of fires.

The burn intensity of fires inside California PAs also differs by the time of fire occurrence and land cover types. Among all five severity classes, unburned to low severity occupied a much greater burned area in the early fire season from May to June (Figure 4.5). As

the fire season continued, burned area at moderate and high severity grew and peaked in August. Areas burned during the peak of fire season were also where most post-fire increased greenness occurred. Comparing the two major land cover types in burned area, shrubland had a much higher moderate severity of burn, while evergreen forest had greater area burned at the high severity (Figure 4.6).

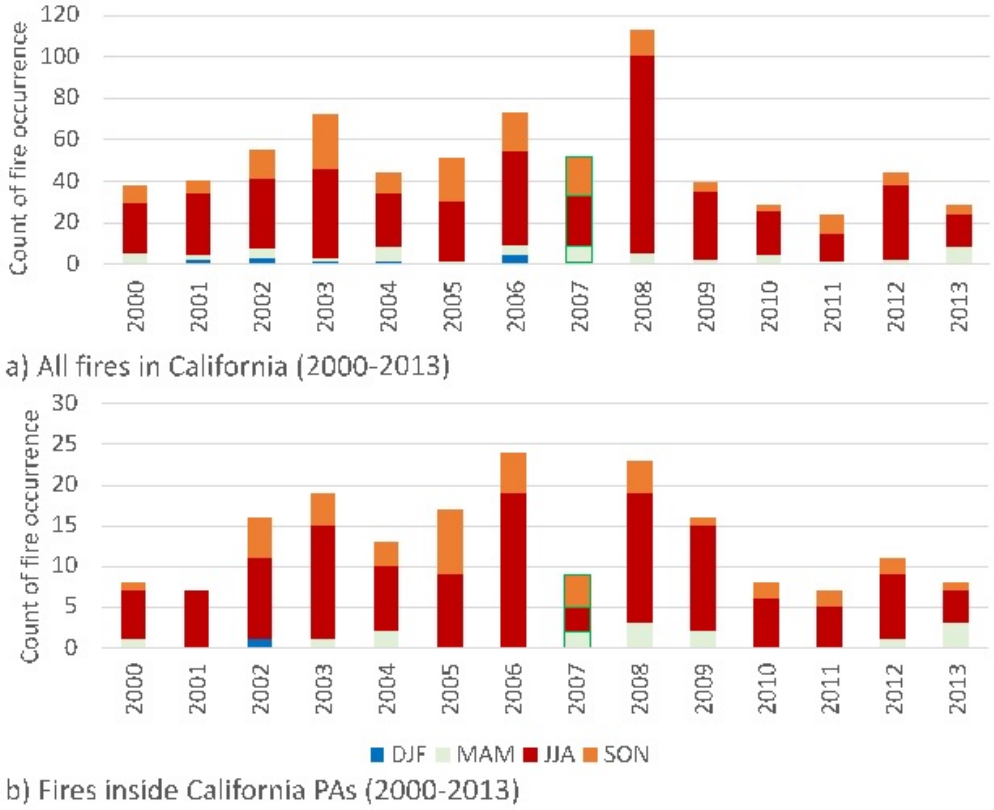

Figure 4.1: Frequency of fire occurrence in California and only PAs of California from 1999 to 2013. Note that the two plots have different value ranges. Bar of the year 2007 is highlighted with green outline.

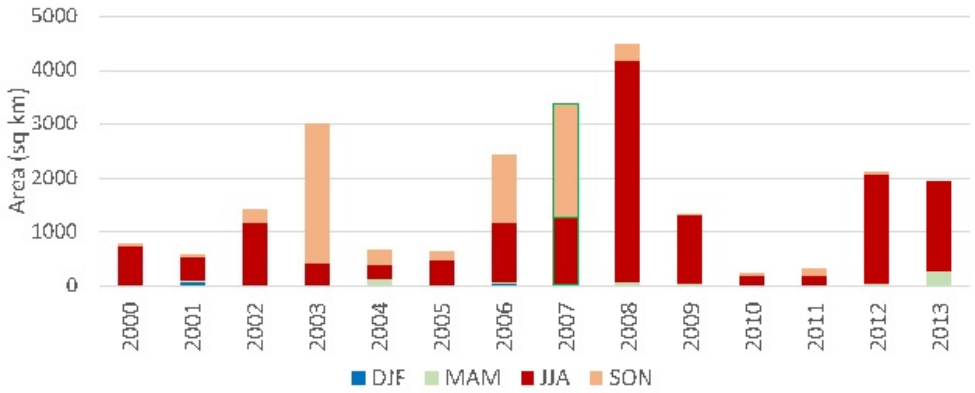

Figure 4.2: Total area of fire in California PAs from 2000 to 2013, shaded by month of occurrence. Months are grouped by season (winter, DJF; spring, MAM; summer, JJA; fall, SON). Bar of the year 2007 is highlighted with green outline.

4.3.2 Post-fire Vegetation Response

4.3.2.1 Fire as the Major breakpoint in NDVI

The difference between fire occurrence and the major break detected by B-FAST on the biggest twenty-three fires indicates that most fires were effectively recorded by NDVI time series, with a discrepancy from the actual fire occurrence date between 0 and 60 days, i.e. four NDVI data points (Figure 4.7a). And these areas consisted the majority of all areas analyzed with B-FAST model (Figure 4.8). Such discrepancy ranged from 0 to 15 days in most California shrubland, indicating almost no offset between the major breakpoint from BFAST and the fire occurrence date. The offset in evergreen forest was slightly larger, with more areas ranging between 15 and 30 days (Figure 4.7a and 4.8a). Almost all fires burned in fall were marked as the major break in NDVI within 30 days after fire, while the summer burned areas had a greater range in the discrepancy (Figure 4.8b). Areas with high and moderate burn severity also had a relatively smaller offset between the major NDVI breakpoint and the fire occurrence date (Figure 4.7c). However, two major outliers were detected. The occurrence of Rush fire (2012 August) and Rim fire (2013 August) were not detected as the major breakpoint in the NDVI time series from 2000 to 2013, with the major

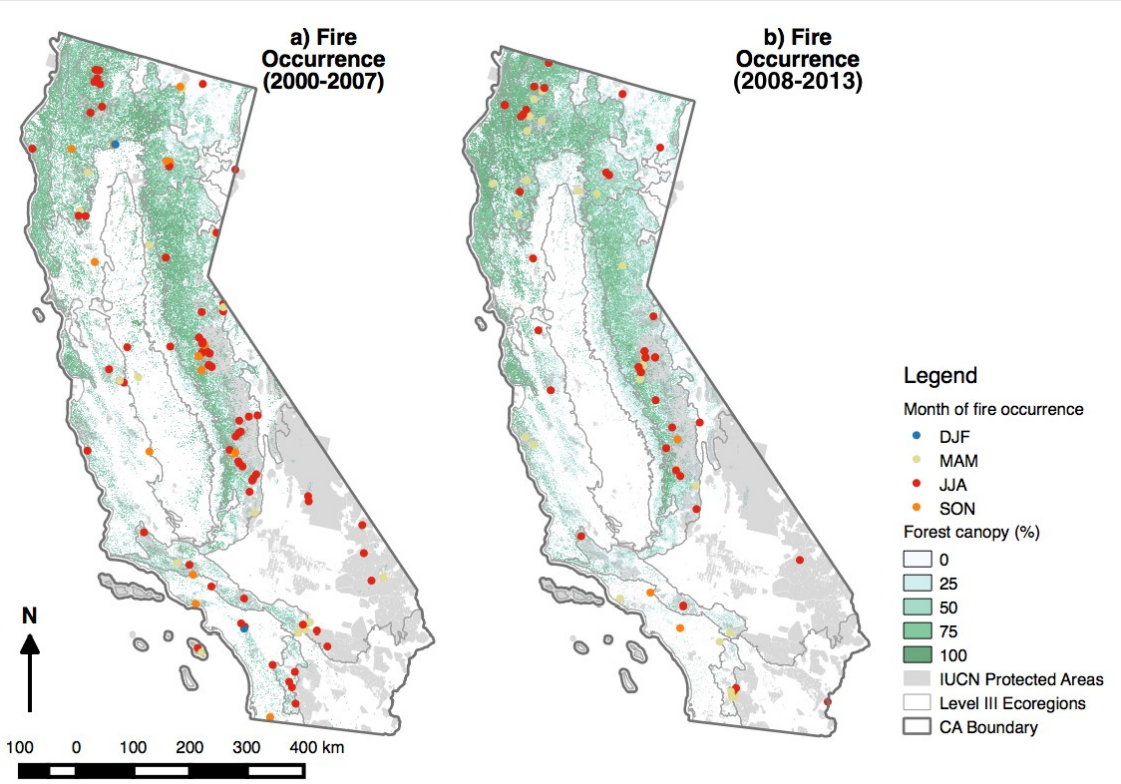

Figure 4.3: Fire occurrence in PAs of California from 2000 to 2013, shaded by month of occurrence. Months are grouped by season (winter, DJF; spring, MAM; summer, JJA; fall, SON). Fires before and after 2008 are mapped separately. NLCD forest canopy coverage in percentage is added as the background (2001 forest canopy for Panel a and 2011 forest canopy for Panel b).

breakpoint detected a long period before the fire occurrence date (Figure 4.7a).

4.3.2.2 Post-fire phenological influence

Comparing the slope of the linear fit between pre/post-fire NDVI sections detected by B-FAST with time, we found that there was a downward trend in the pre-fire NDVI time series, while the post-fire NDVI bounced back with an upward trend. Areas with both pre- and post-fire NDVI increased were also detected (Figure 4.8b). For the post-fire NDVI, areas

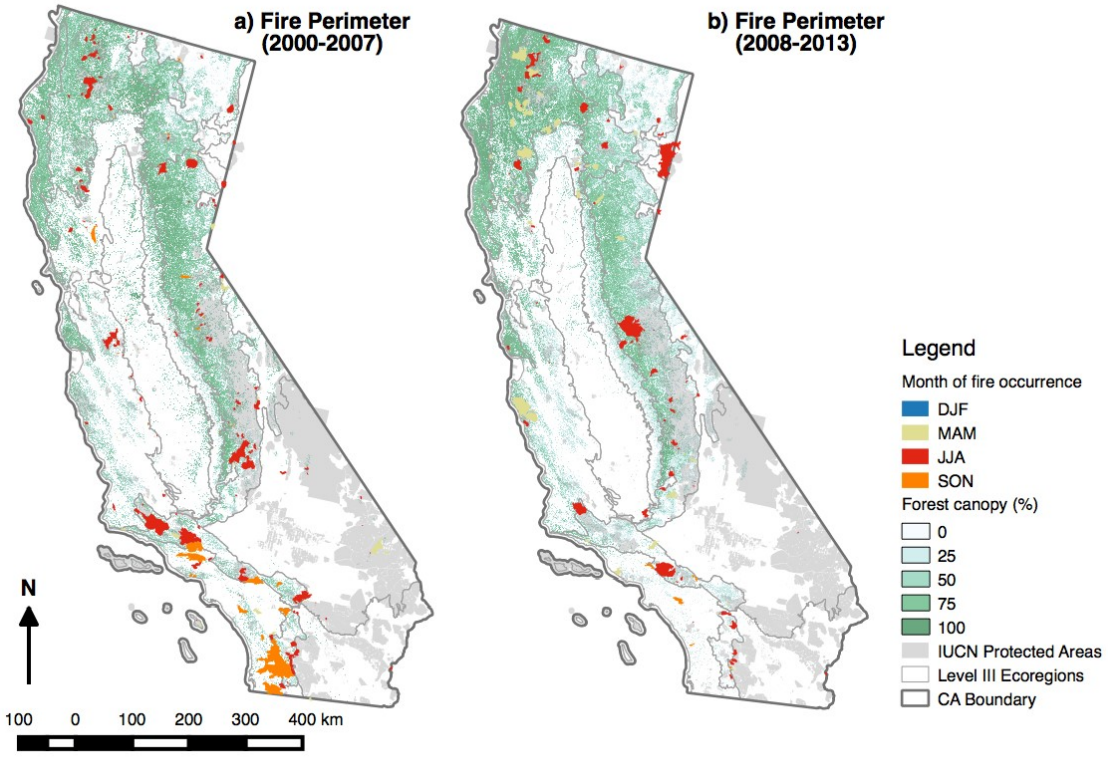

Figure 4.4: Perimeter of fire occurred in California PAs from 2000 to 2013, shaded by month of occurrence. Months are grouped by season (winter, DJF; spring, MAM; summer, JJA; fall, SON). Fires before and after 2008 are mapped separately. NLCD forest canopy coverage in percentage is added as the background (2001 forest canopy for Panel a and 2011 forest canopy for Panel b).

burned at a high severity all had an increasing trend, which set a basis of quantifying the relationship between the burn severity and post-fire response.

Land cover type was a major factor that differentiated the start, peak, and length of immediate post-fire growing season. More burned areas had a later than usual SOST regardless of land cover type (Figure 4.9a and 4.10a). Shrubland and evergreen forest both had majority of areas with positive difference from median during the fire prevailing period of each (2000-2007: shrubland, 2008-2013, evergreen forest), indicating a delayed SOST. The

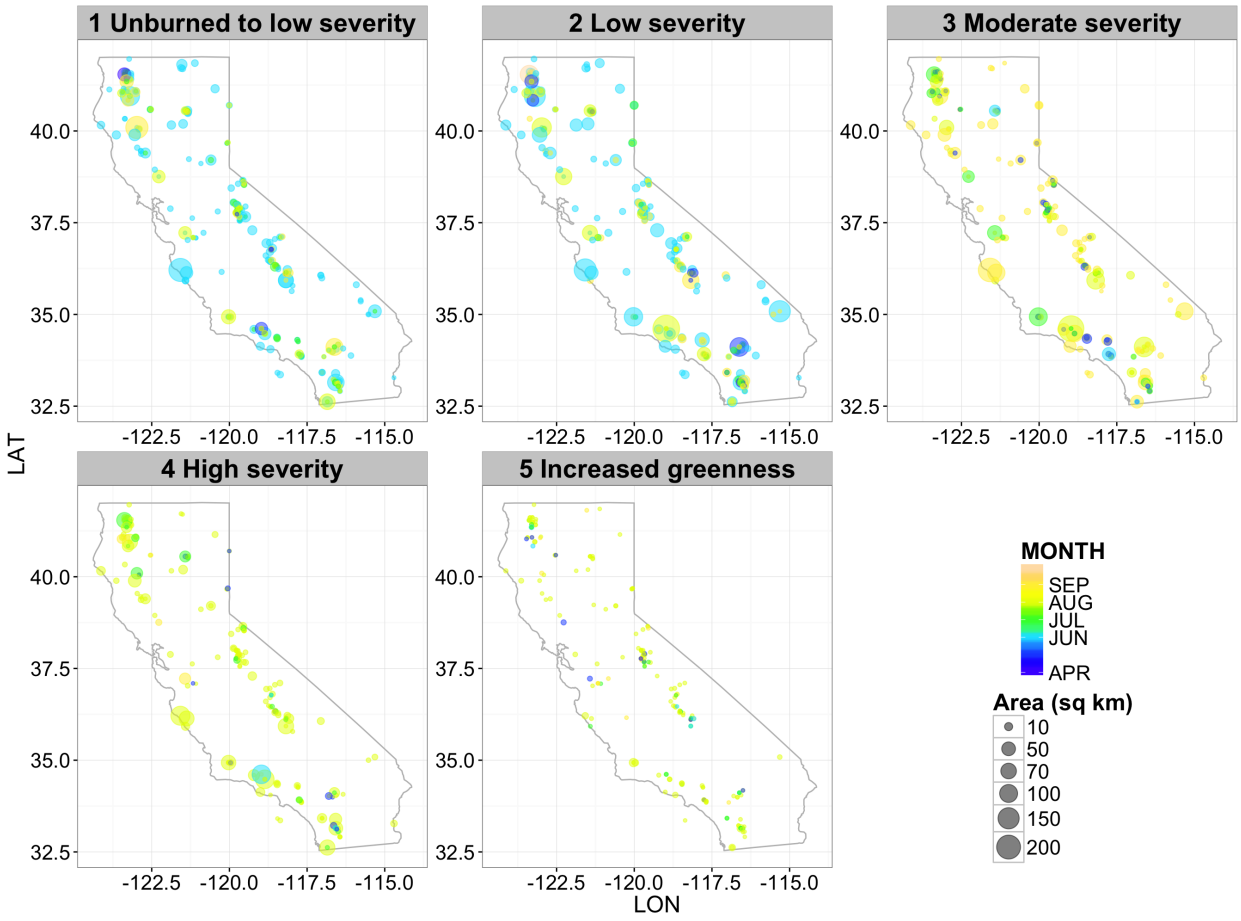

Figure 4.5: Burn severity of fires inside California PAs from 2000 to 2013. Fire occurrence are mapped by the size of area at each burn severity class, colored by the month of fire occurrence.

southern California shrubland also had a more consistent pattern of delay (between 15 and 90 days) than evergreen forest, with most areas with a similar color in Figure 4.9a. However, there was a peak of earlier than usual SOST in burned area of shrubland after 2008, which reflects changes in post-fire behavior after 2008. The departure from usual in MAXT was not as great as SOST, with a large proportion of burned area having a zero to fifteen-day discrepancy compared with median (Figure 4.9b and 4.10b). For the difference between land cover types, the shrubland had an earlier than usual MAXT than evergreen forest, mostly because of the advanced peak of season in the perimeter of the Cedear Fire. Excluding these

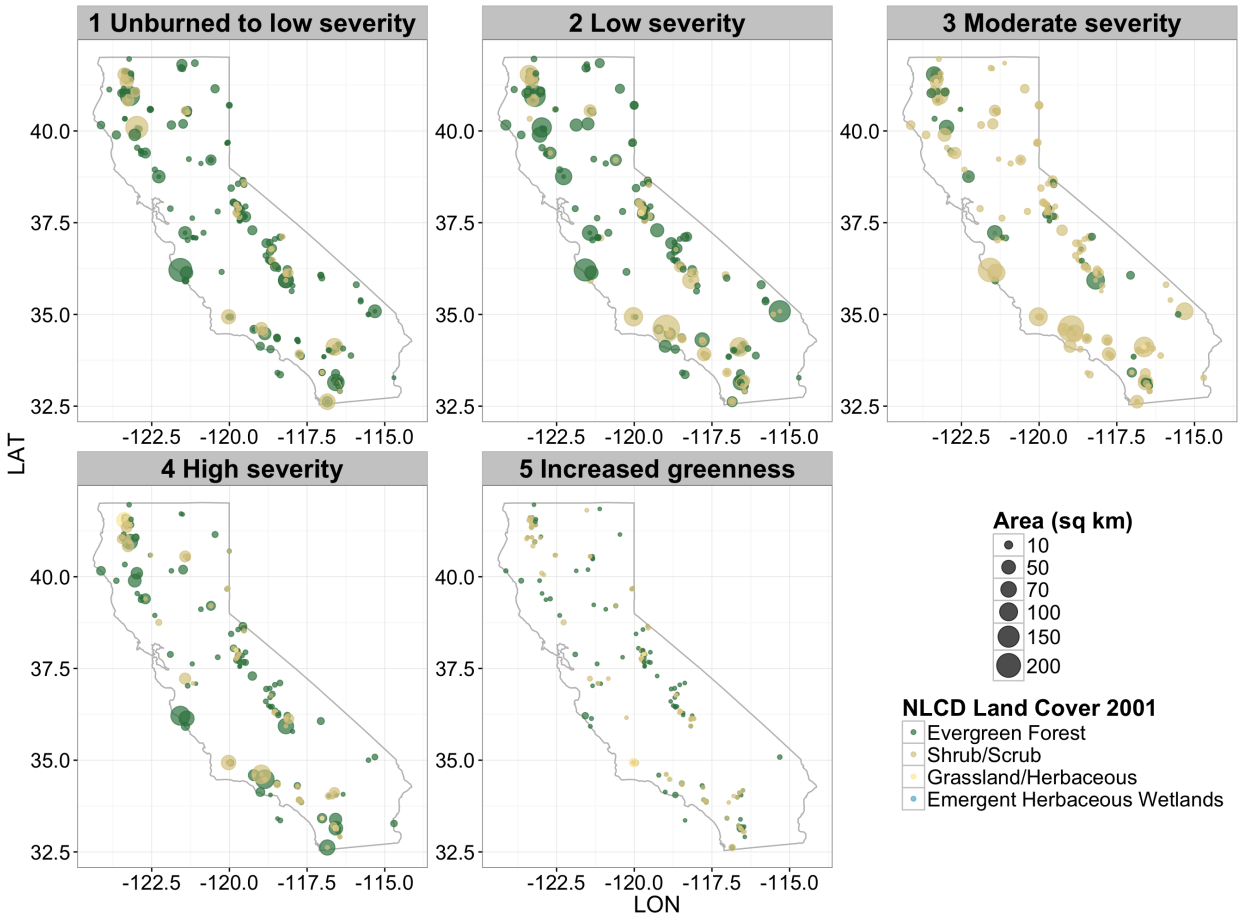

Figure 4.6: Burn severity of fires inside California PAs from 2000 to 2013. Fire occurrence are mapped by the size of area at each burn severity class, colored by NLCD land cover (2001) of the fire centroid.

areas, the peak time was generally delayed, especially for burned areas in evergreen forest after 2008 (Figure 4.10b). The burned areas also had a much shorter duration of growing season for both shrubland and evergreen forest (Figure 8c and 9c). Among all fires investigated, the Rush fire burned in August, 2012 was an outlier in the prevailing delay of SOST and shorten of DUR. Burned at a low severity, the area experienced a much earlier than usual SOST and a longer than usual duration (DUR) of growing season (Figure 4.9).

The NDVI values at two key time points (SOSN, MAXN) had a more consistent pattern than the time-based pheno-metrics. The growing season of burned area started and peaked

at a lower than usual NDVI, while the peak had a greater decrease in NDVI than the start (Figure 4.10a, 4.10b, 4.11a, 4.11b). Such decrease was more significant in evergreen forest after 2008, where the peak of histogram was more negatively shewed than before (Figure 4.11b). As the difference between MAXN and SOSN, the change in AMP in most areas was negatively skewed but at a small level because of the decrease in both items (Figure 4.10c and 4.11c). The Rush fire was also the major outlier. With a low burn severity, its immediate post-fire SOSN was greater than usual (Figure 4.10).

4.3.2.3 Correlation between dNBR and Key Pheno-metrics

We found that the most burned area experienced a weakened immediate post-fire growing season from the above analysis on the departure from usual. And such weakening was investigated with quantitative measurement of burn severity (dNBR) to evaluate the influence of fire intensity on post-fire phenology. The generalized additive models between dNBR and departure from normal for pheno-metrics revealed the similar weakening of the post-fire growing season as observed in previous results. Though highly significant ($p < 0.001$), the correlation coefficients of GAMs between dNBR and the departure from median for key pheno-metrics were mostly low, even if the models were separately calulated by the fire season, land cover types, and thematic classes of burn severity (Figure 4.12-4.14). Major outliers can be clearly detected from the modeling results (e.g. Rush Fire, 2012 and Rim Fire, 2013). The weakening of the immediate post-fire growing season was aggravated with the increase of burn severity (Figure 12-14). SOST and MAXT both had a positive shewed distribution and an increased trend with a higher dNBR for fire seasons (JJA and SON).

Compared with SOST and MAXT, the NDVI-based pheno-metrics (SOSN and MAXN) had a better correlation with dNBR and a more consistent inter-season and spatial pattern. Similar as SOST and MAXT, burned area in shrubland had a more significant correlation between SOSN and dNBR than evergreen forest (Figure 4.13a). Such difference was less observed between MAXN and dNBR (Figure 4.13c). It Is important to note that the Rim Fire had a much lower than usual SOSN and MAXN, with a significant negative correlation

with the increase of dNBR.

The change in the duration of growing season (DUR) was at a smaller magnitude compared with SOST and MAXT. But it followed the similar inter-seasonal and spatial pattern: the correlation between the departure from DUR median and dNBR was greater for shrubland, especially for area burned in fall (Figure 4.14a). Compared with SOSN and MAXN, AMP had a very weak correlation with dNBR. As the difference between MAXN and SOSN, with both items decreased, the change of AMP was expected to be small. However, a slightly decreasing trend was still observed, especially for shrubland burned in fall as evidence of weakened growing season, as shown in all of the pheno-metrics above.

Besides the immediate post-fire growing season, we also investigated the relationship between pheno-metrics and dNBR up to 13 years after fire occurrence, depending on the year of fire. The R^2 and p value of Pearsons correlation indicated that the correlation between burn severity and the measurements of phenology in burned area after fire became weak during the first four to five years after fire, then remained stable at a low level (Figure 4.15). Although outliers can still be observed, such pattern was better reflected during the prevailing fire season (summer and fall) and between the measurements based on NDVI (SOSN, MAXN) and the dNBR. The correlation calculated for fires burned in winter and spring was mostly insignificant or free of trend. Seasonal difference was also obvious for the most significant correlation. The correlation between SOSN and dNBR in fall remained at a relatively high level during the first four post-fire growing seasons for evergreen forest, and even had a slight increase in the second post-fire growing season for shrubland. In contrast, this early year plateau was missing in fires burned in summer. The R^2 constantly decreased from the first year to the fifth year after fire, then remained stable at a low level, regardless of the land cover type of burned area.

We also observed difference between land cover types in the quantitative evaluation of post-fire response for multiple years after fire. Considering the most significant correlation (SOSN vs.dNBR) during the fire prevailing season, R^2 of fires burned on shrubland was generally higher, especially during the early years, then decreased at a higher magnitude

during the first four or five years. The early year decrease of R^2 for burned area in evergreen forest was not as drastic and usually started at a lower level. A major outlier in the decreasing momentum of influence from burn severity on post-fire phenological response was an increase of post-fire SOSN from the immediate post-fire season to the second year after fire, for burned area in shrubland. Considering the similar number of degree of freedom (df) in the calculation and the significant p value, the higher R^2 during the second year of fire provided evidence for a recently recognized post-fire recovery pattern of California shrubland [Keeley et al., 2008].

4.4 Discussion

4.4.1 A Shifting Fire Regime

Although fluctuation exists, the fire occurrence and burned areas in our study area started off at a low level because of the consumption of available fire fuels during the previous peak, then climbed to the maximum in about 4 years. Although the climate conditions during the recent few years were fire-favoring, there was not a significant upward trend in fire occurrence and burned areas, which reflects many long-term simulations of wildfire for the western U.S. [Baker, 2013, Baker, 2015]. The drying trend in climate may not necessarily lead to an overall increase of fire, but it influenced the shift in fire-prone land cover type and season by controlling the fuel availability and fuel moisture.

As reflected in the background map in Figure 4, the tree canopy percentage [Homer et al., 2015], PAs in Klamath ecoregion had been accumulating fire fuels in recent years. Experiencing an increased dryness, the densified canopies became more fire-prone, and finally led to an increase of fires in this region, which had been confirmed by Parks et al. (2014) in their empirical analysis of fire occurrence in the western U.S. Furthermore, the changing of climate regime may increase the chance of lightning [Carle, 2015a], which was another major cause of fire in mountainous evergreen forest.

The recent disappearance of fall fires in southern California shrubland can also be ex-

plained by the recent increase of drought and the missing of a major Santa Ana event, which is the key controlling factor to the fire size and intensity of fires in the fall season. Fire activity is highly influenced by fuel moisture, usually represented by water deficit (WD) or relative humidity (RH). The prolonged drought increased the chance of ignition for plant communities with an enough amount of production by limiting the fuel moisture [Parks et al., 2014]. However, some shrubland in southern California may have reached the bottom line of fuel loads enough for being ignited, because of the loss of aboveground photosynthetic active part during the drought. The lack of biomass decreases the chance of fire or controls the extent of burn. In this case, the shrubland will become less fire-prone [Krawchuk and Moritz, 2011]. The increased dryness also limits the availability of production and slows down the post-fire recovery, which in turn reduces the chance of fire returning because of the shortage in fuel, especially after several active years of fire occurrence. Besides physical factors, human inducement such as fire suppression strategies applied in these areas also lead to removal or thinning of fire fuels. The short distance from many fire-prone PAs to the major metropolitan areas in southern California increases the necessity of fire suppression, including small-scale prescribed fires and reduction of fuel density [Keeley, 2002]. The above factors interacted with each other to limit the potential of fire burning and lead to the significant drop of fire in southern California shrubland.

However, it is also important to note that our study of fire regime covered a relatively short time period (2000–2013), during which the large scale and long term effect from the climate factors may not become prominent. Recent studies focusing on the fires driven by Santa Ana winds (SA fires) revealed that the number of SA winds increases during years when relative humidity during Santa Ana events and fall precipitation were below average [Jin et al., 2014, Liu and Wimberly, 2015]. The 2003 and 2007 Santa Ana firestorms are considered as a hundred-year event. The significant drop of fires in the fall (mostly SA fires) can also be related to the missing of an intensive Santa Ana event after a major breakout in 2007. Therefore, the shift we have observed since 2008 can possibly be a temporary decrease due to the natural fluctuation of Santa Ana events. The SA fires can resume during a major

Santa Ana event in the future.

4.4.2 Difference between Land Cover Types for a Weakened Immediate Post-Fire Growing Season

Although most burned areas had an increase of NDVI as a bounce back from the fire in the long-run, the immediate growing season after the fire was generally weaker than usual, as revealed in the analysis comparing the post-fire year pheno-metrics with their medians from 2000 to 2013 (Figure 4.10-4.11). And such weakening was more prominent if the area was at a higher burn severity. Because of the ecological difference as fuel of fire and the post-fire phenological response, difference between shrubland and evergreen forest was significant. The correlation between dNBR and pheno-metrics also not only confirmed the increase of magnitude in the post-fire response of burned area with burn severity, but also revealed a difference in the sensitivity of response between the time-based and NDVI-based phenological measurements among different land cover types. The different fuel moisture and phenology of these two types of landscape were the explanatory factors.

According to the fire ecology of California shrubland, the expansion of fire can be rapid because of its relatively low level of fuel moisture, especially for fires driven by Santa Ana events (SA fires), which include most of fires burned in the fall season. SA fires are strongly affected by moisture conditions of fuel, as demonstrated in the well noted Santa Ana firestorm in 2003 and 2007 [Jin et al., 2015, Jin et al., 2014]. The removal of surface senescence during SA fires in shrubland is more intensive than non-SA fires, which are usually located in evergreen forest, leaving very limited vegetation mass aboveground. The eradication of aboveground biomass can create it easier to detect the immediate post-fire drop in NDVI, which has been shown in Figure 6a and 7a. The difference in the intensity of the removal of aboveground biomass made the weakening of the immediate post-fire season in shrubland greater than evergreen forest. Through the correlation with dNBR, we observed a greater decay of major pheno-metrics in shrubland than evergreen forest (Figure 4.12-4.14). Such decay was greater at the beginning of the growing season than the peak, which also

demonstrated the great influence from the eradication of aboveground vegetation by fire.

Compared with shrubland, evergreen forest had a weakened immediate post-fire growing season at a lower magnitude, because of the higher level of fuel moisture and a larger fuel amount. The expansion of burned area in evergreen forest takes a longer time even during a crown fire (Sugihara 2006). The longer gap between the detection of NDVI drop and the fire occurrence date was partly due to the time necessary for wetter and denser standing senescence to burn (Figure 4.7a). In other words, the immediate post-fire response of evergreen forest was less time-sensitive than shrubland. The much smaller correlation in evergreen forest between the departure of key time pheno-metrics (SOST, MAXT) and dNBR also revealed the similar pattern (Figure 4.12,4.14). The delay of SOST and MAXT and the shortening of DUR in evergreen forest existed but was less prominent than shrubland, indicating the weakening of the immediate post-fire growing season is less intensive on a temporal basis. For evergreen forest, such weakening is better presented in NDVI-based pheno-metrics (SOSN, MAXN) as direct measurement of aboveground biomass. A great number of fires occurred in evergreen forest were crown fires that expand rapidly by connecting the crowns of trees. The burned areas usually lose a great part of canopy that is photosynthetically active and eventually a significant drop in NDVI.

From the previous comparison, we can also observe a difference of sensitivity in the measurement of post-fire vegetation behaviors between shrubland and evergreen forest. While NDVI-based pheno-metrics are sensitive in depicting the weakened immediate post-fire growing season, the time-based ones had different behaviors in two land cover types. Compared with evergreen forest, such weakening was effectively detected by SOST, MAXT, and DUR in shrubland, indicating weakening of growing season in shrubland was often reflected in terms of time. This high sensitivity in time for shrubland can be explained by the style of aboveground mass removal by fires occurred in this type of land cover. A moderate to high severity of fire in shrubland was likely to remove both the photosynthetic active parts (leaves) and the supporting senescence, and easily created gaps between plants. Losing most of its aboveground mass, it usually took a longer time to recover for shrubs, which eventu-

ally resulted in a longer delayed SOST and MAXT. In contrast, the removal of aboveground senescence (i.e. trunks) for evergreen forest is limited, although it sometimes caused the nutrient cycling become dysfunctional. Thus recovery growth can resume with a much smaller gap than shrubs. However, the fundamental removal of photosynthetic part of trees usually led to a sensitive response in NDVI, considering its higher start off level in canopy coverage.

The above difference in sensitivity and the explanation by the styles of senescence removal was also reflected in the major outlier of each land cover type, the Rush Fire for shrubland and the Rim Fire for evergreen forest. A proportion of the Rush Fire perimeter featured a much earlier than usual SOST and MAXT (Figure 4.12, dark green shaded points). Considering its relatively low burn severity and location (northwest of the Great Plain, adjacent to Nevada), the growing cycle was not completely turned off by the fire, and the burning may facilitate the rapid post-fire re-growth by thinning the canopy and removing the competitors. Burned in a region with a long history of fire suppression, the Rim Fire distinguished itself with a much lower than usual SOSN and MAXN (Figure 4.13, yellow shaded points). As fires burned in area with a long history of fire absence, the Rush Fire and the Rim Fire differed from each other on the basis of the best measurement as an outlier.

4.4.3 Determinants of the Post-Fire Vegetation Behaviors in California PAs

The three physical factors, land cover, seasonality, and burn severity interact with each other to shape the fire regime, and eventually the post-fire vegetation behaviors of burned areas in California, but in different manners. Land cover is the most frequently studied determinants of fire regime and post-fire response from vegetation. Without any external influence, it is also the most significant determinant of the spatial pattern of fire regime and post-fire response from vegetation. However, the basic characteristics determined by land cover can vary by the meteorological conditions of fire, which can partly be explained by the seasonality and the pre-fire meteorological situation, e.g.a prolonged drought or abnormally high air temperature.

As discussed before, land cover and seasonality are often overlapped with each other. The fire-prone season of a given land cover type is usually similar, which was confirmed in the results of correlation between departure from median of pheno-metrics and dNBR. The difference of model performance between evergreen forest and shrubland was prominent and the inter-seasonal variation was small (Figure 4.12, 4.14. However, separating season and land cover helps to distinguish the influence from major fires. Considering the limited number of fires burned in each season on different land cover surface, the major fires can overshadow the influence from other smaller fires and contribute greatly to post-fire vegetation response.

Unlike land cover and seasonality, the burn severity is a relative measurement and varies between fires. The thresholds to determine the MTBS thematic burn severity classes vary by fires, and each fire has its own low/moderate/high burned areas. We expected a greater destroy on the local vegetation and a larger departure from usual if the burn severity increases as a short-term influence on burned area. Such relationship was confirmed by the correlation between the departure from median of key pheno-metrics and dNBR, which revealed a significant negative correlation between the phenological measurements of the immediate post-fire growing season and burn severity (Figure 4.12, 4.14. And such influence was better reflected in the change of NDVI than the change of time. However, there was a great variance in such relationship, mostly because of the spatial heterogeneity between fires included in this study. The outliers (Rush Fire and Rim Fire) were good examples of such variance by location, indicating the influence of fire burn severity is highly fire-specific. The general measurements of spatial heterogeneity, including land cover and seasonality are not effective enough to explain some local characteristics, such as fire history and land management, which have been demonstrated to be other non-physical determinants of fire regime and post-fire response.

Considering the speed of turnover and recovery in our study area, the influence on phenology from fires may not last long. According to Keeley et al. (2008), the solid re-establishment of shrub in previously burned area usually takes about three to four years. Significant at the beginning, the influence of fire decays over time, as we can find in an inter-annual comparison of model performance between multiple years after fire (Figure 4.15). Focusing on

the major fire season (summer and fall), the correlation between burn severity and NDVI-based pheno-metrics of post-fire growing seasons significantly dropped at the beginning, and became insignificant four or five years after fire. However, the higher correlation between burn severity and the start of season NDVI during the second year after fire occurrence in shrubland may provide evidence to support the short-term increase of NDVI in heavily burned shrubland from alien species of grass. The more intensive eradication of aboveground biomass in shrubland leads to more space for the coverage from invasive alien species, which usually establish within two years of fire. Since then, the surface condition becomes more heterogeneous and can be less explained by the intensity of fire. The significant drop of R^2 between SOSN and dNBR from two to three and four years after fire in shrubland indicated the influence of the previous fire eventually decays.

4.4.4 Recommendations for Local Policy Makers to Address the Risk of Wildfires in PAs

The findings discussed above have conveyed important facts regarding to the risk of wildfires in California PAs, especially under a changing fire regime because of the prolonged drought and projected change in climate regime. Considering the difference in the fire regime between the two major land cover types (shrub/scrub and evergreen forest), we provide the following recommendations for local policy makers to accomondate the challenges on wildfires inside PAs.

First, the prolonged drought on California shrubland, especially the southern California chaparral community is two-fold. It can negatively influence the post-fire recovery of shrub plants, thus delay the returning of fire to the same burned area because of the inavailability of fuel source. On the other hand, for PAs dominated by alive shrub and scrub that are experiencing a moisture deficit, the prolonged drought can cause withering or mortality of alive plants, turning them into ignitable fuel source. According to our comparison on fire occurrence and perimeters before and after 2008, the first possibility was observed more frequently: there was a significant decrease in the fire of shrubland in southern California

chaparral. However, given a longer time, the returning of fires in this region is highly possible, because the influence from the moisture deficit of plants needs time to become significant. Therefore, the local land managers should monitor the influence of drought at a more intensive level to track the change of local plants. Necessary prescribed fires and mechnical treatment of harzard fuels in these areas to reduce the thickness of fuel source are also necessary to reduce the risk of major wildfires. For areas that have experienced recent wildfires but struggled to recover because of drought, it is also important to monitor the recovery and provide necessary assistance. For these burned areas, local land managers should also pay special attention to the erosion and land degradation caused by the absence of the aboveground biomass.

Second, the deficit of moisture in evergreen forest has increased the risk of wildfires in these areas, especially considering the thickening of plants during the fire absence period. The increase of fire risk can be boosted by the high mortality of trees because of drought, sometimes associated with the outbreaks of bark beetles for the Sierra Nevada ecoregion [USDA Office of Communications, 2016, Buis, 2016]. The above fact not only underscores a budget fix on fire management, but also urges for efforts on protecting watersheds in this region and restoring forest from drought and threat of bark beetles to make them more resilient to fire in the future. In addition, a comparison between the forest canopy of 2006 and 2011 from National Land Cover Database (NLCD) has revealed there was an increase of forest canopy in the north of California from 2006 to 2011 [Coulston et al., 2013, Jin et al., 2013]. An increase of fire occurrence was observed in this area (section 4.3.1), which can be reasonably attributed to the decrease of fuel moisture on a densified forest community during the previous period of fire absence. The focus of local land managers in this region should be the land management strategies to reduce fuel thickness. At the same time, tracking the change of fuel moisture is also an important element to protect the evergreen forest in the north of California from more disastrous wildfires.

4.5 Conclusion

Unlike most previous studies that are usually focused on selected fires at a finer spatial scale, we provided a comprehensive analysis of the change in fire regime in all fires for California PAs, as well as the post-fire vegetation response of all burned areas inside California PAs, where almost one third of fires from 2000 to 2013 in California occurred. We analyzed the three key factors shaping the fire regime and the post-fire vegetation behavior, including seasonality, land cover, and burn severity. It provided a good test on existing fire ecology knowledge, which were usually obtained by field observations and site-based. There were three notable trend and patterns in the fire regime and the post-fire behaviors of vegetation as revealed in the above analysis.

Although most fires followed the normal fluctuation cycle of four years and occurred during the major fire season, there was a shift in fire regime before and after 2008 in California PAs. A significant drop happened in fires burned in southern California shrubland during fall season since 2008, while an increase of early fire season (late spring) burning occurred in the northern California evergreen forest, mainly inside the Klamath Mountain ecoregion. The former drop can be attributed to the shortage of fire fuels related to the prolonged drought suppressing the production of surface biomass, as well as a natural absence of the strong meteorological driver after an intensive fire burning period from 2005 to 2007 because of the abnormally strong Santa Ana events, especially in the southern California shrubland. The increase of fire occurrence in late spring was mainly due to the densified forest canopy in the Klamath Mountain ecoregion since 2001, which has been demonstrated in the recent two NLCD land cover imagery (2006 and 2011).

A weakened immediate growing season is usually expected after fire, which has also been detected from our analysis on the spatial and temporal distribution of the post-fire vegetation response. From the time and NDVI-based pheno-metrics of the immediate post-fire growing season, we found that most fires experienced a delayed start and peak, a lower than usual NDVI at the above two time points, and a shortened length. However, such weakening

was at a higher magnitude in shrubland compared with evergreen forest. In shrubland, the removal of aboveground senescence by fire is much more intensive than evergreen forest, which usually leads to a more rapid drop of vegetation coverage on surface, as detected by NDVI. In addition, it takes a longer time to burn out the wetter and denser evergreen forest than the drier and sparser shrub. The above weakening in immediate post-fire growing season was confirmed by the correlation between the key pheno-metrics and dNBR, with some outliers in area with a long history of fire suppression and with fires burned at an extraordinary extent and intensity.

Although the present study developed a comprehensive understanding of recent change in fire regime of California and tested the recognized pattern of post-fire vegetation response with key factors in fire ecology, several improvements can be made. The shift in the fire regime noted in the study requires more investigation on a longer time series and should involve climatic conditions explicitly, especially the major fire driven meteorological events like Santa Ana winds. The high residual in the correlation between burn severity and post-fire pheno-metrics, as well as the significant aggregation of observations of the same fire indicates the existence of more determinants of post-fire response. In order to improve the explanatory ability of the model, other environmental factors should also be involved, such as post-fire climate conditions, concentration of nutrient in the soil, fire history of burned area and fire returning interval. Furthermore, considering the uncertainty of dNBR in measuring burn severity, applying other measurements of fire intensity is another way to improve the current model.

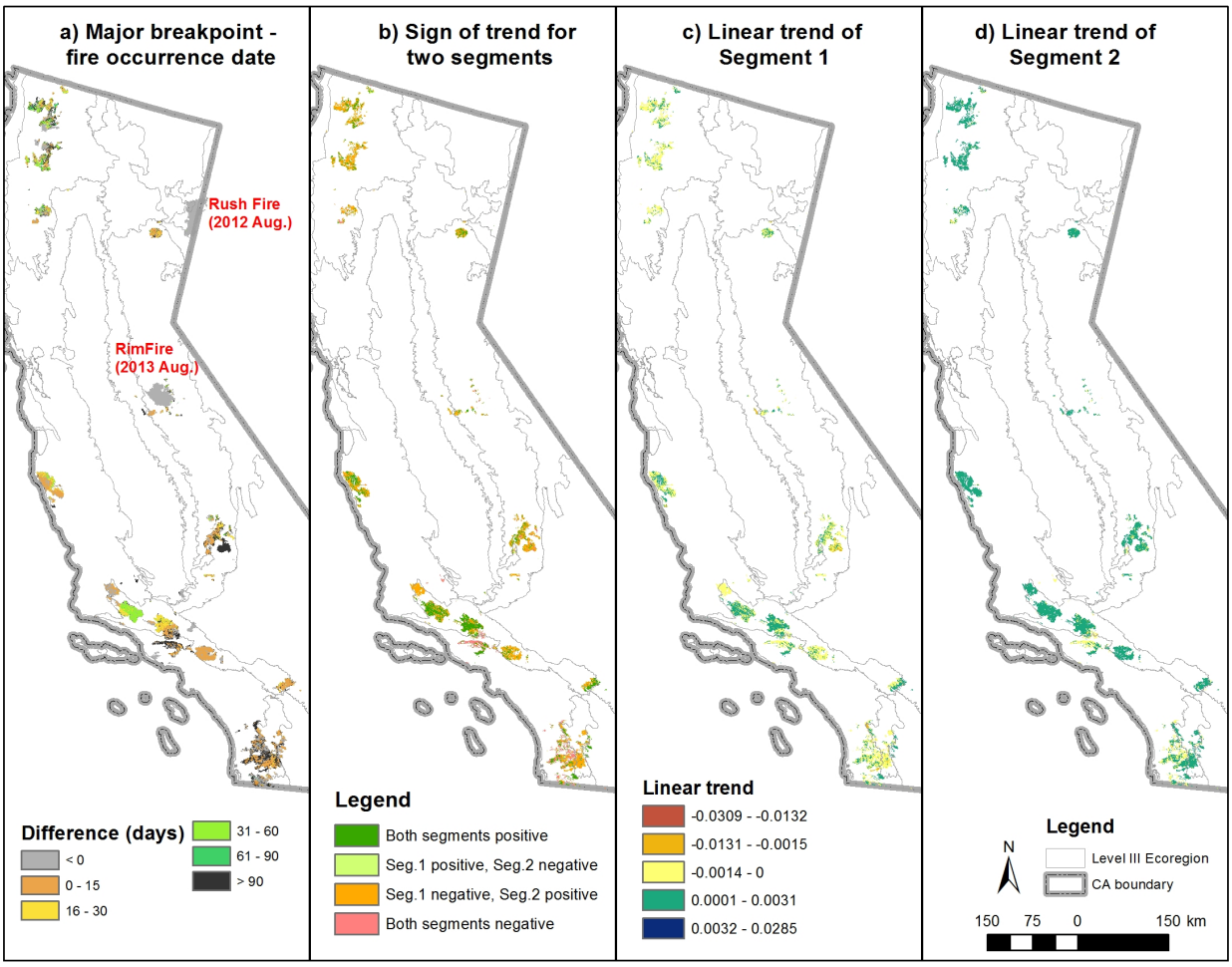

Figure 4.7: Frequency of difference in days between the major breakpoint and the fire occurrence date. Top three panels plot the difference between 0 and 90 days are shaded by land cover (a), fire occurrence season (b), burn severity (c). Full results are plotted in (d).

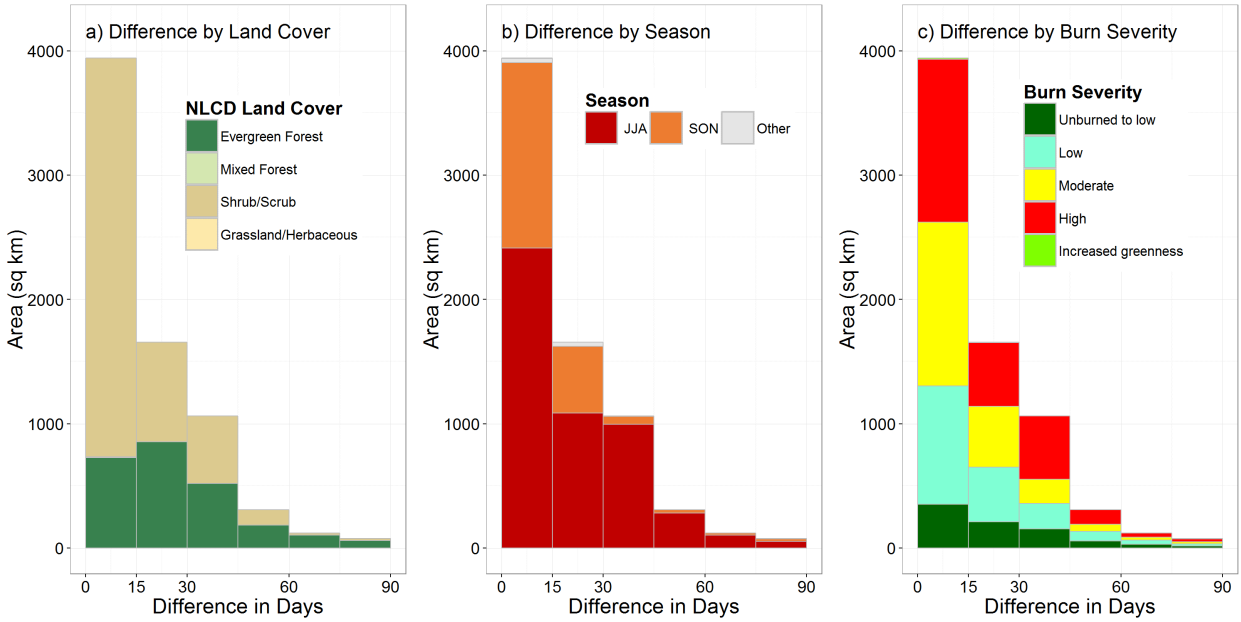

Figure 4.8: Compare major breakpoints of NDVI and the fire occurrence date for 23 major fires in California PAs from 2000 to 2013. Description of each panel: a) illustrates the difference between the major breakpoint detected and the fire occurrence, positive (negative) difference means major breakpoint occurred later (earlier) than the fire; b) compares the sign of linear trend between two segments divided by the major breakpoint for area with a positive difference (Segment 1 and Segment 2, before and after); c) and d) map the value of linear trend of Segment 1 and 2 respectively for area with a positive difference.

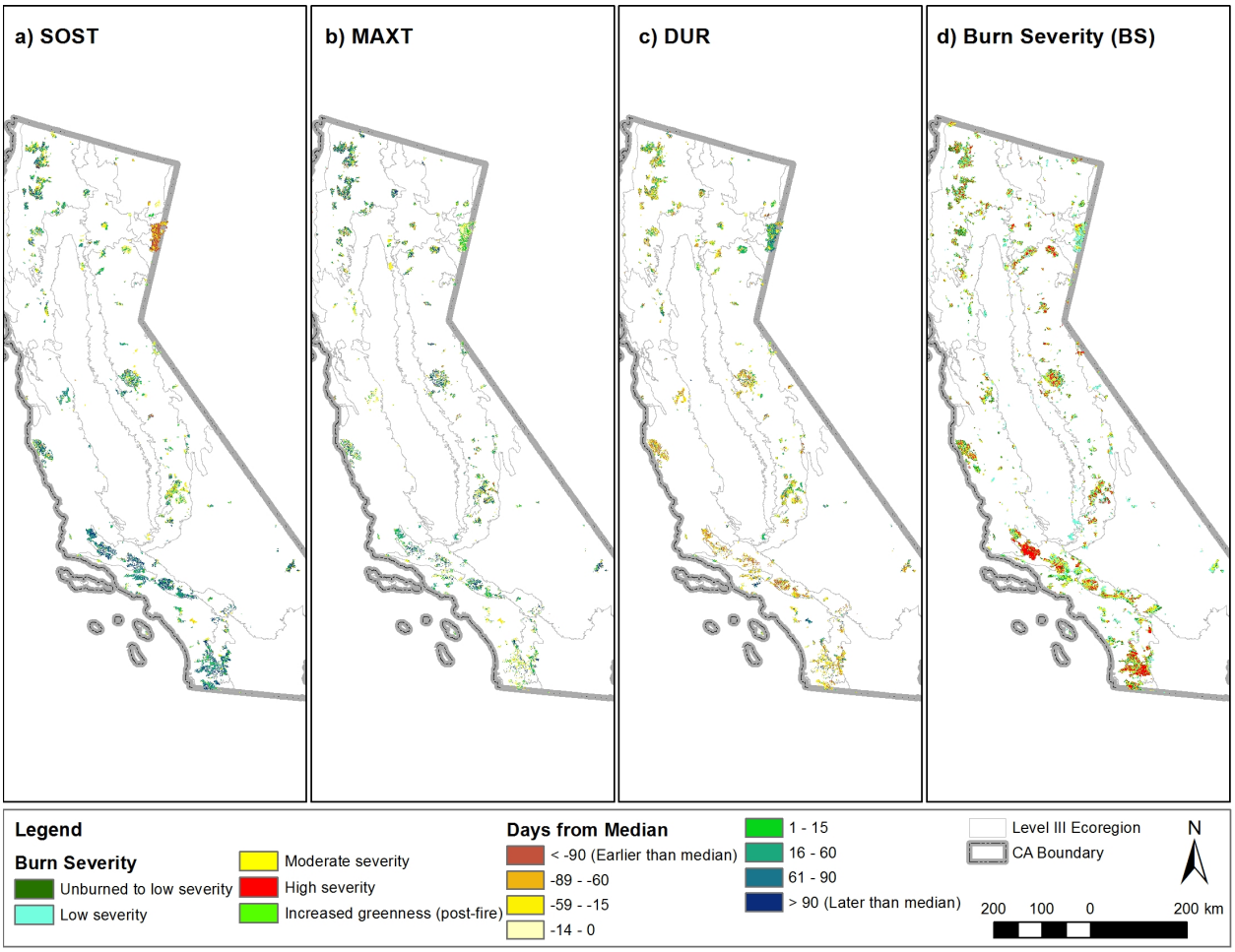

Figure 4.9: Difference between the key time pheno-metrics (SOST, MAXT, DUR) of the following year after fire occurrence and the medians from 2000 to 2014. A negative (yellow-ish) day from median means the phenometrics of the following year after fire occurred earlier (shorter for DUR) than usual. A positive (blue-ish) day from median means the phenometrics of the following year after fire occurred later (longer for DUR) than usual. Burn severity from MTBS data is mapped in d) as a reference of intensity of burning.

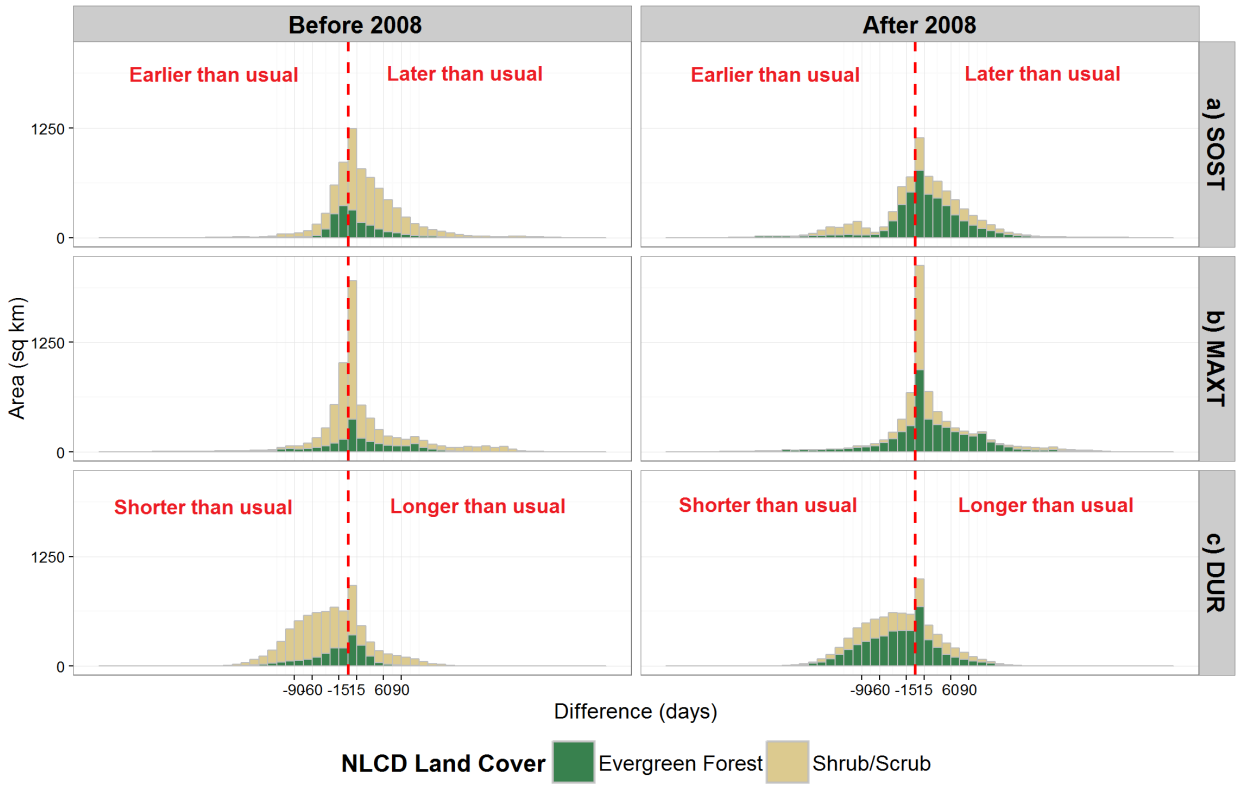

Figure 4.10: Frequency of difference between key time pheno-metrics (SOST, MAXT, DUR) and medians from 2000 to 2014. Fires before and after 2008 are plotted separately, shaded by the major land cover type from NLCD.

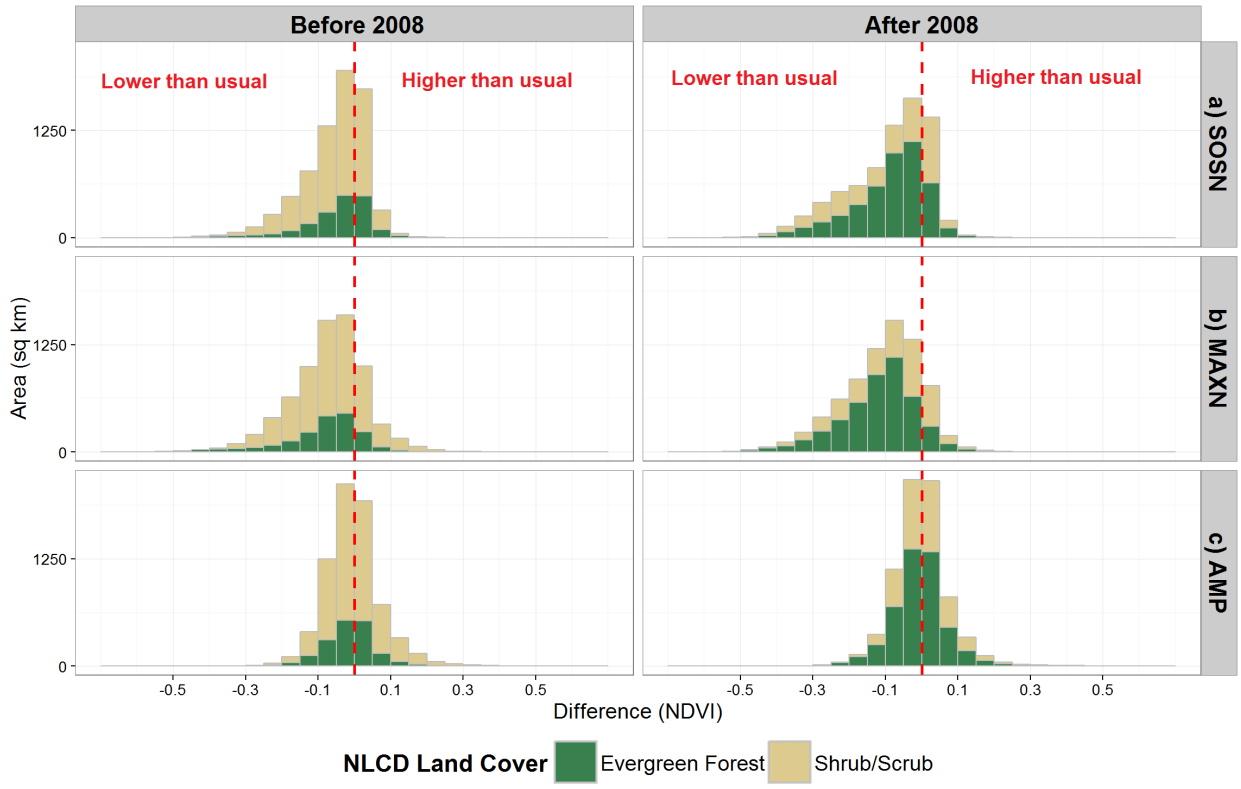

Figure 4.11: Frequency of difference between key time pheno-metrics (SOST, MAXT, DUR) and medians from 2000 to 2014. Fires before and after 2008 are plotted separately, shaded by the major land cover type from NLCD.

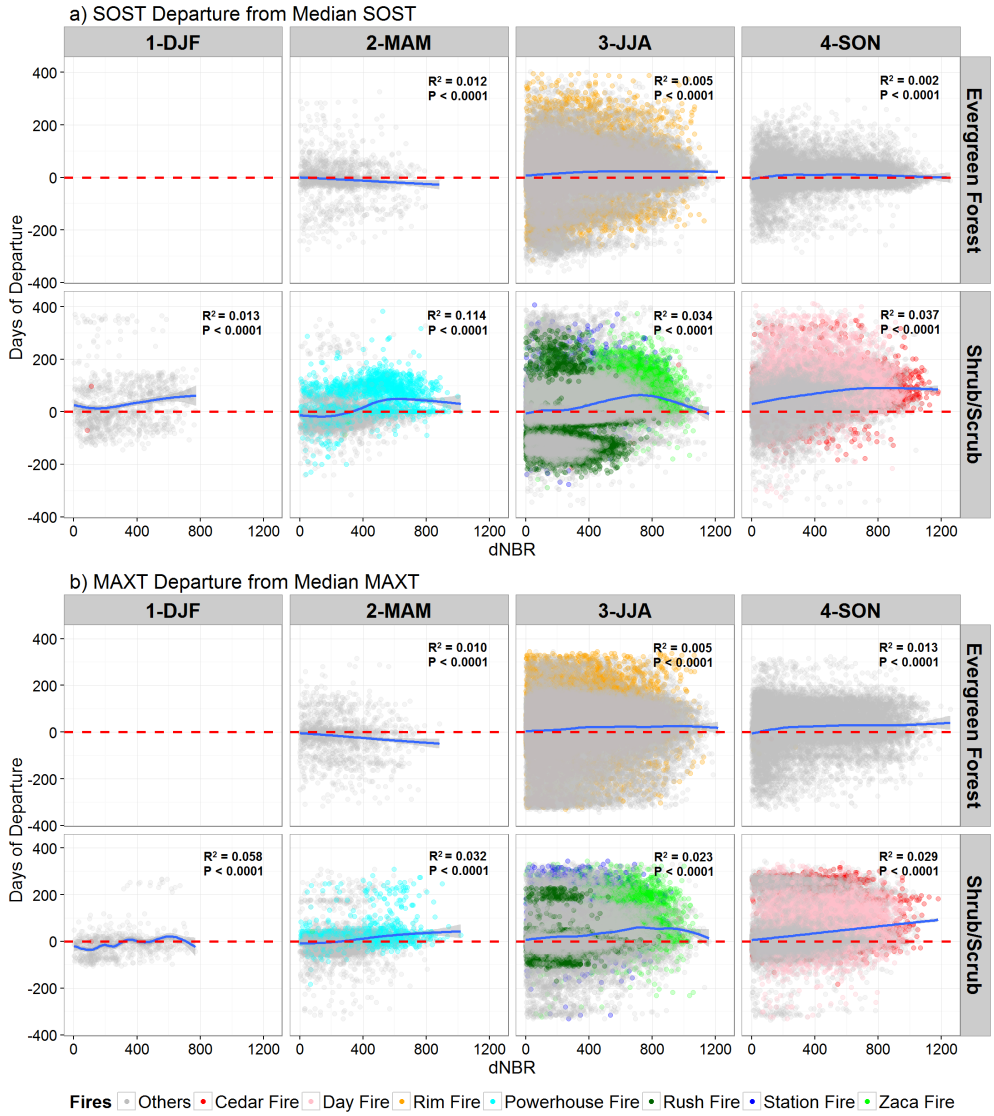

Figure 4.12: Correlation between dNBR and the departure from median SOST (a) and MAXT (b) for the year after fire. A positive departure means the SOST or MAXT of the year after fire occurs later than usual, while the negative departure means the opposite. The two major land cover types, evergreen forest and shrubland are mapped separately for different fire occurrence season. Seven largest fires occurred in California PAs from 2000 to 2013 are colored as shown in the legend.

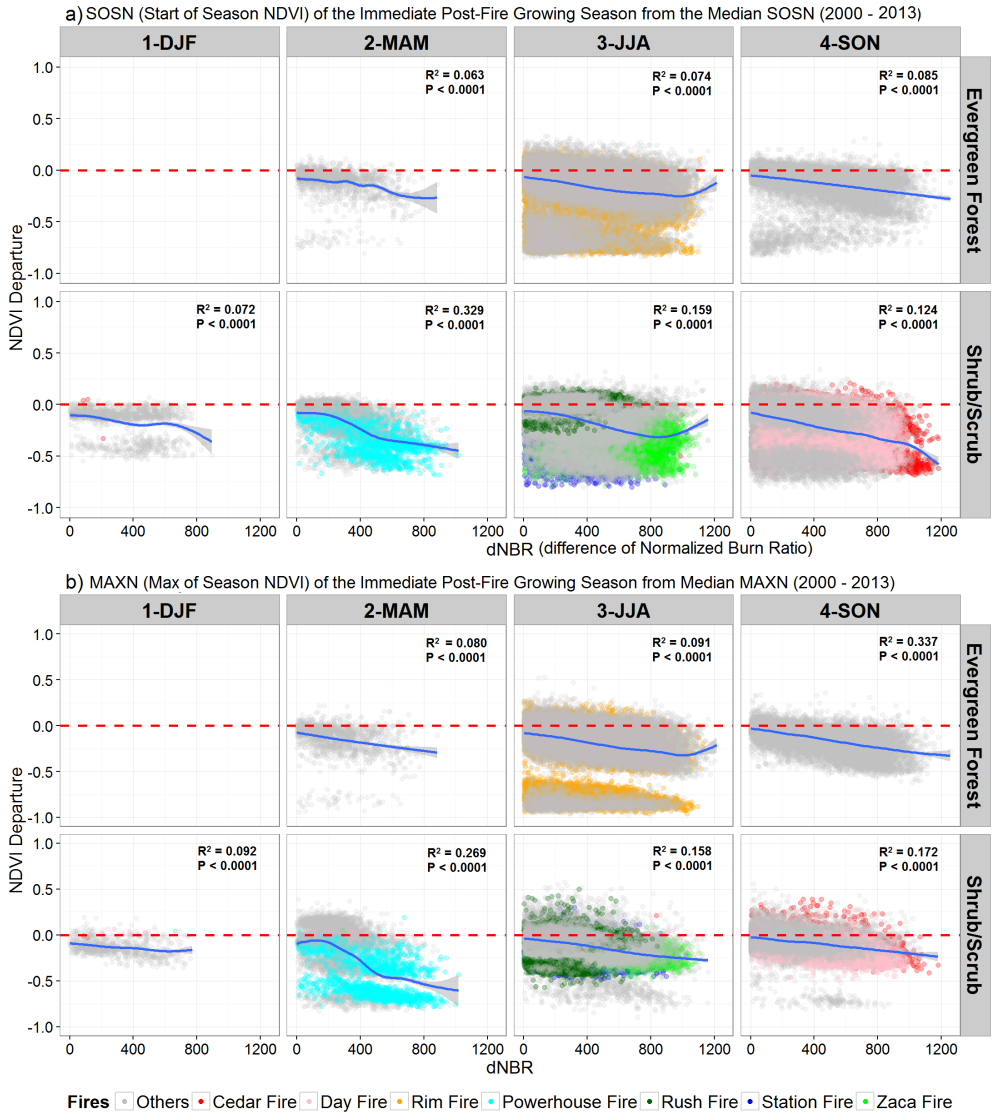

Figure 4.13: Correlation between dNBR and the departure from median SOSN (a) and MAXN (b) for the year after fire. A positive departure means the SOSN or MAXN of the year after fire is lower than usual, while the negative departure means the opposite. The two major land cover types, evergreen forest and shrubland are mapped separately for different fire occurrence season. Seven largest fires occurred occurred in California PAs from 2000 to 2013 are colored as shown in the legend.

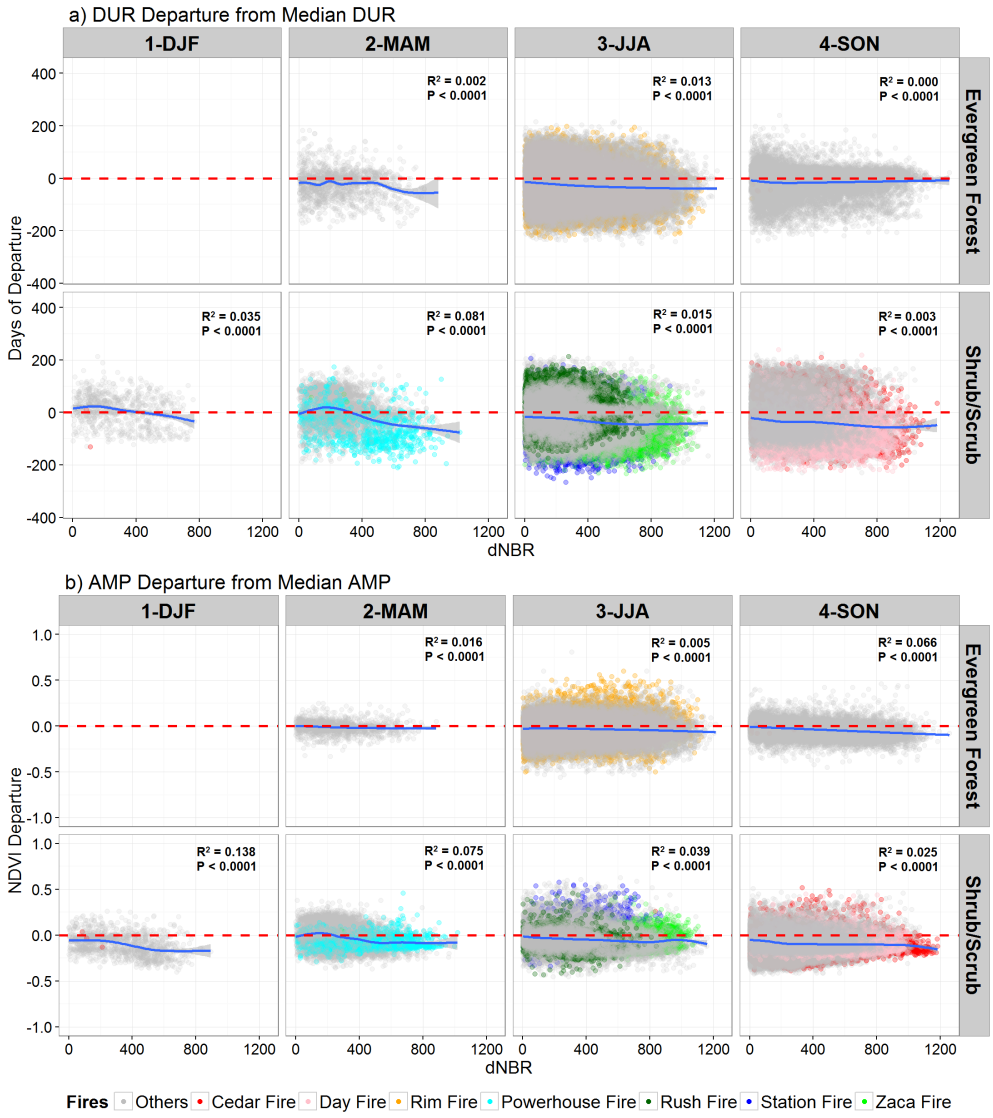

Figure 4.14: Correlation between dNBR and the departure from median DUR (a) and AMP (b) for the year after fire. The two major land cover types, evergreen forest and shrubland are mapped separately for different fire occurrence season. Seven largest fires occurred occurred in California PAs from 2000 to 2013 are colored as shown in the legend.

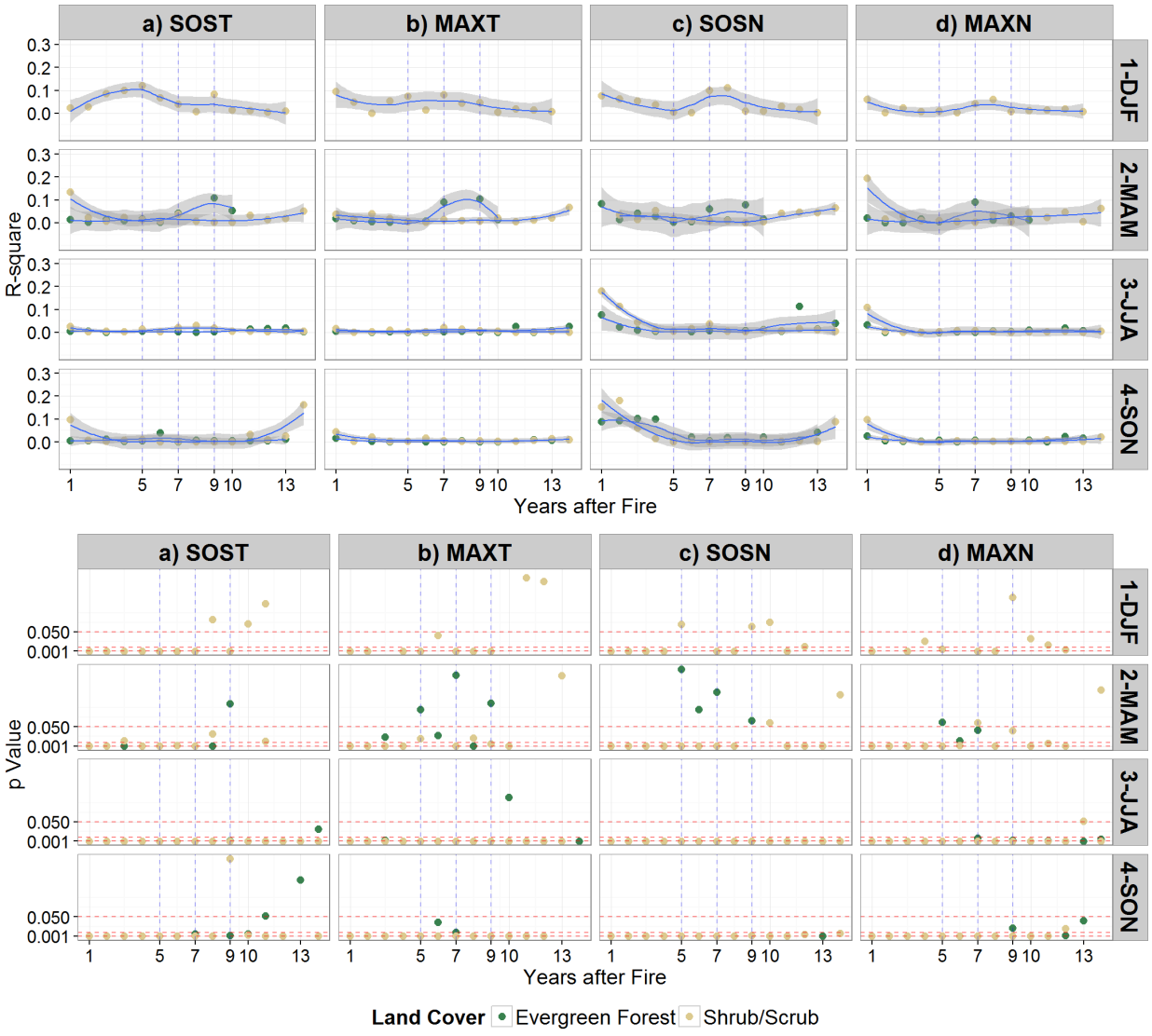

Figure 4.15: Correlation between dNBR and the departure from median SOST (a) and MAXT (b) for the year after fire. A positive departure means the SOST or MAXT of the year after fire occurs later than usual, while the negative departure means the opposite. The two major land cover types, evergreen forest and shrubland are mapped separately for different fire occurrence season. Seven largest fires occurred in California PAs from 2000 to 2013 are colored as shown in the legend.

CHAPTER 5

Detecting the Human Activity in Protected Areas of California with DMSP-OLS Nightlight Data

5.1 Introduction

The influence of human activities in the protected areas (PAs), especially on the biodiversity and the conservation of wilderness of these areas has become a key research topic ever since the awareness of the ecological importance of wilderness by international community and the establishment of PAs globally. Controlling and managing the intensity and extent of human activities inside PAs and the adjacent areas is a key factor to restore and protect the wilderness of the earth. IUCN classified PAs into six different categories based on the degree of protection and the level of human activity in or near PAs that can keep an equilibrium between the wilderness and the anthropogenic disturbance (class I to VI, high to low protection) [Chape et al., 2003]. For different classes of PAs, there is a different acceptable level that the intensity of human activity can reach, which needs the evaluation on the potential risks of the introduction and the spread of human activities in or near PAs [Lovejoy, 2006, Chape et al., 2005, Geldmann et al., 2013], as well as a baseline study about past and present levels of human activities in these areas.

A number of well documented socioeconomic variables have been employed as proxies of human development and activities to answer the question that how, and by what extent the human activities have shaped and influenced the PAs [Wilson et al., 2015a]. These variables

include population [Sleeter and Gould, 2007, Sanderson et al., 2002, Wittemyer et al., 2008], house density [Geldmann et al., 2014], road density [Sanderson et al., 2002], electricity production and consumption [Hernandez et al., 2015, McDonald et al., 2009]. Most of the above studies focused on comparing the socioeconomic variables with the degree of wilderness adjacent to or inside PAs to evaluate the influence of current degree of human activities, or analyze the possible outcomes under different scenarios of the extent and intensity of human development [Wilson et al., 2012, Wilson et al., 2014, Sleeter et al., 2012]. However, studies adopting socioeconomic variables as the proxies of human activities and developments have been mostly limited to the global level [Mcdonald et al., 2008, Mcdonald et al., 2009b, Geldmann et al., 2014], in many cases because of the limited availability of socioeconomic variables at an adequate scale to effectively track the human activities in or near PAs. Although the coverage of imperviousness and other land cover change products can be considered as a direct measurement of human activity in or near PAs, most of these products are only available on a five or ten year basis [Fry et al., 2011, Homer et al., 2015, Fry et al., 2011], which cannot effectively track the dynamics of the extent and intensity of human activities. In the yearly available remote sensing products of land cover, such as MODIS Land Cover product (MCD12Q1), the signal of human activities inside PAs was usually suppressed by the great wilderness thus mostly undetectable directly from the images. Besides socioeconomic variables and land cover, stable nighttime light can be considered as another effective measurement human activity and development, which is a proxy of electricity consumption[Mellander et al., 2015, Henderson et al., 2012, Henderson et al., 2012, Liu et al., 2012, Rybnikova and Portnov, 2014, Ghosh et al., 2013]. The in situ measurement of light glow in night sky is a good example, such as the Night Sky program of National Park Service in the U.S. [Cinzano and Elvidge, 2003, Cinzano and Elvidge, 2004, Duriscoe et al., 2007, Duriscoe, 2013]. The ground-based measurement of night sky provided accurate observation of the influence from human activities on areas with high wilderness such as national parks. However, with the short time span of the available observation, the measurement was usually inconsistent and with very limited spatial coverage. On the other

hand, the remotely sensed stable nighttime light product can provide temporal and spatial continuous observation as a proxy of human activities and has large enough spatial coverage to conduct the analysis at different scales, which was employed as the main data source for analysis in this study.

The remotely sensed nighttime light products, especially the stable nightlight yearly products from Defense Meteorological Satellite Programs Operational Line Scan system (DMSP-OLS) from 1992 to 2013, as well as the latest nightlight focused remote sensing product from VIIRS Suomi NPP [Miller et al., 2012, Elvidge et al., 2013] have been widely applied to studies to investigate the temporal trend, spatial extent , and intensity of human activities [Mellander et al., 2015, Henderson et al., 2012]. Considering its global coverage and spatial resolution at 1 km, this yearly available nighttime light product with atmospheric correction can track the temporal dynamic and the change of spatial extent of human activities more effectively and accurately than socioeconomic variables. After it became available at a global extent, most studies employed the stable nighttime light products by DMSP-OLS were focused on studying the process of urbanization and the economic development of different countries/regions/cities [Seto et al., 2011], while its significance on studies about biodiversity, conservation of wilderness and the effectiveness of PA establishment was less recognized. Among the studies on biodiversity and conservation of wilderness, many were focused on the influence of light pollution on threatened species [Chepesiuk, 2009, Kachelriess et al., 2014, Gaston et al., 2012]. Most studies studying the human pressure on ecosystem with stable nightlight data were concentrated on the outskirt of major metropolitan areas, specifically focusing on the ecological pressure of urban sprawl [Bennie et al., 2014, Geldmann et al., 2014] rather than directly pointing at the PAs. However, a global assessment of light pollution impact on PAs revealed that the direct and indirect (as proxy pressure of human influence) lighting impact in PAs cannot be ignored, especially in two biomes, temperate broadleaf and mixed forests as well as the Mediterranean forests, woodlands, and scrub [Aubrecht et al., 2010]. Considering the high coverage of Mediterranean biomes and the ecological pressure from population in California, there is

a need to investigate the temporal change and spatial extent of stable nighttime light inside California PAs.

By employing the continuous record of stable nighttime light products from DMSP-OLS, we concentrated on four research questions in this study focusing on California PAs: 1) is there a significant increase or decrease of stable nighttime light in California PAs since the DMSP-OLS data became available in 1992, 2) how did the ecoregions inside California differ from each other in terms of change in stable nighttime light, 3) how did the hotspot of stable nighttime light inside PAs change in space since 1992, 4) how to explain the temporal and spatial change of stable nighttime light by socioeconomic variables.

5.2 Data and Method

5.2.1 Data

In this study, we employed the cloud-free and ephemeral lights free nighttime lights time series and the available global radiance calibrated products from the Defense Meteorological Satellite Program Operational Line Scanner (DMSP-OLS) as the main data source for analysis. One of the biggest challenges in exploiting DMSP-OLS nighttime lights for inter-annual comparison and analysis was that the inter-satellite calibration was missing from the original data products, leading to the discrepancy between images obtained from satellites of DMSP-OLS launched in the last two decades [Elvidge et al., 1999, Elvidge et al., 2014, Elvidge et al., 2013]. Saturation problem in developed areas is another issue of this product. The limited dynamic range of DMSP-OLS sensors was not able to accommodate bright source [Hsu et al., 2015]. Thus, the original nighttime light products do not carry the details for bright areas, assigning them with the highest value of the dynamic range (DN = 63). Researchers need to address the above two issues if an inter-comparison is necessary between images obtained from different satellites or for study areas covering cities and other bright sources.

Several socioeconomic indicators, including human footprint index (HFI) and population were also included in this study to provide a reference baseline of the level of human activities in California PAs (Figure 5.1). It can also be used as a possible explanatory variable of the detected temporal and spatial dynamics of human activities. The global HFI was developed by Wildlife Conservation Society (WCS) and Center for International Earth Science Information Network (CIESIN), Columbia University, and is available at the spatial resolution of 1 km. Generated based on population, traffic density, urban areas, and other indicators of human development, HFI is a well-recognized and effective composite measurement of anthropogenic impact on the earth [Sanderson et al., 2002]. The population data used in this study were obtained from two datasets of the U.S. Census, the census tract level population of 2000 and 2010 census as well as the American Community Survey (ACS) of 2005, 2009, 2011 and 2012.

5.2.2 DMSP-OLS Nighttime Light Pre-processing

In order to eliminate the discrepancies between satellites for inter-annual comparison, we calibrated the cloud-free yearly nighttime light images obtained from different satellites with the polynomial regression model. The coefficients of the calibration model were calculated based on a series of stable objectives on the surface, which has no or very limited change in brightness through the past two decades (Elvidge et al. 2009, Elvidge et al. 2014). All available image obtained from different years and satellites were calibrated to a selected year. We compared the R2 of the calibrated images and the reference images between three widely applied polynomial or linear regression models [Elvidge et al., 2014, Liu et al., 2012, Wu et al., 2013, Elvidge et al., 2009]. The polynomial model mentioned in Elvidge et al. [2014] yielded the best R^2 and was selected as the calibration model for images from 1992 to 2012 (Figure 5.2). The year 2013 was not included in the following analysis since the stable coefficients of the polynomial regression were not available. We also calculated and compared the sum of light (SOL) and the average DN between the original and the calibrated nighttime light images to evaluate the performance of inter-calibration model (Figure 5.3-5.4). The

SOL is the sum of DN values above 6 of all available years for the same satellite (Elvidge et al. 2014). The difference between SOL of the same year from different satellites after a successful calibration is expected to be very small. And the transition between sections of different satellites is expected to be negligible and smooth (Figure 5.3-5.4). Since there was more than one image for the overlapped years between satellites, we compared the R2 between the multiple options for the same year and only employed the calibrated image with the highest R^2 in the following analysis (Table 5.1).

However, the calibration method cannot completely eliminate the discrepancies between satellites. The inter-satellite offset still existed after calibration (Figure 5.3-5.4). And the offset between satellites may vary by location, which makes a universal polynomial model difficult to calibrate and address. Therefore, the analysis results based on the calibrated nighttime images should be carefully evaluated and discussed. In order to address the saturation issue in the bright source (e.g. cities), we also employed the global radiance calibrated images for available years. The radiance calibrated product was provided for representative years with other years blended together to increase the dynamic range to provide details of the originally "saturated" bright areas from 1996 to 2010 [Hsu et al., 2015]. The inter-annual calibration was also applied to eliminate the discrepancies for inter-annual comparison. Radiance calibration data of the year 2005 was used as the reference image.

5.2.3 Statistical Analysis on Temporal Dynamics and Spatial Extent of Stable Nightlight

In this study, we applied a series of descriptive statistical analysis and t-test over the inter-calibrated nighttime light analysis for all PAs in California to investigate the temporal and spatial change of low, medium and high lit areas in the PAs from different aspects. The purposes of the above statistical analysis were listed in Table 5.2.

In additional to the descriptive statistics, we classified DN values into six classes [Henderson et al., 2012], including non-lit (< 1), low (3–5), medium low (6–10),

Table 5.1: Selection of calibrated DMSP-OLS data for analysis based on R^2. Bold numbers are R^2 values of the selected data. The nighttime light of 1999 from satellite F12 is the reference image for calibration, thus has the R^2 value of 1.

Year	F10	F12	F14	F15	F16	F18
1992	**0.908**					
1993	**0.936**					
1994	0.924	0.907				
1995		**0.918**				
1996		**0.932**				
1997		**0.925**	0.910			
1998		0.954	**0.972**			
1999		**1.000***	0.972			
2000			0.928	**0.932**		
2001			0.945	**0.959**		
2002			0.920	**0.966**		
2003			**0.943**	0.931		
2004				**0.948**	0.904	
2005				0.934	**0.939**	
2006				0.939	0.920	
2007				0.901	**0.951**	
2008					**0.945**	
2009					**0.892**	
2010						**0.846**
2011						**0.910**
2012						**0.939**

Table 5.2: Statistical calculation applied to track the temporal dynamics of stable nightlight.

Name	Spatial extent	Value restriction	Purpose
Average	All PAs in California	$DN > 0$	Trend of change in DN
			PAs in each ecoregion
			Trend of change in DN for each ecoregion
Quantile	All PAs in California	$DN > 0$	Trend of change at different levels of DN
	PAs in each ecoregion		Trend of change at different levels of DN for each ecoregion
Histogram	All PAs in California	$DN > 0$	Frequency of distribution
		$0 < DN <$3rd quantile	Frequency of distribution for low DN
		$DN >$3rd quantile	Frequency of distribution for high DN
Histogram	PAs in each ecoregion	$0 < DN <$3rd quantile	Frequency of distribution for low DN in each ecoregion
		$DN >$3rd quantile	Frequency of distribution for high DN in each ecoregion
Skewness	All PAs in California	$DN > 0$	Asymmetry of distribution of DN
Kurtosis	All PAs in California	$DN > 0$	Tailedness (presence of outliers) of DN
t-test	PAs in each ecoregion	1992 and every following year	Evaluate the significance of change compared with 1992
		Current year and the previous year	Evaluate the degree of fluctuation

medium (11–20), high (21–62), and very high (> 62), then employed two types of analysis based on the classification to study how the nighttime light inside PAs moved along the gradient of development from 1992 to 2012. The first was to detect the change of HFI at different levels of DN from 1992 to 2012. This helped to translate the spatial change of DN to a more meaningful indicator of human activity. For example, a decrease of average HFI for a given class of DN from 1992 to 2012 indicates this class moves to a traditionally (2004 level) less developed area. The second was to calculate the transition matrices of six levels of DN values between three key timing points (1992, 2000, and 2012) to obtain the from-to change between different levels of DN values. The trend detected by the inter-class conversion reflected the spatial migration of hotspot of stable nighttime light.

We also mapped the spatial distribution of nighttime light in multiple years to provide intuitive illustration of change in space. However, the small proportion of lit area ($DN > 0$) in California PAs made it difficult to map and detect the hotspots of change in stable nighttime light. We calculated the kernel density for several years of significance with the search radius of kernel (bandwidth) determined by the standard distance [Mitchell, 2005].

The kernel density maps not only smoothed the lit area to obtain a more intuitive mapping of stable nighttime light, but also illustrated the concentration and compactness of lit clusters (hotspots) in PAs. By mapping and comparing the kernel density of nightlight between different years, we can track the migration of the hotspots of lit area.

5.2.4 Spatial Modeling between Socioeconomic Variables and Stable Nighttime Light

We conducted geographic weight regression (GWR) models for years with census tract level demographic data available to investigate the relationship between population and the stable nighttime light inside PAs. We employed the GWR models to address the significant spatial autocorrelation between the explanatory and dependent variables [Fotheringham et al., 2003, Pez et al., 2011]. Only a subset of census tracts with the centroid located inside the PAs were included in the modeling to minimize the uncertainty introduced by the boundary offset between census tracts and PAs. The geographic weight matrix was generated using the Gaussian scheme [Fotheringham et al., 2003]. We reported the local R^2 at each census tract, the quasi-global R^2 and the Akaike information criterion corrected for finite sample sizes (AICc) as the measurements of model performance.

5.3 Results

5.3.1 Trend of Lit DN in California PAs (1992–2012)

The average, quantiles, pattern of frequency distribution, as well as the kurtosis and skewness of non-zero DN (hereafter referred as lit DN) from 1992 to 2012 in California PAs all demonstrated a decreasing trend, although fluctuation existed and trend was different between radiation calibrated and non-radiation calibrated nighttime light products.

The average lit DN in California PAs had a decreasing trend in general starting from 1992 (Figure 5.4a). The average lit DN started off at a relatively high level, followed by a

sharp decrease, then reached a stable level with a slight increase from 1994 to 1999 and a decrease from 2000 to 2004, when the inter-calibrated nighttime DN reached the minimum of the entire time series. After 2004, an increase occurred, but the time section from 2004 to 2012 was relatively stable. Although the discrepancies existed between satellites, the sharp decrease from 1992 to 1994, the decrease from 2000 to 2004, and the increase from 2004 to 2009 can be identified from the nighttime images obtained by the same satellite in different periods (Figure 5.4b). Combining both calibrated and not calibrated nighttime light images, the trend of lit DN values in PAs started off at a relatively high level and decreased until the early 2000s, followed by an increase at a low magnitude.

The limited years available for radiance calibrated products made it difficult to evaluate the trend at the same length of time series as above. By comparing the radiance calibrated products with the non-radiance calibrated equivalent, we found the decreasing linear trend was consistent, except for the outlier in radiance calibrated data of 2004 (Figure 5.4a and Figure 5.5). The above comparison on average lit DN values between three stable nighttime light products (original, inter-calibrated, radiance calibrated) indicated that the average lit DN inside PAs generally decreased from 1992 to 2012, despite some inter-annual fluctuation.

Change in quantiles reflected the dynamic of lit DN values at low, medium, and high values. Despite the relatively stable time series of the minimum lit DN, the first, second, and third quantile of inter-calibrated lit DN values inside California PAs decreased consistently from 1992 to 2012, which was parallel to the trend detected in average lit DN. The magnitude of decrease was greater in larger quantiles (Figure 5.6). The similar trend was also detectable from lit DN without inter-calibration. The downward trend was consistent in different levels of lit DN, while the higher DN values contributed greatly to define the overall trend in average. Sometimes it even overrode the opposite trend of the lower values. The trend of lit DN in radiation calibrated data was a good example. Although there was a slight increasing trend in lower lit DN values, the decrease in the third quantile cancelled out the opposite trend of the smaller DN values, which made the average lit DN values decrease from 1996 to 2010 (Figure 5.7). The great gap between the median and average of lit DN in PAs (29% to

44% of average) should be addressed in the following analysis to understand the temporal change of lit DN.

5.3.2 Change of DN Value at Different Levels

The inter-annual comparison between the shape of frequency distribution revealed the different roles of lower and higher lit DN values in defining the overall temporal trend of stable nighttime light inside PAs. Both skewness and kurtosis indicated the distribution of lit DN moved to lower DN values and the high to very high values became less available during the past two decades (higher kurtosis). Despite some fluctuation (1996–1997, 2007–2009), both the skewness and kurtosis increased significantly from 1992 to 2012 (Figure 5.8), so does the radiance calibrated data (Figure 5.9). The increase of a positive skewness indicated the distribution of frequency becomes left-skewed, associated with a movement of peaks toward the lower values. The increase of kurtosis indicated that the distribution of frequency contained more outliers, which were mostly the high DN values. The presence of high value outliers was associated with the increasingly left-skewed DN distribution.

A detailed comparison between peaks and tails from 1992 to 2012 confirmed the above trend detected from skewness and kurtosis. Peaks of histogram were mostly located near the minimum of lit DN (3–5), especially from 1992 to 2003. These peaks at lower values either grew higher or moved leftward from 1992 to 2012 or during the years with lower DN average, both indicating a downward change of lit DN (Figure 5.10-5.11). The histogram focusing on DN values lower than the third quantile illustrated such pattern with more details (Figure 5.12). Although years with higher average DN had a longer tail in frequency distribution, frequency of DN with high or very high value was not high enough to define the overall trend. On the basis defined by the peaks at low DN, medium DN values (6-15) greatly contributed to the overall trend through the relatively high frequency than higher DN and the greater DN values. And this was the value range of most third quantiles from 1992 to 2012 (Figure 5.6). In this value range, years with higher average DN usually had a higher frequency (e.g. 2004 in Figure 5.12). From the above comparison, we found that the medium values greatly

contributed to decreasing trend through the higher DN with enough frequency to become significant, while the lower DN values played an important role in defining the trend of lit DN values inside PAs because of the high frequency.

The comparison between different value ranges of DN provided a more detailed analysis of the difference in contribution to shape the decreasing trend in lit DN. Consistent with the average DN inside PAs, the areas with medium to high values ($DN > 10$) decreased from 1992 to 2010 (Figure 5.13), which supported the significant contribution to the downward trend of the average from higher DN values. The low DN values (3–5) experienced an increase from 1992 to 2004, which was consistent with the growth of low value peaks in the histogram during this period. After 2004, there was a significant increase in medium low DN values, reflecting the slight increase in the lit average.

The simultaneous increase/decrease between DN classes can be better understood by the transition matrices between 1992, 2000, and 2012. From 1992 to 2000, the three lowest DN value classes were the biggest change-to classes, while the greatest change-to percentage was found in DN between 5 to 10. The medium and high value DN classes mostly converted to the closest lower DN class (Table 5.3a). For example, the greatest percentage of change occurred from DN between 10 and 20 to DN between 5 to 10 (77.83%). The same decreasing trend continues from 2000 to 2012. The highest DN value class ($DN = 6263$) was completely converted to a lower level (Table 5.3b). In summary, the conversion from 1992 to 2012 was dominated by a conversion from higher DN to lower DN (Table 5.3c), which also confirmed the decreasing trend detected by average, quantiles, and distribution of frequency.

5.3.3 Difference of Changes between EPA Level III Ecoregions

The trend in average and the quantiles of all ecoregions was mostly consistent with the overall decreasing from all PAs, though spatial heterogeneity existed. All ecoregions had a relatively sharp decrease from 1992 to 2000, then followed by a stable period or even an increase in mid to late 2000s (e.g.Central Basin & Range, Northern Basin & Range), despite

Table 5.3: Transition matrices between 1992, 2000, and 2012 in California PAs, using calibrated nighttime light series. Area above 20% were shaded in red.

a) 1992-2000

		DN <=1	3<DN<=5	5<DN<=10	10<DN<=20	20<DN<=62	62<DN<=63
1992 DN Values	DN <=1	97.46%	1.55%	0.95%	0.04%	0.01%	0.00%
	3<DN<=5	39.39%	25.76%	34.85%	0.00%	0.00%	0.00%
	5<DN<=10	12.78%	16.60%	68.53%	2.04%	0.04%	0.00%
	10<DN<=20	0.47%	0.07%	77.83%	20.31%	1.33%	0.00%
	20<DN<=62	0.00%	0.00%	1.04%	35.11%	63.62%	0.23%
	62<DN<=63	0.00%	0.00%	0.00%	0.00%	36.84%	63.16%

b) 2000-2012

		DN <=1	3<DN<=5	5<DN<=10	10<DN<=20	20<DN<=62
2000 DN Values	DN <=1	99.48%	0.17%	0.35%	0.00%	0.00%
	3<DN<=5	69.03%	8.02%	22.95%	0.00%	0.00%
	5<DN<=10	19.14%	3.25%	76.66%	0.93%	0.03%
	10<DN<=20	1.75%	0.29%	53.14%	41.17%	3.65%
	20<DN<=62	0.17%	0.00%	2.41%	33.51%	63.92%

c) 1992-2012

		DN <=1	3<DN<=5	5<DN<=10	10<DN<=20	20<DN<=62
1992 DN Values	DN <=1	98.68%	0.28%	1.01%	0.02%	0.00%
	3<DN<=5	67.68%	8.08%	24.24%	0.00%	0.00%
	5<DN<=10	29.29%	6.48%	63.20%	0.98%	0.04%
	10<DN<=20	1.60%	0.00%	90.08%	7.52%	0.80%
	20<DN<=62	0.00%	0.00%	14.48%	41.83%	43.68%
	62<DN<=63	0.00%	0.00%	0.00%	0.00%	100.00%

the great difference in the average (Figure 5.14). Similar as found in all lit DN of PAs, the change of quantiles was consistent with the average in all ecoregions. However, the higher values (the third quantile and the maximum) played a more important role in defining the shape of dynamic at the ecoregion level (Figure 5.15), especially for ecoregions with a lower average lit DN (e.g. Cascades, Klamath Mountains) or containing a stable developed area (e.g. Central California Foothills & Coastal Mountains, Central California Valley, Southern California & Northern Baja Coast). The lit area with higher DN values was not evenly distributed between ecoregion. Such difference resulted in the amplified contribution from higher DN values to ecoregions with high wilderness.

Despite the downward trend was detected from most ecoregions, we also evaluated the significance of the change and the magnitude of fluctuation observed from the inter-annual difference of DN values in PAs. Two groups of t-test results indicated that the significance of downward trend and fluctuation differs by space (i.e. ecoregion in this study). In the $t-test$ between the year 1992 and all the following years, 7 out of 12 ecoregions had more than 75%, if not all years after 1992 significantly different from their initial status, including three ecoregions with all years significantly different from 1992 ($p < 0.05$) (Figure 5.16a). The rest ecoregions with much less significant difference compared from 1992 indicated the value difference detected in above results was not great enough to fundamentally change the lit levels at night in these ecoregions. This study helps to identify the ecoregions worth for the following analysis of change. On the other hand, the t-test between the current and the previous year of all years after 1992 helped to identify the key period of great fluctuation. The most frequently found period with significant fluctuation compared with the previous year was around 2000 (Figure 5.16b), which indicated the following analysis should also include 2000 as a key transition year to understand the temporal trend of lit DN in California PAs.

Similar as for all lit areas in California PAs, we also compared the change of lit areas at different DN value ranges to understand the contribution from different DN levels to the overall trend of lit DN between ecoregions. Despite the offset between area percentage of each class, all ecoregions in our study followed the same pattern and had the same turning point at 2004, though spatial heterogeneity existed (Figure 5.17). Because of the high proportion in lit area of PAs, DN from 3 to 5 and 6 to 10 were the most distinguishable classes in most ecoregions, except for Southern California & Northern Baja Coast. The latter had a much higher percentage of relatively high DN values than rest of ecoregions.

5.3.4 Migration of Hotspot of Lit DN along the Gradient of Human Development

The conversion from high to low DN values since 1992 reflected a shrinkage of medium to high DN pixels in PAs, but cannot answer the question that which direction along the

gradient of human development level these areas migrated to. There is a need to interpret such change and conversion with a baseline of human development level (e.g. HFI). Despite the relative stable max DN above 62, the average HFI inside medium to high DN values ($DN > 10$). In contrast, the average HFI of lower DN values decreased after 2004, when the conversion from higher to lower DN classes accelerated (Figure 5.18). Combining both results, we found that areas with higher DN did not just shrink, but shrank to the area closer to the core development regions, while the areas with lower DN expanded apart from the more developed regions.

The above changes detected by comparing average HFI inter-annually were also found in the maps of kernel density for lit nightlight area. Taking the region with the largest lit area (southern California) as an example, the core area of high nightlight DN values (yellow part, kernel density between 0.92 and 5.4 in Figure 5.19) continued to grow smaller in 1992, 2000, and 2012. And these areas moved toward the more developed major metropolitan areas such as Los Angeles and San Diego. In contrast, areas with a lower DN value expanded from more rural area toward the metropolitan regions (green part, kernel density between 0.045 and 0.17). The only exception in southern California was the corridor along highway I-15 (penetrating into Mojave Desert). The lit area along this corridor became more connected from 1992 to 2012. The similar shrinkage of high DN areas and the expansion of low DN areas was also detected in all PAs inside California in our analysis (Figure 5.20a-c), both the Bay Area and Southern California PAs experienced the same trend. However, the radiance calibrated results were different, mostly because of extraordinary high average lit DN in 2004. Comparing the earliest (Figure 5.20d) and the latest radiance calibrated results (Figure 20f), the area with the highest kernel density was smaller, yet the medium DN value areas had a higher coverage. Generally speaking, the magnitude of decrease detected from the radiance calibrated was smaller than the non-radiance calibrated products.

5.3.5 Understand the Change of Lit Area in PAs with Population

Considering the availability of socioeconomic variables and the rural location of most PAs, we employed the census tract level population density as the explanatory variable to understand the distribution of lit area inside California PAs. Since there was not enough census tract level data for the period of study, we focused on investigating the spatial distribution of relationship between nighttime light and the population density in multiple years (2000, 2009-2012) by geographic weight regression (GWR) models for all census tracts inside California PAs. The quasi-global R2 of GWR models indicated the correlation between population density and nighttime light was high, especially in census tracts of southern California, inner land desert, and foothills of Sierra Nevada (Figure 21). Such correlation in census tracts in the Bay Area, however, was not as high as other ecoregions. In terms of inter-annual comparison, the GWR model of 2000 worked the best among the five models ($R^2 = 0.722$) because of the high correlation in census tracts along Sierra Nevada foothills. Because of the limited years applied in GWR modeling, we did not report the temporal trend of change in model performance. However, we were able to find during the years when census tract level GWR modeling were applied, only a few census tracts had a significant change in the correlation between nighttime light DN values and population density. They were located along the Sierra Nevada Mountains and the inner land of Mojave Desert, as well as along the Coastal Ranges (Figure 5.21). In summary, the correlation between non-zero nightlight DN and population density was significant and relative stable, but varied across different ecoregions in California.

5.4 Discussion

5.4.1 Change of Lit Area in Time and Space

The rapid population growth and urban sprawl in California during the past two decades and the increasing of awareness in wilderness conservation were both driving forces of change in

stable nighttime light change in California PAs and can lead to opposite trend of change. Assessment focusing on adjacent area, especially the metropolitan areas close to California PAs revealed the increasingly severe ecological pressure brought by the boom of population and spread of urbanized areas [Aubrecht et al., 2010, Wilson et al., 2015a, Wilson et al., 2015b]. However, the benefits from the establishment of PA networks in California cannot be ignored. With 148 designated wilderness areas and highest number of national parks, California is the an intensively monitored region for conservation. The continued work on constraining human activities and development inside PAs has removed a number of human settlement, mining infrastructure, and animals that used to be a threaten of wilderness. The decreasing trend reflected in previous results through the change of average, quantiles, histograms, skewness/kurtosis, and transition matrices between key timing points demonstrated the effectiveness of PA management and conservation inside the boundaries of PAs.

The large areas covered by low DN values inside PAs made the areas with higher DN an important factor to determine the direction of change, especially if PAs are located close to a major metropolitan area. Evaluating the direction of movement for DN hotspots, toward the core area of development (e.g.metropolitan area) or wilderness, reflected the effective removal of area with high DN. Although some of the low value DN converted back to the medium low class after 2004 and finally caused a slight increase during this period, the elimination of area with high DN was consistent, which contributed greatly in the general decrease of lit area inside PAs. Considering the large radius of influence from the artificial skyglow, limiting the area covered by high DN values, especially the human settlements should be of the great priority to reduce the negative influence to wilderness inside PAs.

However, the decrease of lit area inside California PAs needs more careful scrunity, since the inter-calibration model may introduce uncertainty to the data for analysis. In order to make full use of the available DMSP-OLS stable nighttime light data series, we applied the inter-calibration method designed to cover the longest available time series of nightlight (1992 to 2012). It is also necessary to compare the results yielded from different inter-calibration methods to reduce the uncertainty from data manipulation, which can possibly generate

misleading results regarding to the trend of change [Liu et al., 2012, Wu et al., 2013].

5.4.2 Spatial Heterogeneity in the Correlation between Lit Area in PAs and Population Density

From the analysis above, we can confirm that the lit areas at night in California PAs decreased from 1992 to 2012 in general, though spatial heterogeneity existed in terms of the degree of change. In addition, the lit areas also shrank toward the better developed area and retreated from the core part of PAs. Because of nighttime light is highly correlated with population and other economic variables as indicators of development, we anticipated a higher average nightlight in highly populated census tracts intersecting with PAs. However, the GWR model results for selected years revealed the existence of a great spatial heterogeneity in the correlation between population density and average nightlight. The contrast between southern California and the Bay Area in the correlation is a good example of such difference. We will explain the difference in the performance of GWR in different locations by the spatial characteristics of census tracts and the data manipulation involved in demographic data.

The size of census tracts played an important role in the model performance since it defined how much proportion of PAs was involved in modeling. Regardless of the size and extent of census tract, the demographic data use one population count value (or population density) as the representation of population inside the entire spatial extent defined by the boundary of census tract. In more populated regions, the size of census tract is much smaller than rural area (e.g. the comparison between Bay Area census tracts and Mojave Desert census tracts). In rural area, since a large proportion of PAs fell into the boundary of census tracts (Figure 5.1), the population of these census tracts is a good representation of the stable settlement inside PAs. This explained the relatively higher correlation between population density and the average nightlight in relative larger census tracts of inner land desert and a part of Southern California (Figure 5.19). For smaller census tracts, if the boundaries are highly overlapped with the extent of PAs, the correlation can still be high, such as the relatively high correlation in smaller census tracts near southern California metropolis area.

In contrast, the spatial extent of census tracts in the Bay Area was less overlapped with the boundaries of PAs, which made the GWR modeling results less significant compared with other regions. The biased population measurement used to represent the human settlement inside PAs is the major factor of relatively low local R^2 in the Bay Area.

5.4.3 Evaluating the Explanatory Capability of Population for Lit Area at Night in PAs

Because of the lack of a good continuous demographic time series at or below census tract level from 1992 to 2012, we cannot provide a full picture of the correlation between the lit area at night and population of this period to comprehensively evaluate the effectiveness of explanatory capability of population, the only socioeconomic explanatory variable we used in this study. However, the comparison between multi-year GWR models revealed that such effectiveness was not always high. We can explain the difference in model performance by the uncertainties introduced by both population and nighttime light data.

By comparing the R^2 and AICc of five GWR models, we found although most regions had a stable model performance among the five years, there was a decrease in the general performance of model (Figure 5.21). The year 2012 had the lowest local R^2 in Sierra Nevada, where the most significant difference between GWR models occurred (Figure 5.22). In the year 2012, the population density of Sierra Nevada ecoregion (blue dots in Figure 5.23) were more closely concentrated near zero than the other four years. According to the average of lit DN (Figure 5.14) and t-test results (Figure 5.16), there was not a significant decrease in average nighttime light during this period of study inside this ecoregion, indicating such decrease was not great enough to drive any significant trend in nighttime light, though the maximum DN in this area decreased significantly (Figure 5.15). The explanatory capability of the human settlement on the coverage of lit area at night may have reached its limit because of the high wilderness in the Sierra Nevada ecoregion and the well maintained monitoring network of PAs, indicating no more significant correlation can be detected if the human settlement continued to be removed from this area.

Some limits in the stable nightlight light data we employed in this study also influenced our analysis in the explanatory effectiveness of population. Similar as the lower limit set by the small human settlement in the predictive capability of population to the nightlight, the upper limit of the population-nightlight correlation in this study was generated by the saturation issue of the DMSP-OLS stable nightlight data. Because of the saturation, the correlation between average DN and population density in areas where average DN was greater than 60 was generally poor (Figure 5.23). Since the nighttime DN reached its maximum of dynamic range at 63, there was not a valid nighttime DN to reflect the greater population of these areas. If this section can be excluded, the linear relationship between average DN and population density should be more obvious, indicating an improvement in the effectiveness for population to explain the spatial coverage and temporal dynamics of nighttime light. In summary, although the GWR models indicated the correlation between population density and nighttime light was significant and reliable, there is a need to conduct such evaluation with a better time series data for PAs for both the explanatory variable and the nighttime light itself.

Even if we obtained a solid relationship in space between population density and stable nighttime light, the temporal change of population and the nighttime light as we detected seemed to be contradictory: how to explain the decrease of nighttime light inside California PAs at the same time of a significant increase of population in California? The possible reason can be the effective establishment of PA network and execution of wilderness restoring strategies. Although the population in California increased during our period of study, the establishment of PAs also increased, and the land management strategies inside PAs have been focused on human settlement removal and re-planning during the past two decades. This helped to remove or decrease the residential population inside PAs. By comparing the population density between 2000 and 2012, the population of many inland census tracts remained relatively stable. The increase of population density mostly occurred in southern California (San Diego) and some near the Bay Area. Several census tracts covering PAs even had a loss of population during the study period (Figure 5.24). It challenged the assumption

of a confirmative increase of population in our study area. Considering the spatial migration pattern of different level of nightlight, there was an increase at the low level (DN = 3–10), which can be considered as an evidence of such removal and limitation of high density human settlement. Even if the population of the census tracts intersecting PAs had an increase, such increase was usually restricted outside the boundaries of PAs. Therefore, the population collected at census tract level and by traditional census survey may not always be the most accurate indicator of human activity inside PAs. A more precise measurement of population, or human activity is necessary to improve the quantitative modeling.

5.4.4 Interpreting the Decreasing Lit Area inside California PAs from the View of Policy Makers

The overall decrease of lit area inside California PAs needs locally specific discussion, especially for PAs located close to the major metropolitan regions, such as southern California and the Bay area. Although the comparison between ecoregions have indicated the decreasing trend in lit area was consistent across ecoregions, PAs adjacent to the highly developed areas are still under the influential radius of sky glow from cities, thus need special investigation. For example, the Santa Monica Mountain National Recreation Area (SAMO), located in the neigborhood of the city of Los Angeles, still maintains a number of settlements and receives sky glow from the city of Los Angeles as well as several major interstate or state level highways. Although we can observe a shrinkage of area with high DN value in the ecoregion of southern California mountain (Figure 5.19), PAs like SAMO may not always follow the same trend of the entire ecoregion. For local land managers, it is necessary to focus on the local specific conditions and address the most pressing needs by PAs.

If there was a confirmed decrease in stable nighttime light inside the PA, the local land manager should focus more on evaluating the existing sources of stable nighttime light to find out if it is necessary to eliminate them or reduce the intensity. At the same time, tracking the change of stable nighttime light or human activities at a different format is always a key task of land managers, especially for natural reserves, national parks, national monuments,

and national recreational areas [Gillespie et al., 2016]. If the local change of stable nighttime light or other format of human activity was opposite than what was detected for the entire ecoregion, the local land manager may concentrate on analyzing the recent change of stable nighttime light and find possible restoring strategies to eliminate or reduce the intensity of human activity, especially if it has become a threat toward the protection of wilderness.

5.5 Conclusion

In this study, we investigated the temporal dynamics and the change in spatial extent of stable nighttime light inside California PAs from 1992 to 2012 with a series of descriptive statistics. The comparison between multiple years for all EPA level III ecoregions in California indicated that there was a significant decrease in stable nighttime light of California PAs from 1992 to 2012. Such decrease mostly occurred in areas with relatively high nightlight, while area with relatively low nightlight experienced a slight increase, mostly converted from areas at a higher level of nightlight previously. Spatially speaking, the extent of higher lit area shrank toward the core area of development, while the relatively lower lit area expanded a little, claiming the area covered by higher nightlight before. Temporally speaking, the dynamic of nighttime light had some fluctuation. The turning point of change occurred between 2000 to 2004, when the relatively sharp decrease started from 1992 became more gradual. An increase at a low magnitude even occurred from 2006 to 2009. The GWR modeling between population density at census tract level and nighttime light indicated the population was a good explanatory variable of nighttime light coverage inside PAs in space. However, considering the uncertainties brought by both the spatial extent of census tract and the nighttime light data, this relationship requires further investigation. The significant decrease of lit area at night can be considered as a success of implementation of wilderness restoration and the establishment of PA network. And such success needs to be preserved by strict execution of natural conserve strategies. Conducted at a regional level, this analysis can also help the PA managers to evaluate the effectiveness of current strategy.

Based on the limits observed from the above result reporting and analysis, a series of improvement can be considered for further analysis. First, there is a need to separately consider the different levels of protection in evaluating the effectiveness of socioeconomic variables. This can help to reduce the uncertainty in GWR modeling. Second, the future studies should explore the possibility on exploiting the radiance calibrated data. In this study, because of the lack in demographic data during the years when radiance calibrated data were available, the regression modeling analysis was conducted on the non-radiance calibrated nighttime light, which may also be a possible source of uncertainty in the modeling. Third, combining nighttime light data from various resources, especially the in situ observation data can also help to address the uncertainty introduced from remote sensing data. For example, the sky quality index (SQI) from CCD camera obtained in a series of sites by NPS can be considered as validation data for calibration of DMSP-OLS stable nighttime light data (Figure 5.25). Last but not the least, the latest development of geotagging in social media can be the next step in collecting human activity information inside PAs, especially for national parks. This technology directly addresses the individual activity of human and provides precise record on the time and space of the activity [Levin et al., 2015]. Given enough consideration on data collection quality and self-trending issue from the access of internet and social media platform, this should be a new direction of studying anthropogenic influence in wilderness.

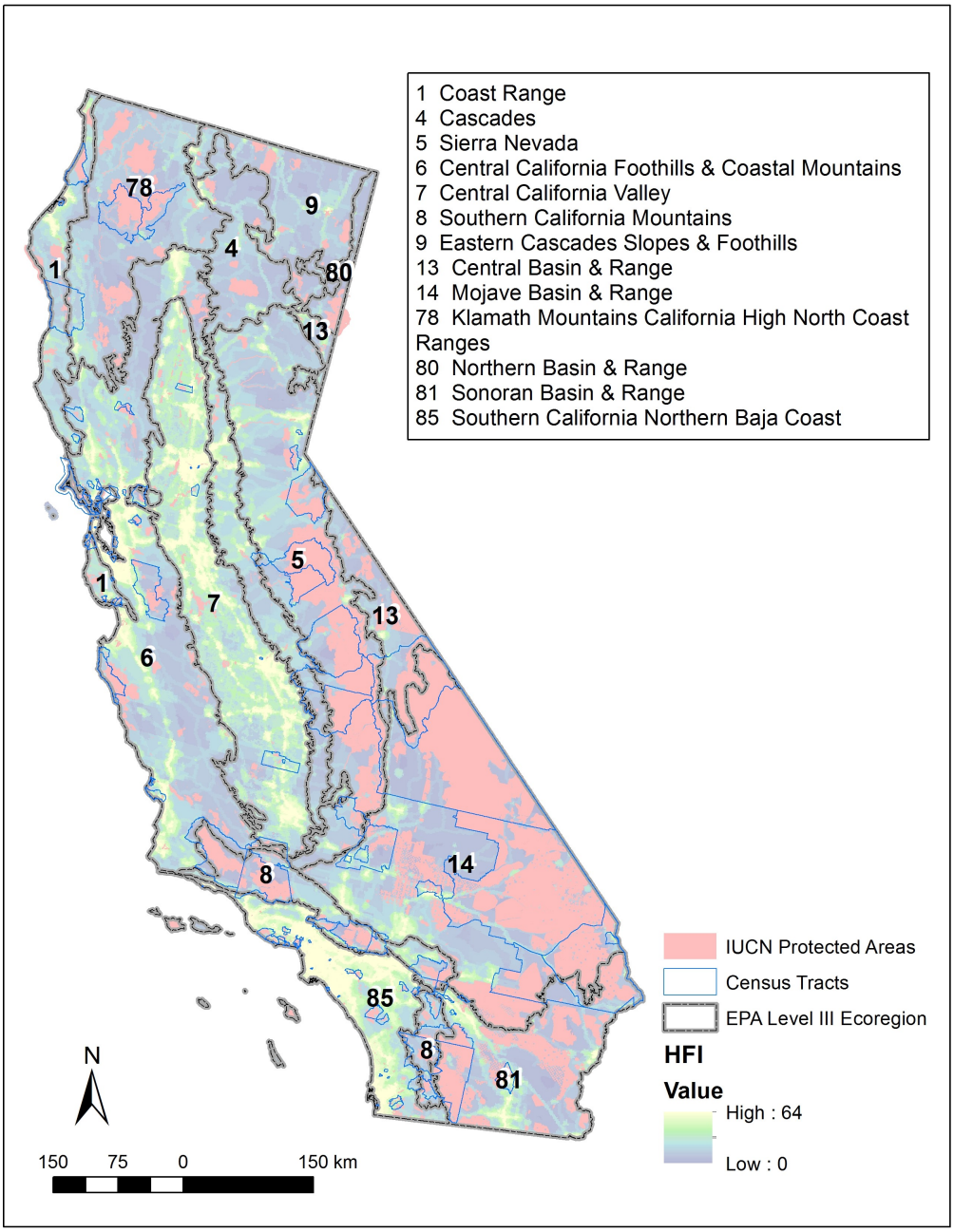

Figure 5.1: IUCN protected areas in California, with the background shaded by Human Footprint Index (HFI). Boundaries of EPA Level III ecoregions and census tracts intersecting PAs are also mapped for reference.

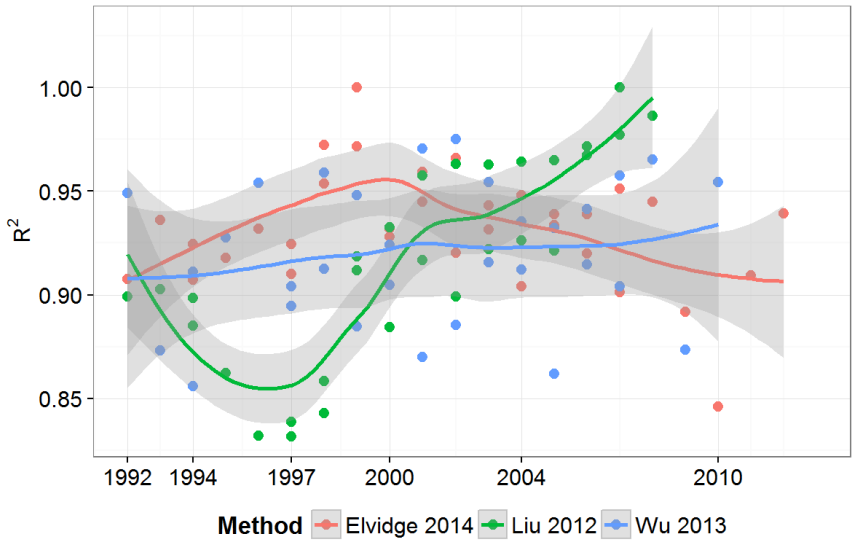

Figure 5.2: Compare three inter-satellite calibration methods. Elvidge 2014 and Liu 2012 used DMSP-OLS data of 1999 and 2007 as reference image, which led to an R^2 value of 1. Labels of x-axis indicate the start year of operation for different sensors.

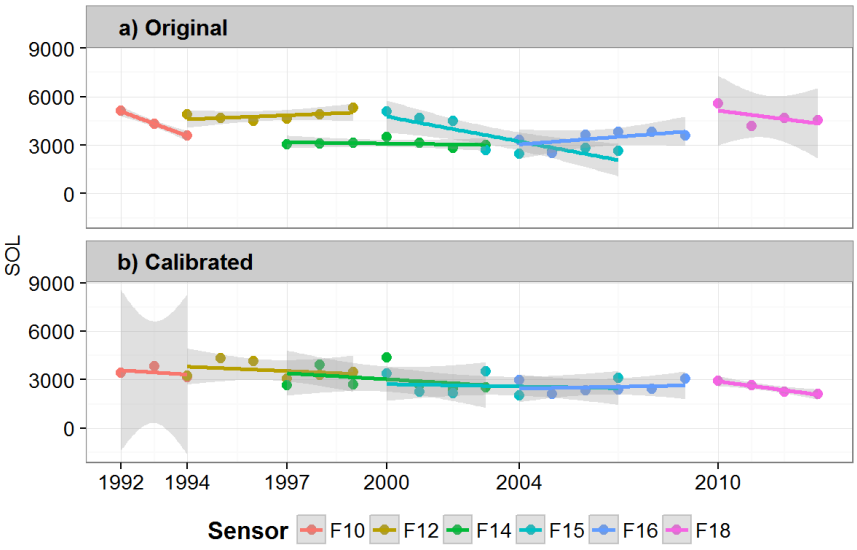

Figure 5.3: Compare Sum of Light (SOL) between non-calibrated and calibrated DMSP-OLS nighttime series. SOL values are shaded by satellilte, including a linear fit for the time series of each satellite.

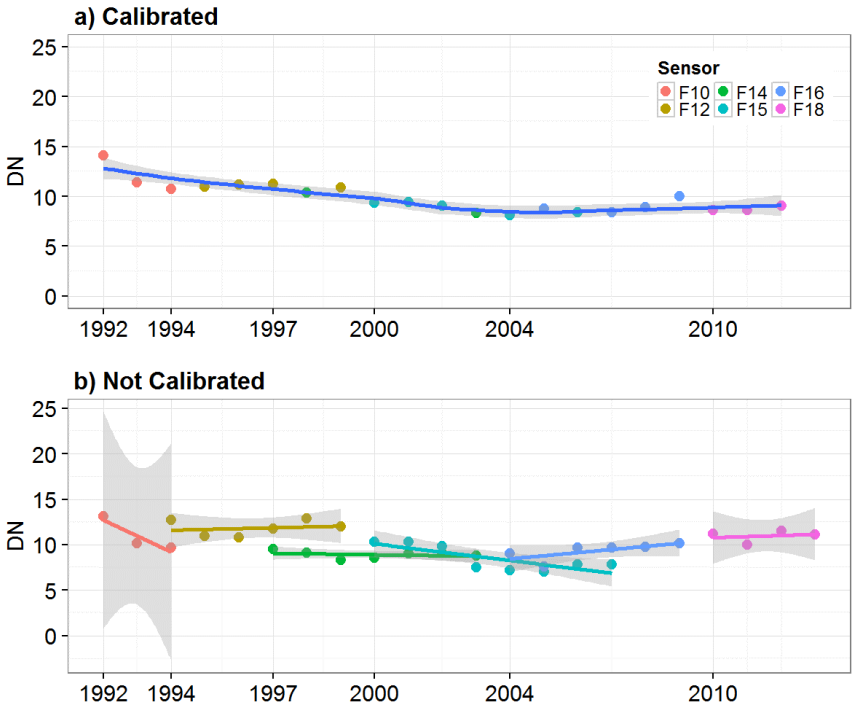

Figure 5.4: Mean of the non-zero nightlight DN in California PAs (1992 – 2013). Selected calibrated data were colored by sensors. Linear fit was added for average of non-calibrated DN values.

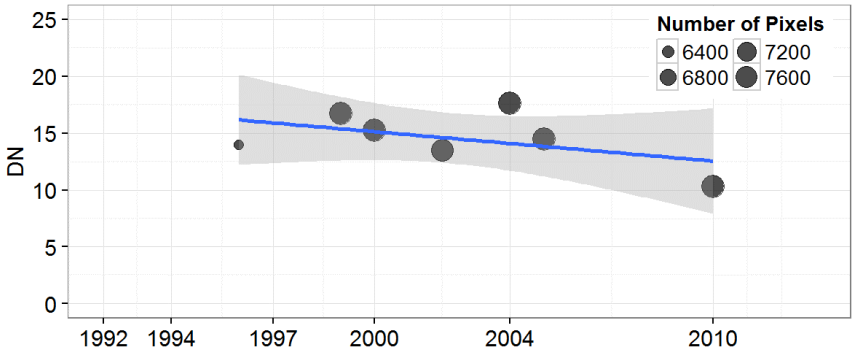

Figure 5.5: Mean of non-zero radiation calibrated nighttime light images in California PAs (1996–2010). Different sizes of points indicate the number of non-zero pixels in the nighttime light images.

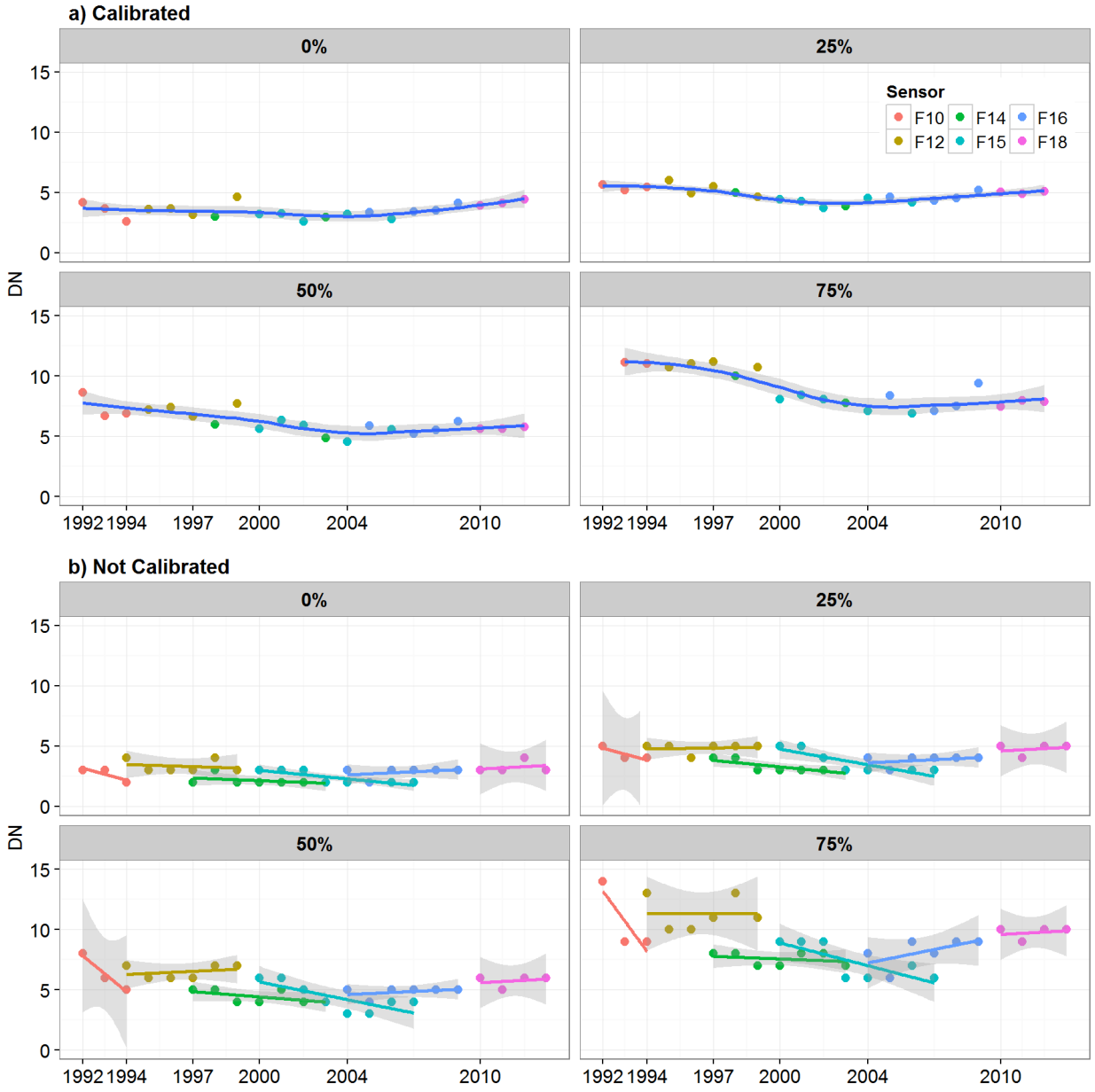

Figure 5.6: Quantiles of Non-Zero nightlight DN in California PAs (1992–2013). Selected calibrated data were colored by sensors. Blue curves in panel a) are loess smoothed fit curves; grey shades are 95% confidence region of curve fitting. Linear fit was added for average of non-calibrated DN values.

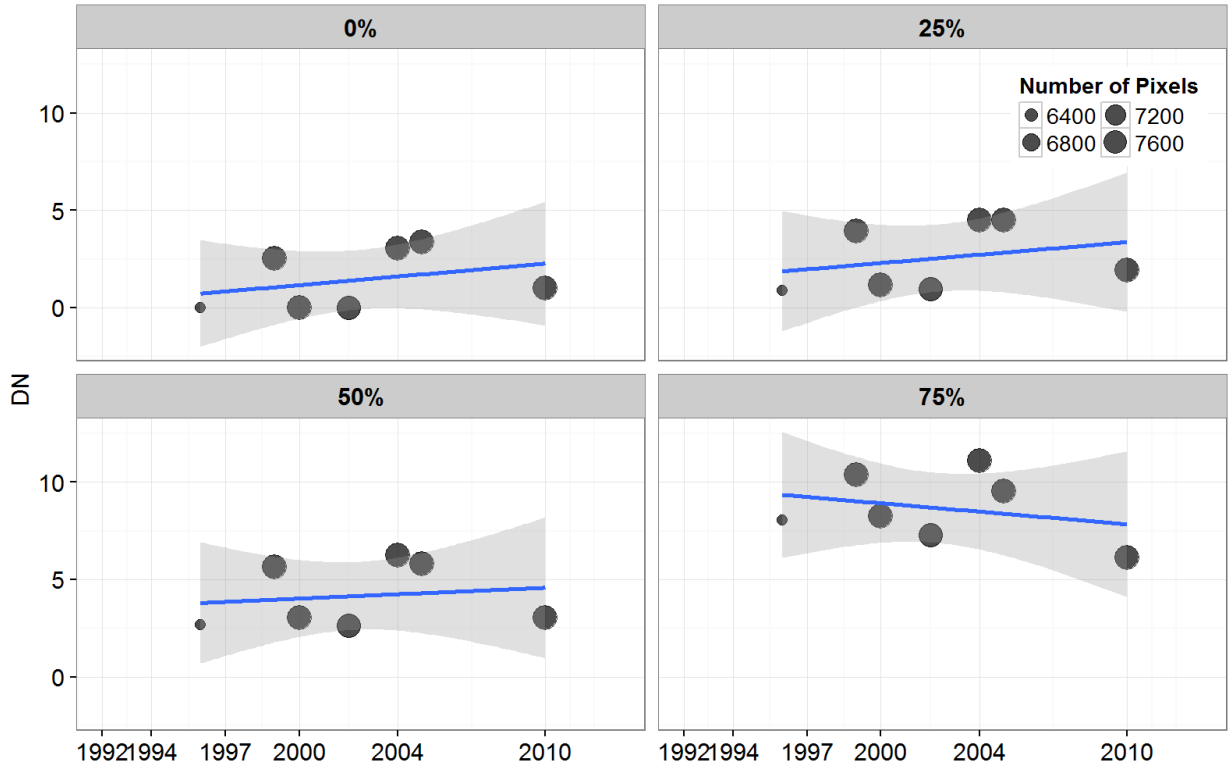

Figure 5.7: Quantiles non-zero radiation calibrated nighttime light images in California PAs (1996–2010). Different sizes of points indicate the number of non-zero pixels in the nighttime light images.

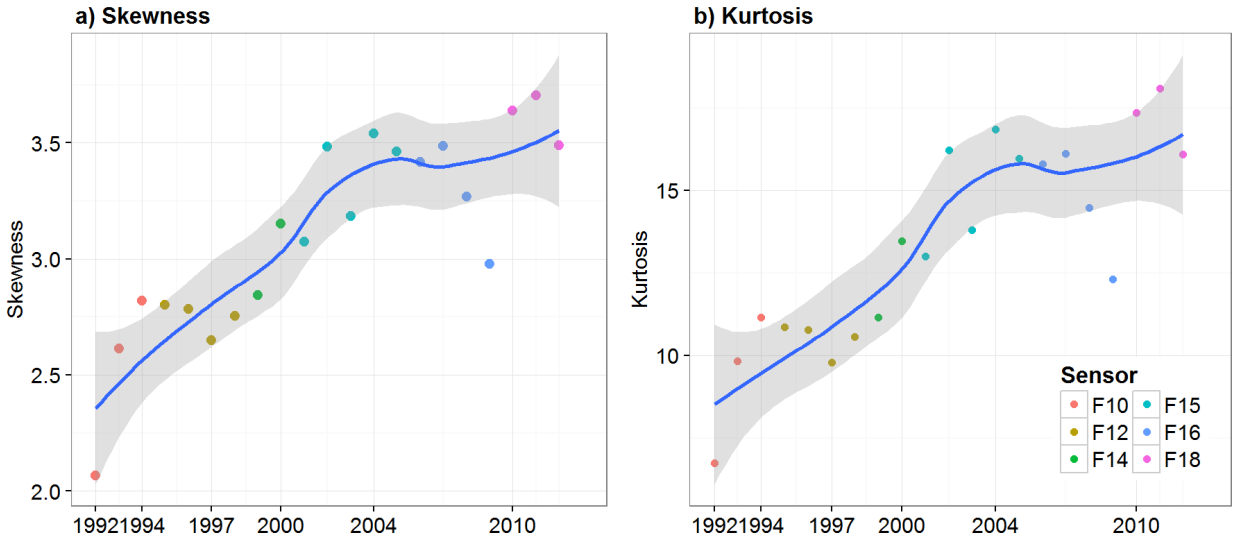

Figure 5.8: Skewness and kurtosis for nightlight above 0 for California PAs. Blue curves are loess smoothed fit curves; grey shades are 95% confidence region of curve fitting. Note that the skewness and kurtosis has different value ranges.

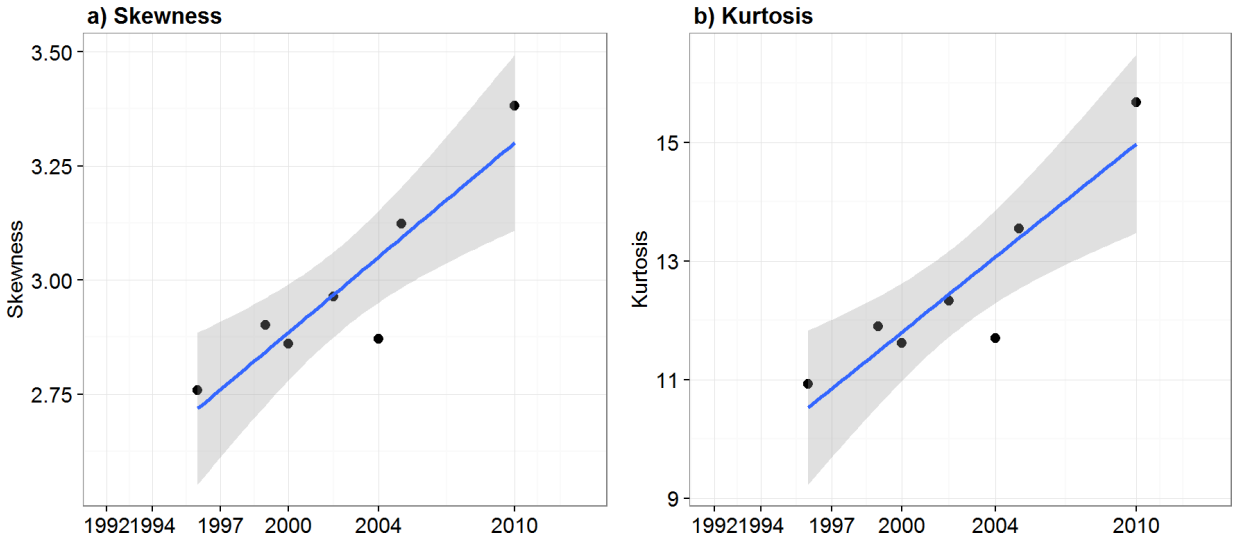

Figure 5.9: Skewness and kurtosis of radiation calibrated nighttime light images (DN = 0 63) in California PAs (1996–2010). Blue curves are linear fit lines.

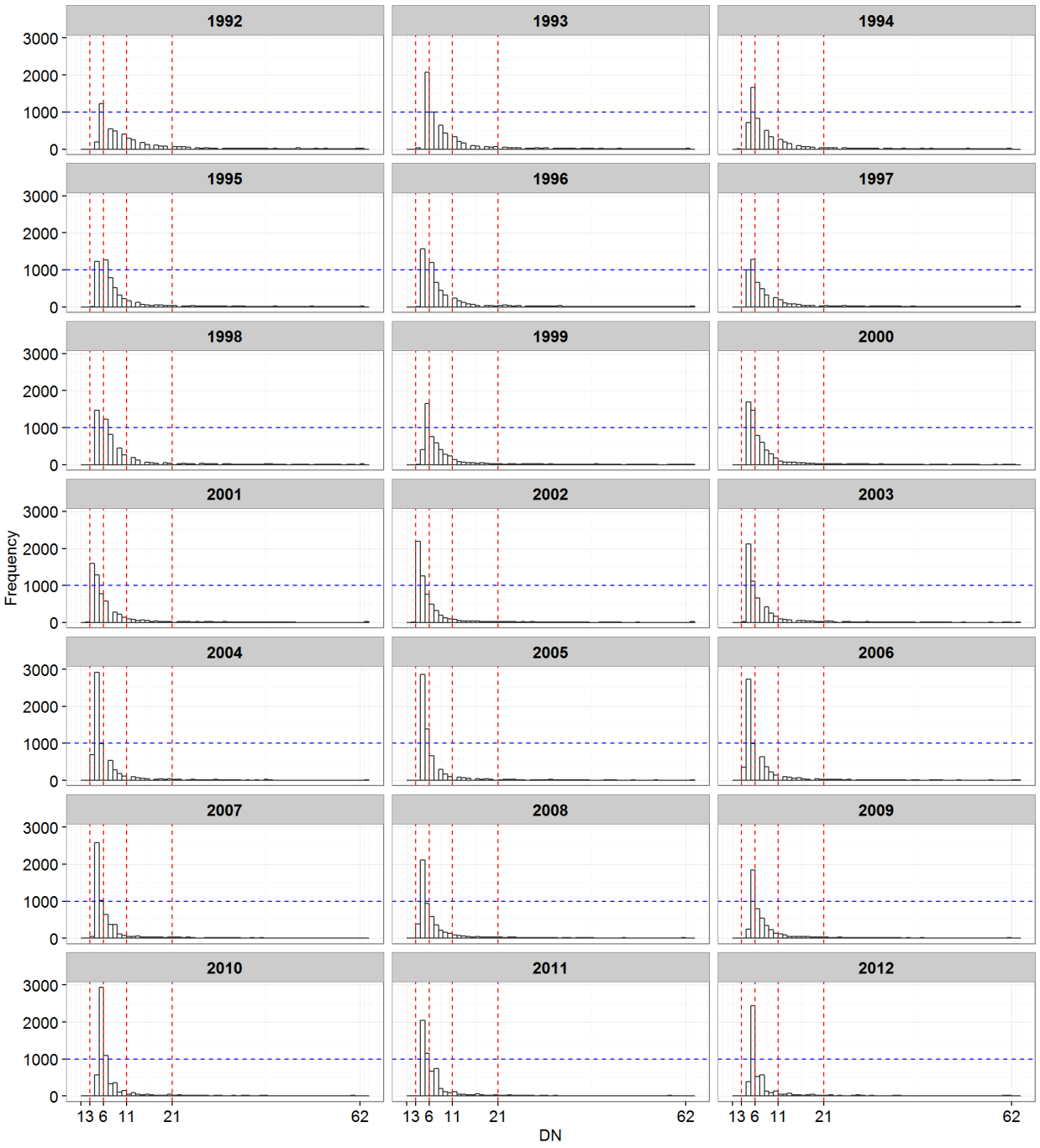

Figure 5.10: Histogram of nightlight above 0 in California PAs. Binsize of bars equals to one. Red dash lines are guidelines at frequency = 1000. DN values are broken into five sections to reflect the very low, low, medium, medium high, and high levels. Red dash line illustrates the different classes of DN values.

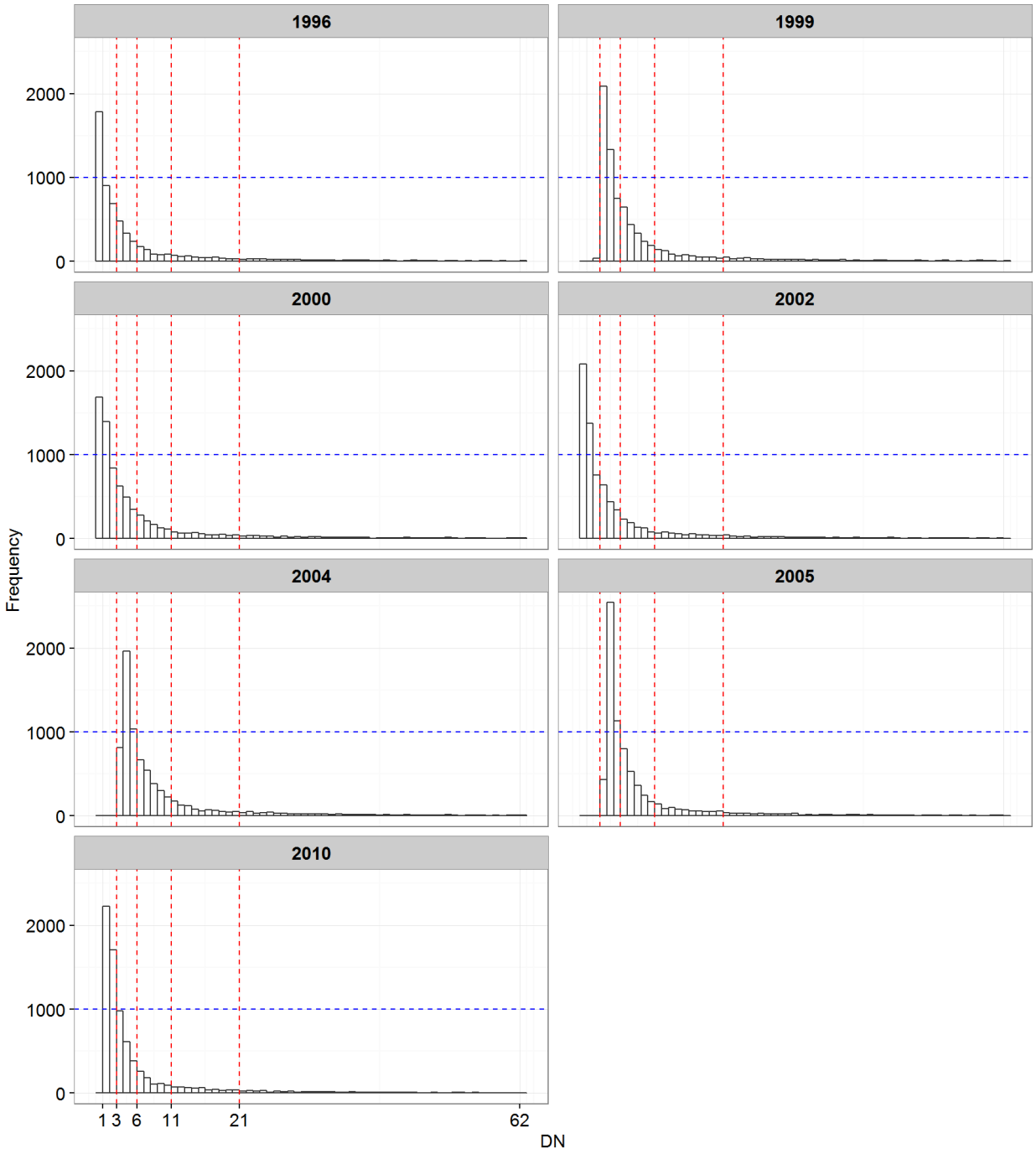

Figure 5.11: Histogram of non-zero radiation calibrated nighttime light images in California PAs (1996–2010). Binsize of bars equals to one. Red dash lines are guidelines at frequency = 1000. DN values are broken into five sections to reflect the very low, low, medium, medium high, and high levels.

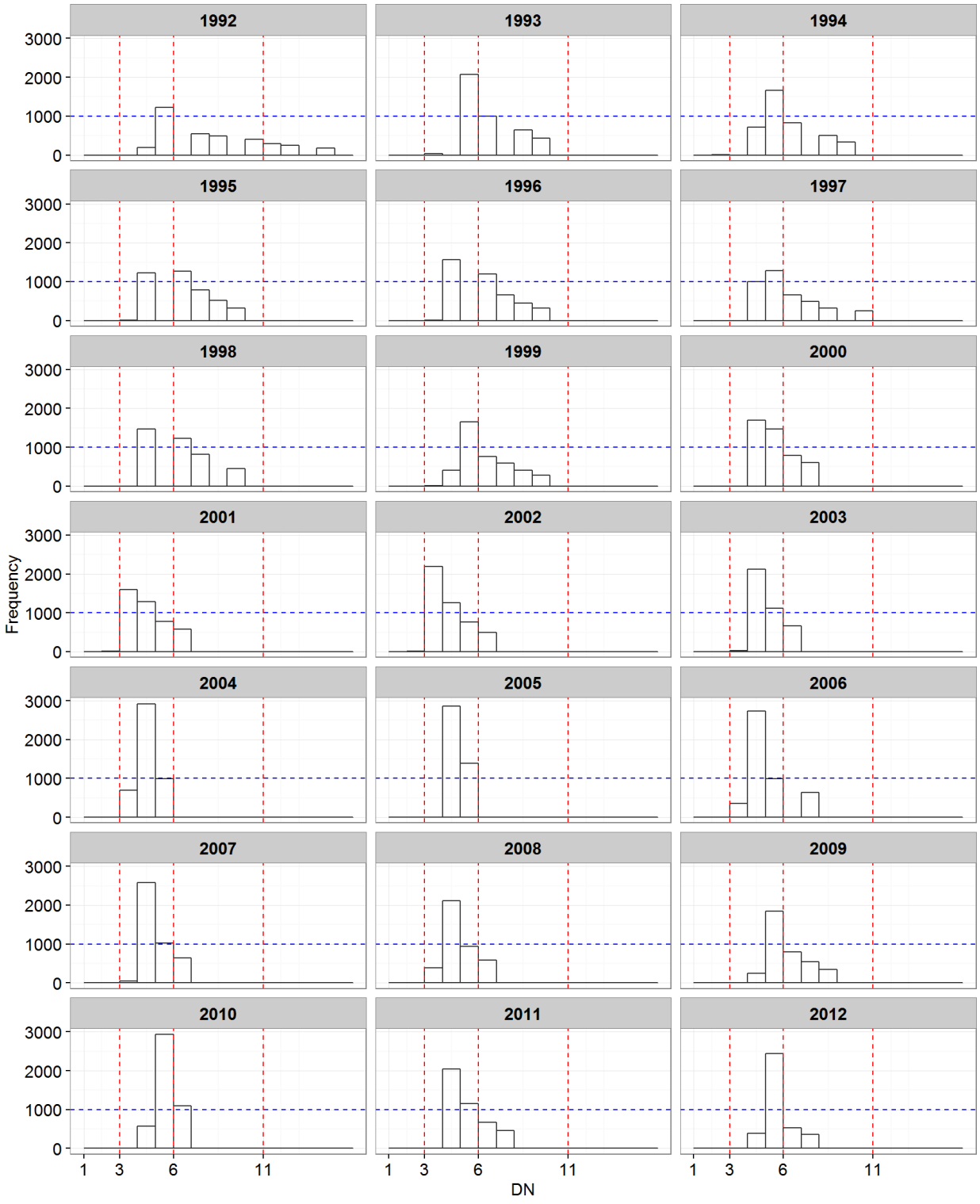

Figure 5.12: Skewness and kurtosis of radiation calibrated nighttime light images (DN = 0–63) in California PAs (1996–2010). Blue curves are linear fit lines.

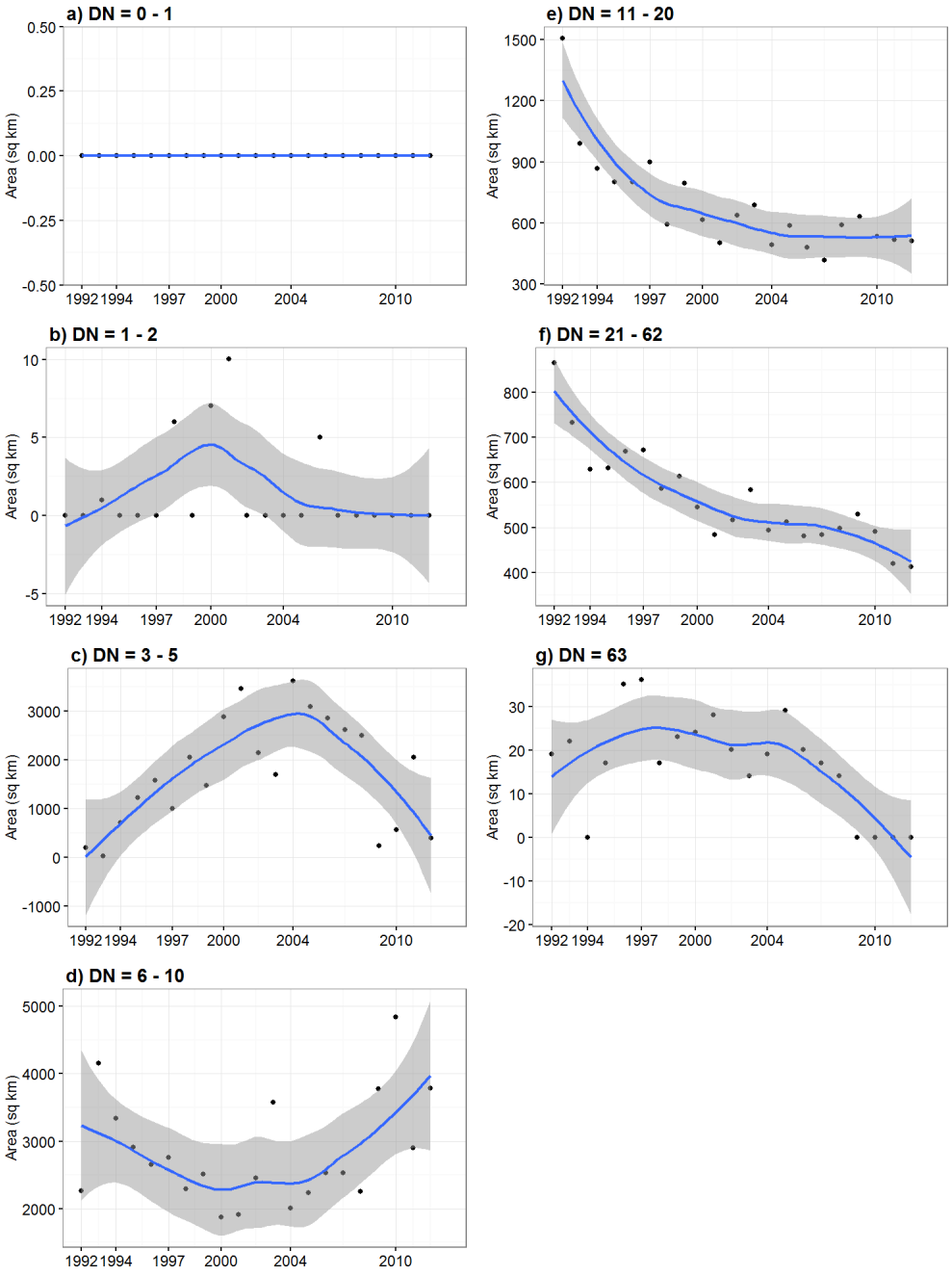

Figure 5.13: Change of area in each non-zero DN value range for Calfornia PAs. DN values are extracted from inter-satellite calibrated nightlight images. Blue curves are loess fitting curves for data of each value range.

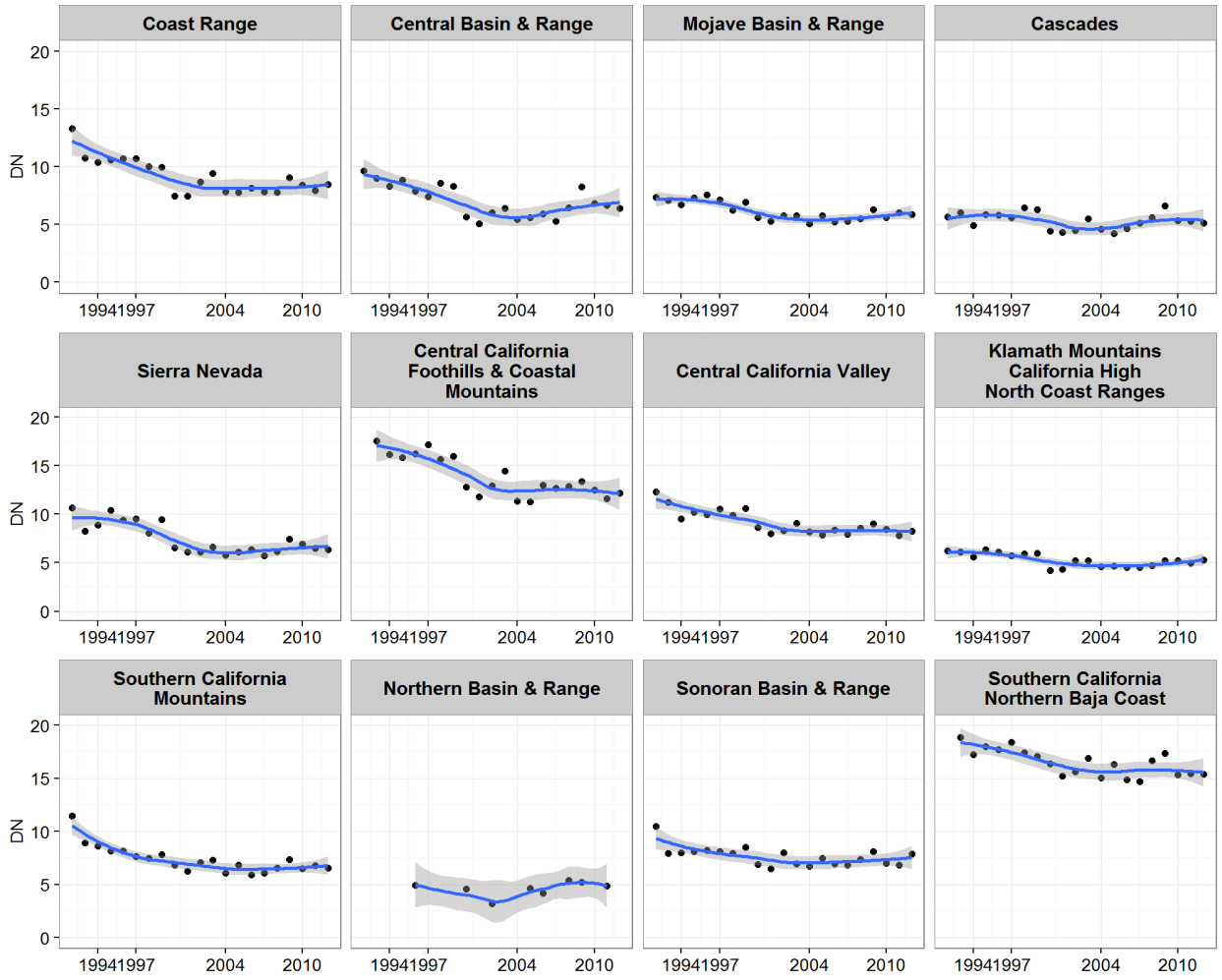

Figure 5.14: Average nightlight of California PAs inside EPA level III ecoregions. Only pixels with nightlight above 1 are included. Blue curves are loess smoothed fit curves; grey shades are 95% confidence region of curve fitting.

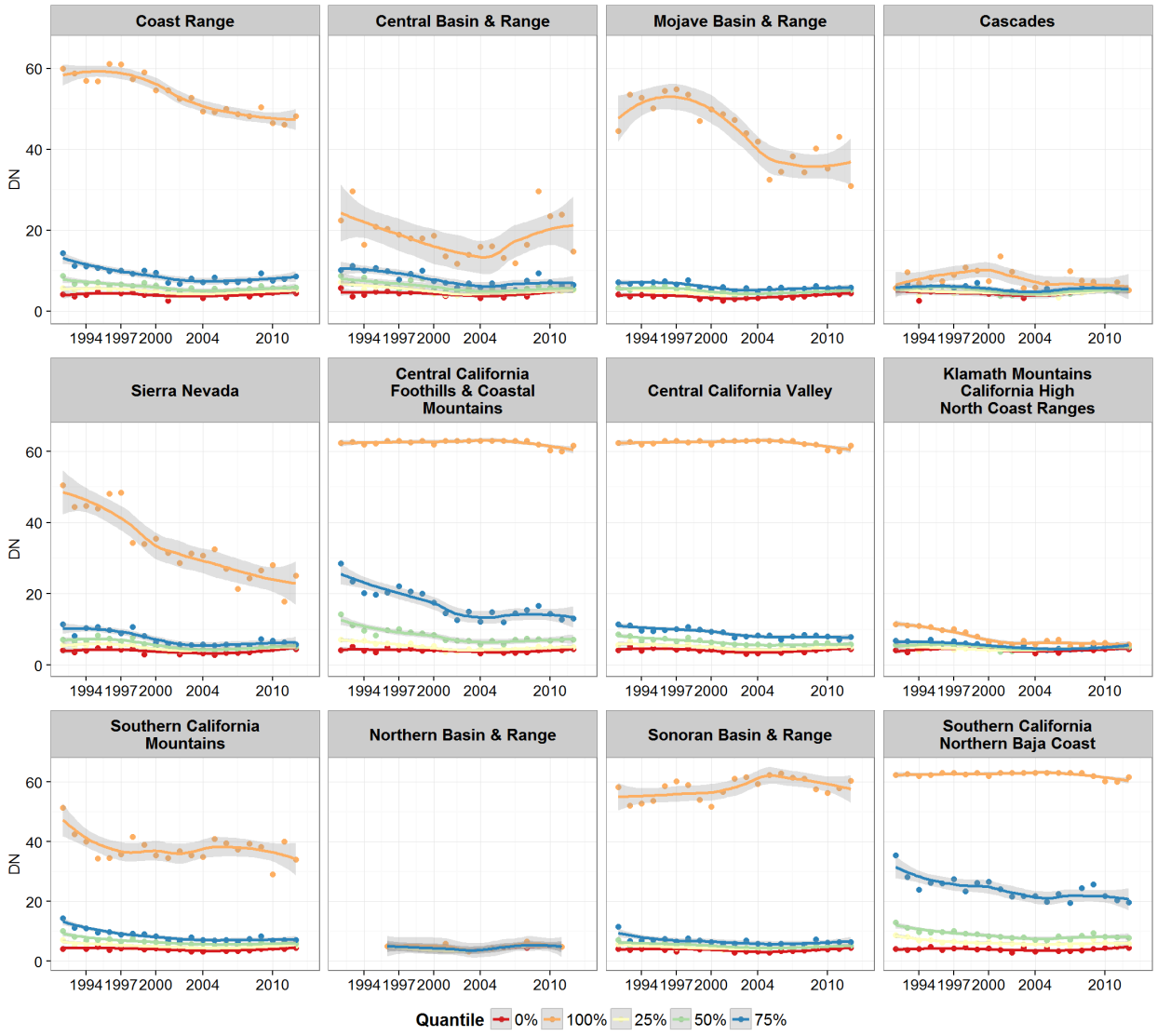

Figure 5.15: Quantiles of nightlight of California PAs inside EPA level III ecoregions. . Only pixels with nightlight above 1 are included. Solid curves are loess smoothed fit curves; grey shades are 95% confidence region of curve fitting.

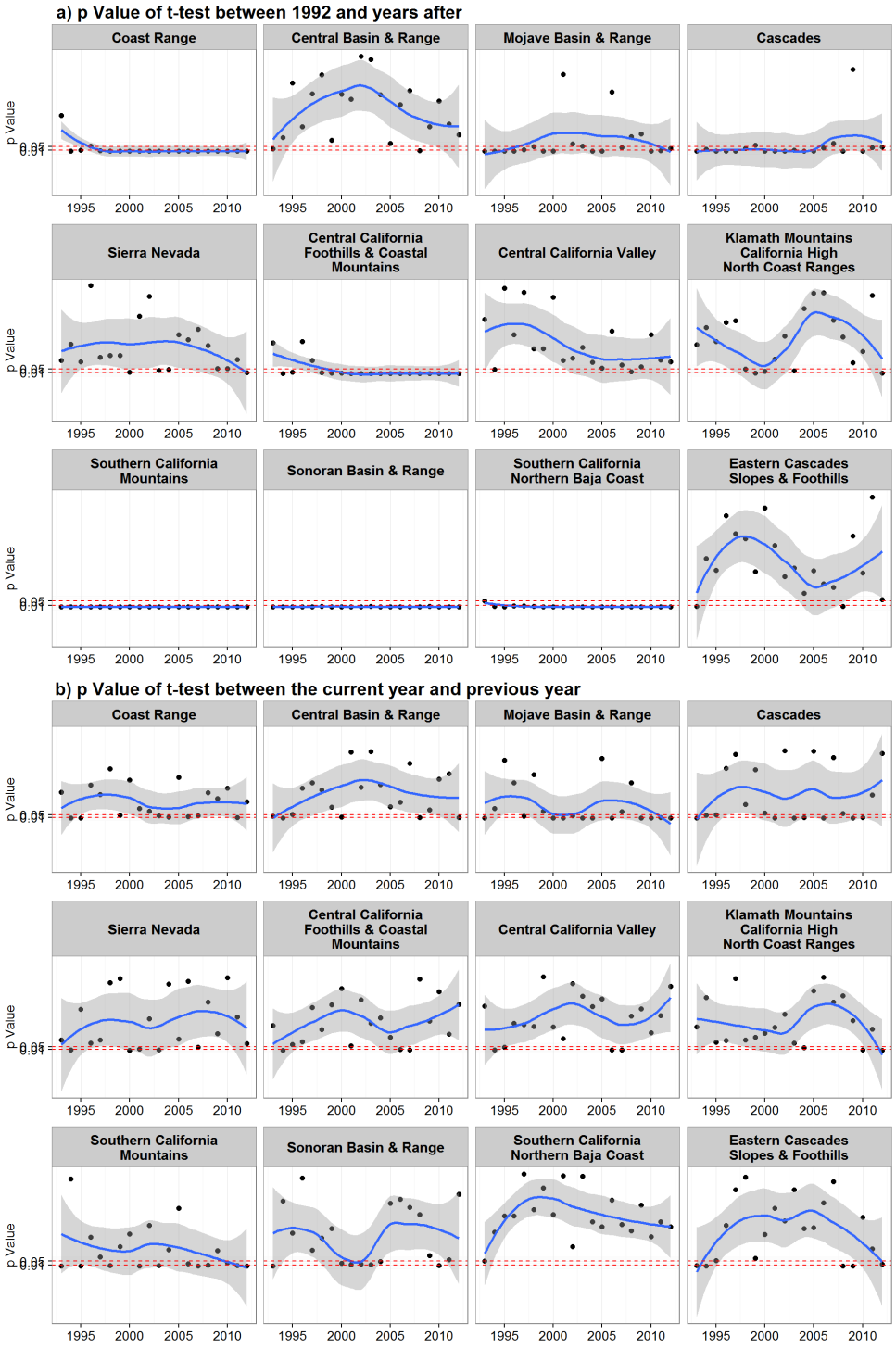

Figure 5.16: t-test for inter-annual comparison of nightlight. Panel a includes t-test p values between the baseline (1992) and all following years; panel b includes t-test p values between current year and the following year. All test results are plotted by EPA level III ecoregions.

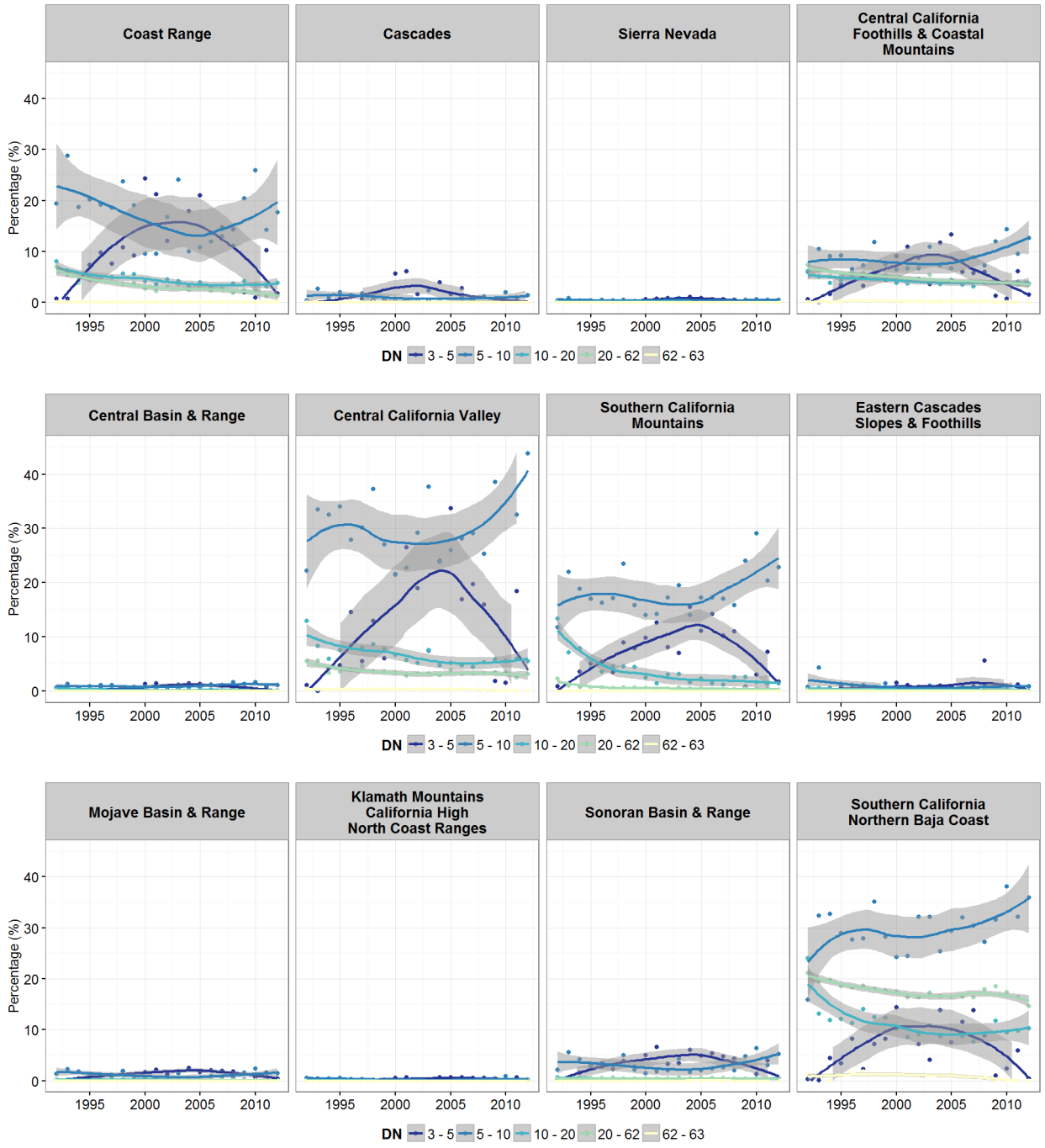

Figure 5.17: Change of area percentage in each value range for different ecoregions. Value ranges with very small area are omitted. Different value ranges are colored in terms of the DN value.

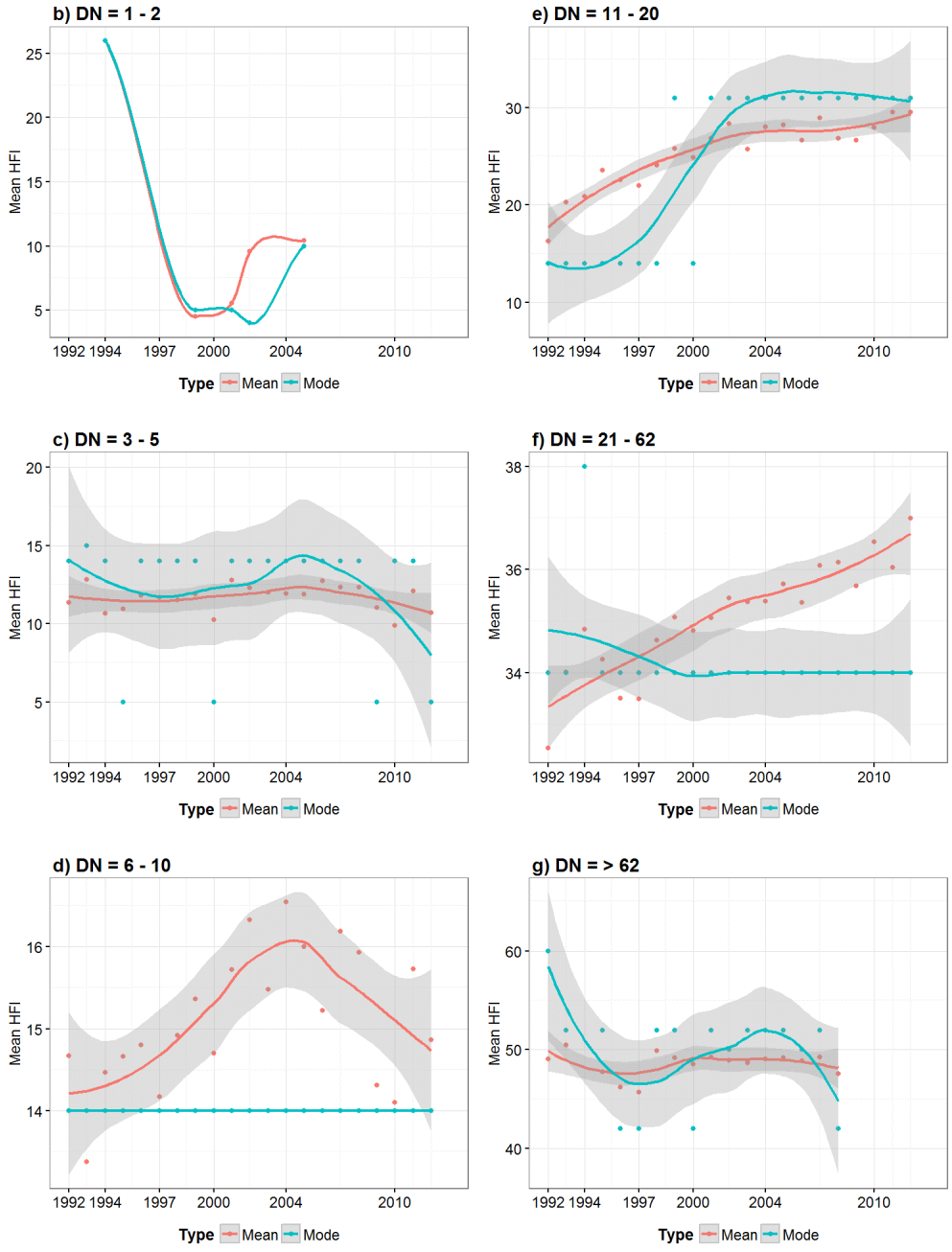

Figure 5.18: Change of mean and mode HFI in non-zero nightlight areas inside California PAs (1992–2012). Some value ranges do not exist in all years. Note that the value range of HFI at each DN class is different.

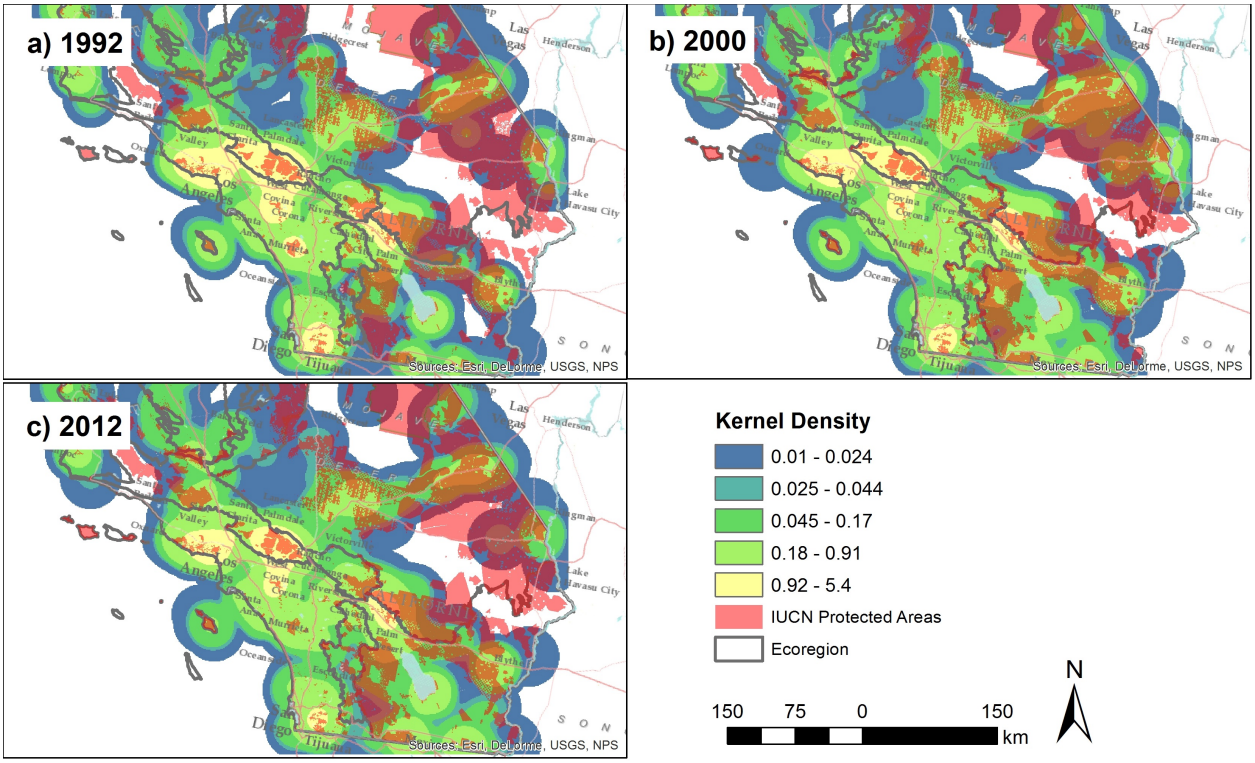

Figure 5.19: Kernel density in non-zero nightlight area of southern California PAs (1992,2000,2012).

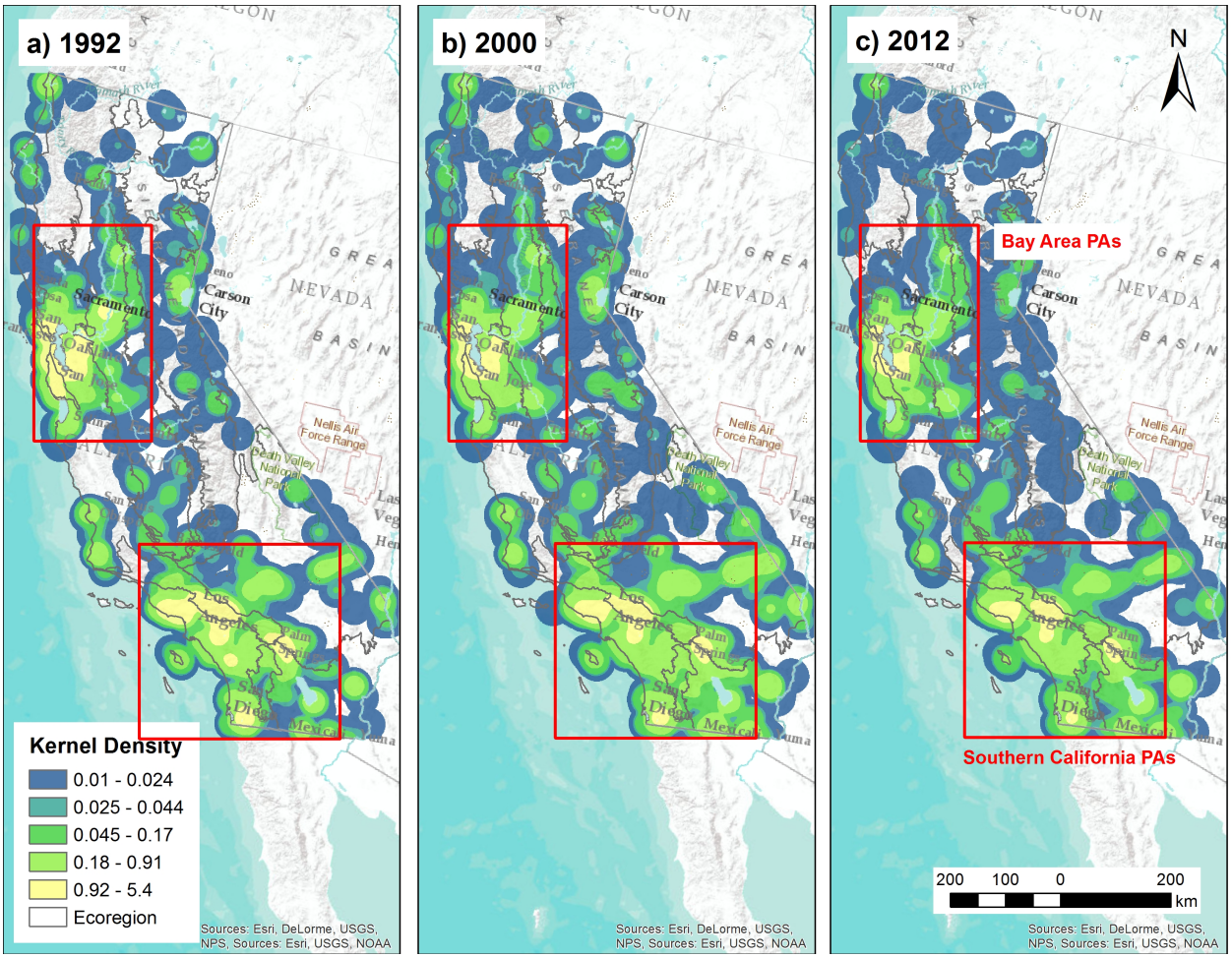

Figure 5.20: Kernel density in non-zero nightlight area of California PAs. Panel a-c map with the kernel density based on inter-satellite calibrated DMSP-OLS nighttime series in 1992, 2000, and 2012. Panel d-f map with the kernel density based on radiation calibrated DMSP–OLS nighttime series in 1996–1997, 2004, and 2010. Note the difference in value ranges between a–c and d–e.

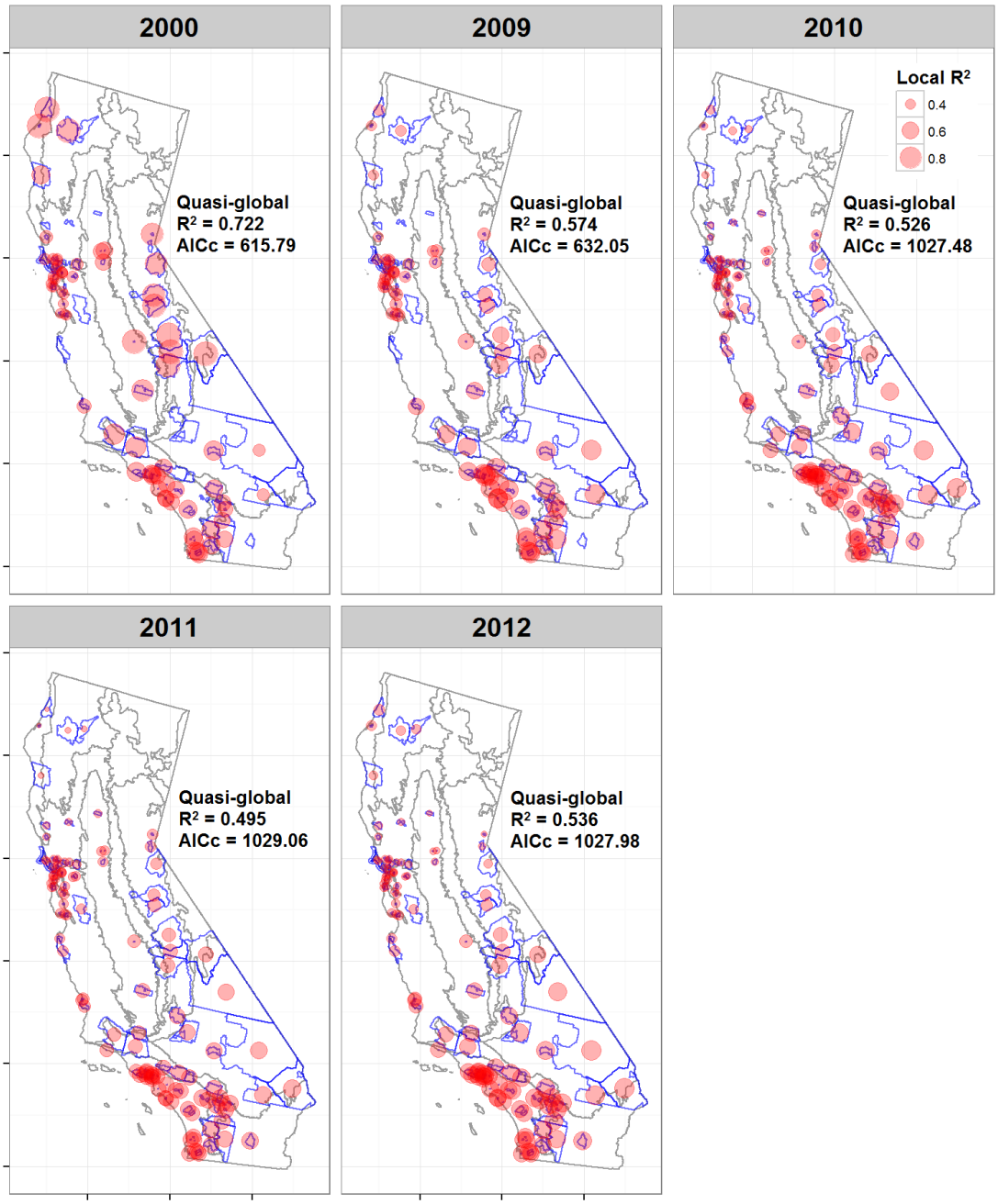

Figure 5.21: Geographic weight regression model adjusted R2 between average DN and population density of census tracts inside California PAs. Quasi-global R^2 and AICc of each GWR model is included in each panel. Only years with population at census tract level available are modeled. The boundaries of census tracts with center inside PAs are colored with blue. The boundaries of EPA level III ecoregions are colored with grey.

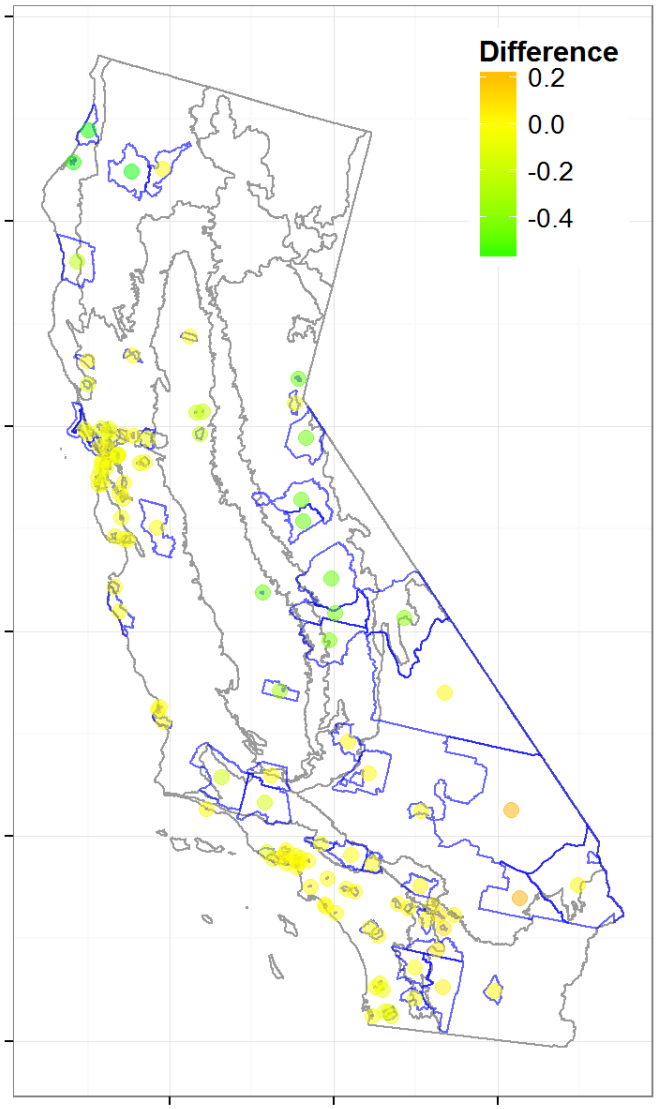

Figure 5.22: Difference of GWR R^2 at the first and last year with population data available. Positive and negative difference is colored as orange and green.The boundaries of census tracts with center inside PAs are colored with blue. The boundaries of EPA level III ecoregions are colored with grey.

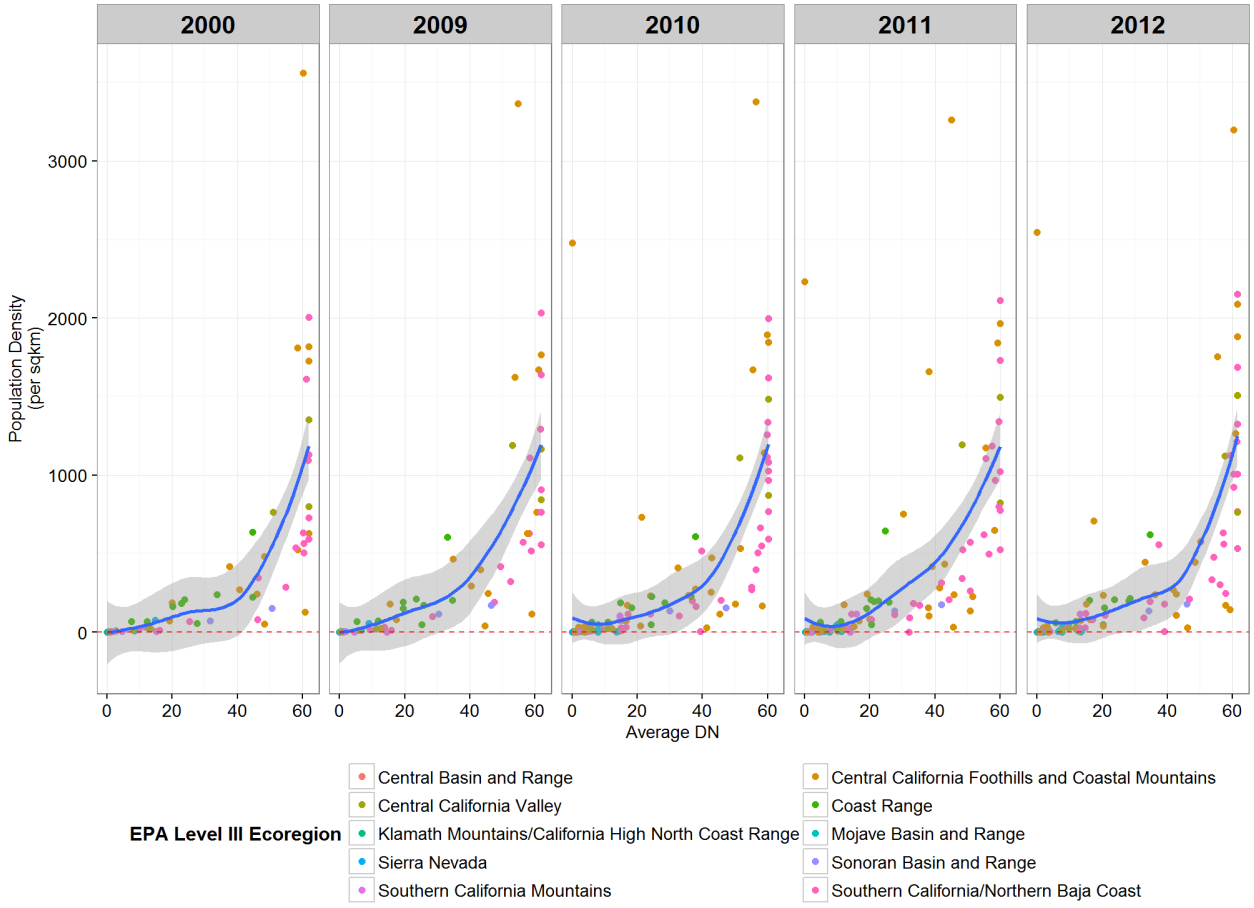

Figure 5.23: Scatterplot of population density vesus average lit nighttime light DN. Points are colored by ecoregions and separated by years.

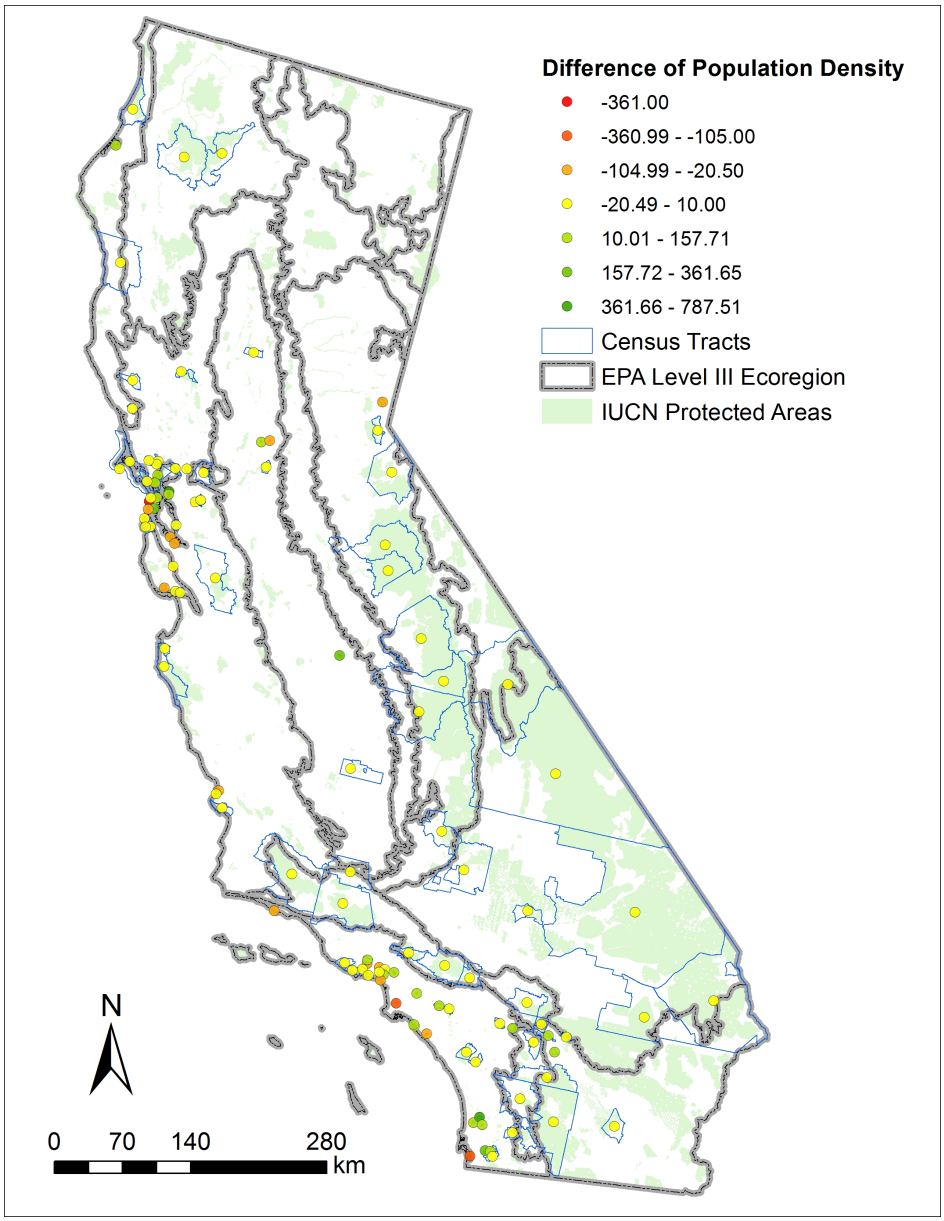

Figure 5.24: Difference of population density for census tracts intersecting California PAs between 2000 and 2012. Gain and loss is colored differently using a divergent color scheme.

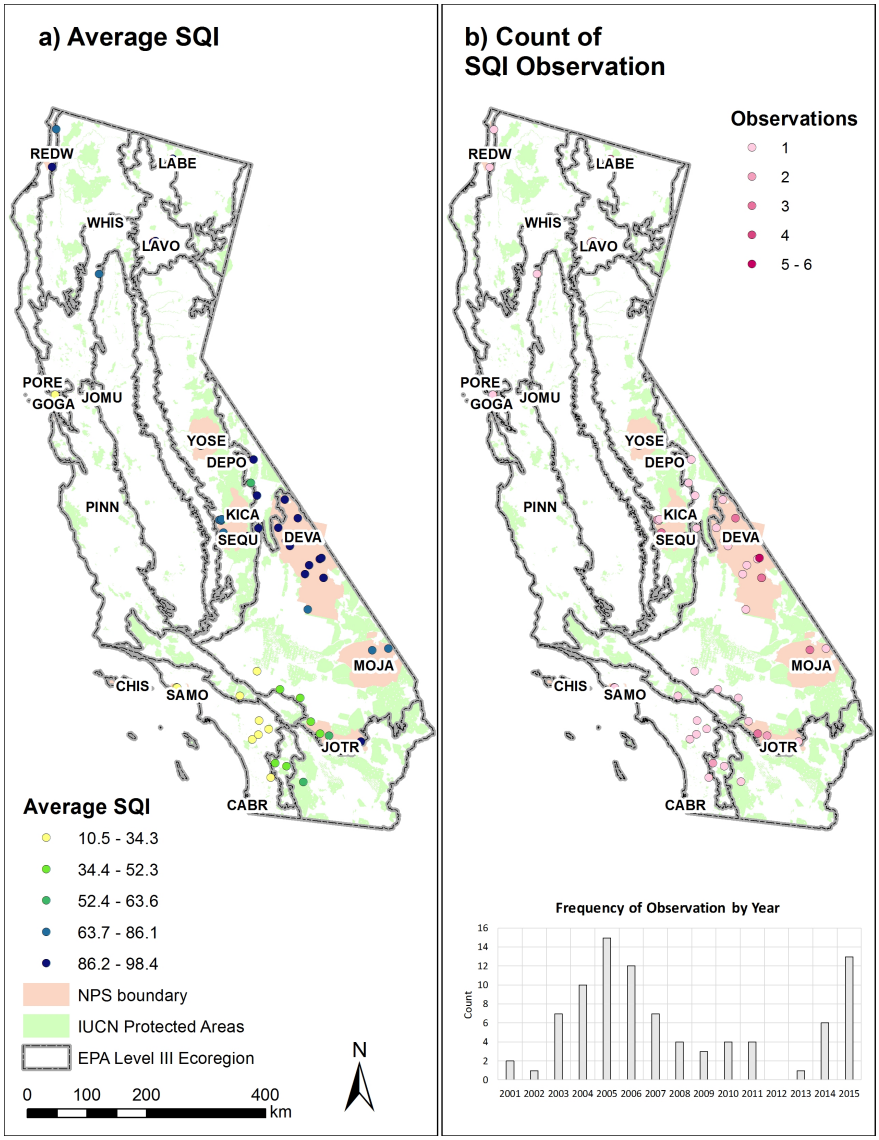

Figure 5.25: Sky quality index (SQI) from CCD camera by NPS night sky program. Average SQI is shaded from low (dark blue) to high (bright yellow). The higher SQI means a greater sky glow.

CHAPTER 6

Conclusion

The dissertation was set out to explore the past and present situation of three major ecological challenges during the recent two decades in protected areas of California, which supports a high species richness and biodiversity and maintains many reserves for wilderness. Besides the scientific significance of the topic, this dissertation was also motivated by the demand of a cost-effective and practical paradigm of preliminary and supportive research for policy-making at a regional level, which is crucial for maintenance and future development of the protected area monitoring system.

With the assistance of satellite remote sensing technologies and geospatial analysis, this dissertation answered the following questions regarding to three major ecological challenges:

- Is there a browning trend in California protected areas as a response of recent increase of drought?
- Has the fire regime changed during the recent years inside California protected areas? If so, what are the consequences of such change, especially in terms of post-fire regrowth of vegetation?
- How did the extent and intensity of human activity inside protected areas changed under the push of an increased population size and the pull of wilderness protecting regulations and executions?

The major findings to answer the above questions were drawn by utilizing various thematic remotely sensed biogeographic and abiotic measurements in a continuous time series. A browning trend was detected in a large number of protected areas of California from 2000

to 2015. Some protected areas were more temporally dynamic then others. A significant shift of fire regime occurred in 2008 in a study period from 2000 to 2013, featuring a great drop of fires in southern California chaparral and shrub/scrub area. The post-fire growing season was weakened more significantly in shrubland than the more humid evergreen forest. The historical record of stable nighttime light, a proxy of human activity and development revealed a decreasing in the intensity as well as a shrinkage in the extent of human activity from 1992 to 2012, though outlier existed. These findings provided a comprehensive understanding of the past and present of the ecological challenges to California protected areas.

Limitation of the above studies is mainly focused on the following three aspects. First, some analysis failed to consider the heterogeneity of protected areas in terms of the protective. The difference between levels of protection may introduce uncertainty to modeling and statistical analysis. Second, lack of understanding on some ecological processes and mechanisms influenced the development of explanatory variables to yield better predictive results when investigating the causal relationship between two or more biogeographic indicators. Third, most analysis excluded the adjacent area to protected areas, which is an important input of disturbance and an ecological corridor to mass and energy exchange between nearby protected areas. Studying the protected areas as isolated islands may harm the interpretation of analysis results, especially considering the geographic scope and the spatial scale of most studies conducted in this dissertation. Last, the diversity between different ecoregions was not sufficiently addressed in analysis. There is a need to group the protected areas based on ecoregions and interpret the analytical results under this framework, which will make the conclusions more accessible to local land managers and policy makers.

Future improvement should address the above limitations and shortcomings, including separating the protected areas by the IUCN protecting categories in both qualitative and quantitative analysis, investigating the ecological processes and modeling to explore the possibility of bridging the gap between remote sensing observations and biogeographic measurements necessary for model implementation, and incorporate the adjacent region of protected

areas for study to utilize theory and knowledge from landscape ecology for a better interpretation of findings. In addition, adopting the latest geospatial computation development also helps to expand the studies of protected areas through remote sensing technologies, such as implementing computation on cloud based computation infrastructure and platform like Google Earth Engine, and exploring the possibility of voluntarily collected geospatial data from social media as a sensor of human activity.

To sum up, the studies of three major ecological challenges on protected areas in California provided a cost-effective and practical paradigm for park managers and policy makers to review, evaluate, and develop a more adaptive land management strategies and policies for environmental conservation. With the increasing awareness of the significance of protected areas and the help of technological development, the network of protected area is under the way of expanding and improving globally. Despite the progress from technology and research, the goal of a sustainable future of the protected area on the Earth cannot be reached without the international corporation and education on sustainability.

References

[Alcaraz-Segura et al., 2009] Alcaraz-Segura, D., Cabello, J., Paruelo, J., and Delibes, M. (2009). Use of descriptors of ecosystem functioning for monitoring a national park network: A remote sensing approach. *Environmental Management*, 43(1):38–48.

[Anderson, 1976] Anderson, J. R. (1976). *A land use and land cover classification system for use with remote sensor data*, volume 964. US Government Printing Office.

[Anselin, 1988] Anselin, L. (1988). *Spatial econometrics: methods and models*, volume 4. Springer.

[Anselin, 2013] Anselin, L. (2013). *Spatial econometrics: methods and models*, volume 4. Springer Science and Business Media.

[Anselin and Arribas-Bel, 2011] Anselin, L. and Arribas-Bel, D. (2011). Spatial fixed effects and spatial dependence. Report, GeoDa Center for Geospatial Analysis and Computation.

[Assuncao and Reis, 1999] Assuncao, R. M. and Reis, E. A. (1999). A new proposal to adjust moran's i for population density. *Statistics in medicine*, 18(16):2147–2162.

[Aubrecht et al., 2010] Aubrecht, C., Jaiteh, M., and de Sherbinin, A. (2010). Global assessment of light pollution impact on protected areas. Technical report, CIESIN and NASA SEDAC, The Earth Institute at Columbia University, Palisades, NY, USA.

[Baker, 2013] Baker, W. L. (2013). Is wildland fire increasing in sagebrush landscapes of the western united states? *Annals of the Association of American Geographers*, 103(1):5–19.

[Baker, 2015] Baker, W. L. (2015). Are high-severity fires burning at much higher rates recently than historically in dry-forest landscapes of the western usa? *Plos One*, 10(9).

[Baltagi and Li, 2001] Baltagi, B. H. and Li, D. (2001). Lm tests for functional form and spatial error correlation. *International Regional Science Review*, 24(2):194–225.

[Barbour et al., 2007] Barbour, M. G., Keeler-Wolf, T., and Schoenherr, A. A. (2007). *Terrestrial vegetation of California*. Univ of California Press.

[Bennie et al., 2014] Bennie, J., Davies, T. W., Duffy, J. P., Inger, R., and Gaston, K. J. (2014). Contrasting trends in light pollution across europe based on satellite observed night time lights. *Scientific Reports*, 4.

[Bond and Keeley, 2005] Bond, W. J. and Keeley, J. E. (2005). Fire as a global 'herbivore': the ecology and evolution of flammable ecosystems. *Trends in Ecology and Evolution*, 20(7):387–394.

[Buis, 2016] Buis, A. (2016). Nasa maps california drought effects on sierra trees.

[California Fire Resource Assessment Program, 2003] California Fire Resource Assessment Program (2003). The changing california forest and range 2003 assessment : assessment summary. techreport.

[Capitanio and Carcaillet, 2008] Capitanio, R. and Carcaillet, C. (2008). Post-fire mediterranean vegetation dynamics and diversity: A discussion of succession models. *Forest Ecology and Management*, 255(3-4):431–439.

[Carle, 2010] Carle, D. (2010). *Introduction to earth, soil, and land in California*. Univ of California Press.

[Carle, 2015a] Carle, D. (2015a). *Introduction to fire in California*. Univ of California Press.

[Carle, 2015b] Carle, D. (2015b). *Introduction to water in California*. Univ of California Press.

[Chape et al., 2003] Chape, S., Blyth, S., Fish, L., Fox, P., and Spalding, M. (2003). *United Nations list of protected areas*. IUCN, Gland, Switzerland and Cambridge, UK and UNEP-WCMC, Cambridge, UK.

[Chape et al., 2005] Chape, S., Harrison, J., Spalding, M., and Lysenko, I. (2005). Measuring the extent and effectiveness of protected areas as an indicator for meeting global biodiversity targets. *Philosophical Transactions of the Royal Society B-Biological Sciences*, 360(1454):443–455.

[Chepesiuk, 2009] Chepesiuk, R. (2009). Missing the dark health effects of light pollution. *Environmental Health Perspectives*, 117(1):A20–A27.

[Cinzano and Elvidge, 2003] Cinzano, P. and Elvidge, C. D. (2003). Modelling night sky brightness at sites from dmsp satellite data. *Light Pollution: The Global View*, 284:29–37.

[Cinzano and Elvidge, 2004] Cinzano, P. and Elvidge, C. D. (2004). Night sky brightness at sites from dmsp-ols satellite measurements. *Monthly Notices of the Royal Astronomical Society*, 353(4):1107–1116.

[Coad et al., 2013] Coad, L., Leverington, F., Burgess, N. D., Cuadros, I. C., Geldmann, J., Marthews, T. R., Mee, J., Nolte, C., Stoll-Kleemann, S., and Vansteelant, N. (2013). Progress towards the cbd protected area management effectiveness targets. *Parks*, 19(1):13–24.

[Cochrane et al., 2012] Cochrane, M. A., Moran, C. J., Wimberly, M. C., Baer, A. D., Finney, M. A., Beckendorf, K. L., Eidenshink, J., and Zhu, Z. (2012). Estimation of wildfire size and risk changes due to fuels treatments. *Int J Wildland Fire*, 21.

[Coppin et al., 2004] Coppin, P., Jonckheere, I., Nackaerts, K., Muys, B., and Lambin, E. (2004). Digital change detection methods in ecosystem monitoring: a review. *International Journal of Remote Sensing*, 25(9):1565–1596.

[Coulston et al., 2013] Coulston, J. W., Jacobs, D. M., King, C. R., and Elmore, I. C. (2013). The influence of multi-season imagery on models of canopy cover. *Photogrammetric Engineering & Remote Sensing*, 79(5):469–477.

[Crabtree et al., 2009] Crabtree, R., Potter, C., Mullen, R., Sheldon, J., Huang, S. L., Harmsen, J., Rodman, A., and Jean, C. (2009). A modeling and spatio-temporal analysis framework for monitoring environmental change using npp as an ecosystem indicator. *Remote Sensing of Environment*, 113(7):1486–1496.

[Curran et al., 2004] Curran, L. M., Trigg, S. N., McDonald, A. K., Astiani, D., Hardiono, Y., Siregar, P., Caniago, I., and Kasischke, E. (2004). Lowland forest loss in protected areas of indonesian borneo. *Science*, 303(5660):1000–1003.

[Davis and Hansen, 2011] Davis, C. R. and Hansen, A. J. (2011). Trajectories in land use change around u.s. national parks and challenges and opportunities for management. *Ecological Applications*, 21(8):3299–3316.

[De Smith et al., 2007] De Smith, M. J., Goodchild, M. F., and Longley, P. (2007). *Geospatial analysis: a comprehensive guide to principles, techniques and software tools*. Troubador Publishing Ltd.

[Dudley, 2008] Dudley, N. (2008). *Guidelines for applying protected area management categories*. IUCN.

[Duriscoe, 2013] Duriscoe, D. M. (2013). Measuring anthropogenic sky glow using a natural sky brightness model. *Publications of the Astronomical Society of the Pacific*, 125(933):1370–1382.

[Duriscoe et al., 2007] Duriscoe, D. M., Luginbuhl, C. B., and Moore, C. A. (2007). Measuring night-sky brightness with a wide-field ccd camera. *Publications of the Astronomical Society of the Pacific*, 119(852):192–213.

[Eidenshink et al., 2007] Eidenshink, J., Schwind, B., Brewer, K., Zhu, Z., Quayle, B., and Howard, S. (2007). A project for monitoring trends in burn severity. *Fire Ecol (Special Issue)*, 3.

[Elvidge et al., 1999] Elvidge, C. D., Baugh, K. E., Dietz, J. B., Bland, T., Sutton, P. C., and Kroehl, H. W. (1999). Radiance calibration of dmsp-ols low-light imaging data of human settlements. *Remote Sensing of Environment*, 68(1):77–88.

[Elvidge et al., 2013] Elvidge, C. D., Baugh, K. E., Zhizhin, M., and Hsu, F.-C. (2013). Why viirs data are superior to dmsp for mapping nighttime lights. *Proceedings of the Asia-Pacific Advanced Network*, 35:62–69.

[Elvidge et al., 2014] Elvidge, C. D., Hsu, F.-C., Baugh, K. E., and Ghosh, T. (2014). National trends in satellite-observed lighting. *Global urban monitoring and assessment through Earth observation*, page 97.

[Elvidge et al., 2009] Elvidge, C. D., Ziskin, D., Baugh, K. E., Tuttle, B. T., Ghosh, T., Pack, D. W., Erwin, E. H., and Zhizhin, M. (2009). A fifteen year record of global natural gas flaring derived from satellite data. *Energies*, 2(3):595–622.

[Faivre et al., 2014] Faivre, N., Jin, Y. F., Goulden, M. L., and Randerson, J. T. (2014). Controls on the spatial pattern of wildfire ignitions in southern california. *International Journal of Wildland Fire*, 23(6):799–811.

[Fancy et al., 2008] Fancy, S. G., Gross, J. E., and Carter, S. L. (2008). Monitoring the condition of natural resources in us national parks. *Environmental Monitoring and Assessment*, 151(1):161–174.

[Fotheringham et al., 2003] Fotheringham, A. S., Brunsdon, C., and Charlton, M. (2003). *Geographically weighted regression: the analysis of spatially varying relationships*. John Wiley and Sons.

[Fox et al., 2008] Fox, D. M., Maselli, F., and Carrega, P. (2008). Using spot images and field sampling to map burn severity and vegetation factors affecting post forest fire erosion risk. *Catena*, 75(3):326–335.

[Fry et al., 2011] Fry, J. A., Xian, G., Jin, S., Dewitz, J. A., Homer, C. G., LIMIN, Y., Barnes, C. A., Herold, N. D., and Wickham, J. D. (2011). Completion of the 2006 national land cover database for the conterminous united states. *Photogrammetric engineering and remote sensing*, 77(9):858–864.

[Gaston et al., 2012] Gaston, K. J., Davies, T. W., Bennie, J., and Hopkins, J. (2012). Review: Reducing the ecological consequences of night-time light pollution: options and developments. *Journal of Applied Ecology*, 49(6):1256–1266.

[Geldmann et al., 2013] Geldmann, J., Barnes, M., Coad, L., Craigie, I. D., Hockings, M., and Burgess, N. D. (2013). Effectiveness of terrestrial protected areas in reducing habitat loss and population declines. *Biological Conservation*, 161:230–238.

[Geldmann et al., 2014] Geldmann, J., Joppa, L. N., and Burgess, N. D. (2014). Mapping change in human pressure globally on land and within protected areas. *Conservation Biology*, 28(6):1604–1616.

[GEO BON Office, 2011] GEO BON Office (2011). Adequacy of biodiversity observation systems to support the cbd 2020 targets. In *A Report Prepared by the Group on Earth Observations Biodiversity Observation Network (GEO BON), for the Convention on Biological Diversity*.

[Gergely and McKerrow, 2013] Gergely, K. J. and McKerrow, A. (2013). Tools and data for meeting america's conservation challenges. Report, US Geological Survey.

[Getis and Ord, 1992] Getis, A. and Ord, J. K. (1992). The analysis of spatial association by use of distance statistics. *Geographical Analysis*, 24(3):189–206.

[Ghosh et al., 2013] Ghosh, T., Anderson, S. J., Elvidge, C. D., and Sutton, P. C. (2013). Using nighttime satellite imagery as a proxy measure of human well-being. *Sustainability*, 5(12):4988–5019.

[Giglio, 2010] Giglio, L. (2010). Modis collection 5 active fire product users guide version 2.4. *Science Systems and Applications, Inc.*

[Gillespie et al., 1990] Gillespie, A., Smith, M., Adams, J., Willis, S., Fischer, A., and Sabol, D. (1990). Interpretation of residual images: spectral mixture analysis of aviris images, owens valley, california. In *Annual JPL Airborne Visible/Infrared Imaging Spectrometer (AVIRIS) Workshop*, volume 2, pages 90–54.

[Gillespie, 1992] Gillespie, A. R. (1992). Spectral mixture analysis of multispectral thermal infrared images. *Remote Sensing of Environment*, 42(2):137–145.

[Gillespie et al., 2008] Gillespie, T. W., Foody, G. M., Rocchini, D., Giorgi, A. P., and Saatchi, S. (2008). Measuring and modelling biodiversity from space. *Progress in Physical Geography*, 32(2):203–221.

[Gillespie et al., 2015] Gillespie, T. W., Willis, K. S., and Ostermann-Kelm, S. (2015). Spaceborne remote sensing of the world's protected areas. *Progress in Physical Geography*, 39(3):388–404.

[Gillespie et al., 2016] Gillespie, T. W., Willis, K. S., Ostermann-Kelm, S., Jenkins, O., Federico, F., Lee, L., and MacDonald, G. M. (2016). Inventory and monitoring nighttime lights distribution and dynamics in the mediterranean coast network of southern california. Technical report, National Park Service.

[Goetz et al., 2005] Goetz, S. J., Bunn, A. G., Fiske, G. J., and Houghton, R. A. (2005). Satellite-observed photosynthetic trends across boreal north america associated with climate and fire disturbance. *Proceedings of the National Academy of Sciences of the United States of America*, 102(38):13521–13525.

[Goetz et al., 2009] Goetz, S. J., Jantz, P., and Jantz, C. A. (2009). Connectivity of core habitat in the northeastern united states: Parks and protected areas in a landscape context. *Remote Sensing of Environment*, 113(7):1421–1429.

[Gorelick, 2012] Gorelick, N. (2012). Google earth engine. In *AGU Fall Meeting Abstracts*, volume 1, page 04.

[Gross et al., 2013] Gross, D., Dubois, G., Pekel, J. F., Mayaux, P., Holmgren, M., Prins, H. H. T., Rondinini, C., and Boitani, L. (2013). Monitoring land cover changes in african protected areas in the 21st century. *Ecological Informatics*, 14:31–37.

[Guarin and Taylor, 2005] Guarin, A. and Taylor, A. H. (2005). Drought triggered tree mortality in mixed conifer forests in yosemite national park, california, usa. *Forest Ecology and Management*, 218(1-3):229–244.

[Guerschman et al., 2009] Guerschman, J. P., Hill, M. J., Renzullo, L. J., Barrett, D. J., Marks, A. S., and Botha, E. J. (2009). Estimating fractional cover of photosynthetic vegetation, non-photosynthetic vegetation and bare soil in the australian tropical savanna region upscaling the eo-1 hyperion and modis sensors. *Remote Sensing of Environment*, 113(5):928–945.

[Guerschman et al., 2015] Guerschman, J. P., Scarth, P. F., McVicar, T. R., Renzullo, L. J., Malthus, T. J., Stewart, J. B., Rickards, J. E., and Trevithick, R. (2015). Assessing the effects of site heterogeneity and soil properties when unmixing photosynthetic vegetation, non-photosynthetic vegetation and bare soil fractions from landsat and modis data. *Remote Sensing of Environment*, 161:12–26.

[Hansen et al., 2014] Hansen, A. J., Piekielek, N., Davis, C., Haas, J., Theobald, D. M., Gross, J. E., Monahan, W. B., Olliff, T., and Running, S. W. (2014). Exposure of us national parks to land use and climate change 1900-2100. *Ecological Applications*, 24(3):484–502.

[Hansen et al., 2013a] Hansen, M. C., Potapov, P. V., Moore, R., Hancher, M., Turubanova, S. A., Tyukavina, A., Thau, D., Stehman, S. V., Goetz, S. J., Loveland, T. R., Kommareddy, A., Egorov, A., Chini, L., Justice, C. O., and Townshend, J. R. G. (2013a). High-resolution global maps of 21st-century forest cover change. *Science*, 342(6160):850–853.

[Hansen et al., 2013b] Hansen, M. C., Potapov, P. V., Moore, R., Hancher, M., Turubanova, S. A., Tyukavina, A., Thau, D., Stehman, S. V., Goetz, S. J., Loveland, T. R., Kommareddy, A., Egorov, A., Chini, L., Justice, C. O., and Townshend, J. R. G. (2013b). High-resolution global maps of 21st-century forest cover change. *Science*, 342(6160):850–853.

[Harris et al., 2011] Harris, S., Veraverbeke, S., and Hook, S. (2011). Evaluating spectral indices for assessing fire severity in chaparral ecosystems (southern california) using modis/aster (master) airborne simulator data. *Remote Sensing*, 3(11):2403–2419.

[Henderson et al., 2012] Henderson, J. V., Storeygard, A., and Weil, D. N. (2012). Measuring economic growth from outer space. *American Economic Review*, 102(2):994–1028.

[Henry et al., 2005] Henry, H. A. L., Cleland, E. E., Field, C. B., and Vitousek, P. M. (2005). Interactive effects of elevated co2, n deposition and climate change on plant litter quality in a california annual grassland. *Oecologia (Berlin)*, 142(3):465–473.

[Hernandez et al., 2015] Hernandez, R. R., Hoffacker, M. K., Murphy-Mariscal, M. L., Wu, G. C., and Allen, M. F. (2015). Solar energy development impacts on land cover change and protected areas. *Proceedings of the National Academy of Sciences of the United States of America*, 112(44):13579–13584.

[Hickman, 1993] Hickman, J. C. (1993). *The Jepson Manual*. University of California Press, Berkeley, CA.

[Homer et al., 2007] Homer, C., Dewitz, J., Fry, J., Coan, M., Hossain, N., Larson, C., Herold, N., McKerrow, A., VanDriel, J. N., and Wickham, J. (2007). Completion of the 2001 national land cover database for the counterminous united states. *Photogrammetric Engineering and Remote Sensing*, 73(4):337.

[Homer et al., 2015] Homer, C., Dewitz, J., Yang, L., Jin, S., Danielson, P., Xian, G., Coulston, J., Herold, N., Wickham, J., and Megown, K. (2015). Completion of the 2011 national land cover database for the conterminous united statesrepresenting a decade of land cover change information. *Photogrammetric Engineering and Remote Sensing*, 81(5):345–354.

[Hope et al., 2007] Hope, A., Tague, C., and Clark, R. (2007). Characterizing post-fire vegetation recovery of california chaparral using tm/etm plus time-series data. *International Journal of Remote Sensing*, 28(6):1339–1354.

[Hsu et al., 2015] Hsu, F. C., Baugh, K. E., Ghosh, T., Zhizhin, M., and Elvidge, C. D. (2015). Dmsp-ols radiance calibrated nighttime lights time series with intercalibration. *Remote Sensing*, 7(2):1855–1876.

[Hughes and Larsen, 1988] Hughes, R. M. and Larsen, D. P. (1988). Ecoregions: an approach to surface water protection. *Journal-Water Pollution Control Federation*, 60(4):486–493.

[IUCN and UNEP-WCMC, 2015] IUCN and UNEP-WCMC (2015). The world database on protected areas (wdpa) [on-line].

[Jardine et al., 2013] Jardine, A., Merideth, R., Black, M., and LeRoy, S. (2013). *Assessment of climate change in the southwest United States: a report prepared for the National Climate Assessment*. Island press.

[Jenkerson et al., 2010] Jenkerson, C., Maiersperger, T., and Schmidt, G. (2010). emodis: a user-friendly data source. Report 2331-1258, US Geological Survey.

[Jin et al., 2013] Jin, S., Yang, L., Danielson, P., Homer, C., Fry, J., and Xian, G. (2013). A comprehensive change detection method for updating the national land cover database to circa 2011. *Remote Sensing of Environment*, 132:159–175.

[Jin et al., 2015] Jin, Y. F., Goulden, M. L., Faivre, N., Veraverbeke, S., Sun, F. P., Hall, A., Hand, M. S., Hook, S., and Randerson, J. T. (2015). Identification of two distinct fire regimes in southern california: implications for economic impact and future change. *Environmental Research Letters*, 10(9).

[Jin et al., 2014] Jin, Y. F., Randerson, J. T., Faivre, N., Capps, S., Hall, A., and Goulden, M. L. (2014). Contrasting controls on wildland fires in southern california during periods with and without santa ana winds. *Journal of Geophysical Research-Biogeosciences*, 119(3):432–450.

[Jones et al., 2009] Jones, D. A., Hansen, A. J., Bly, K., Doherty, K., Verschuyl, J. P., Paugh, J. I., Carle, R., and Story, S. J. (2009). Monitoring land use and cover around parks: A conceptual approach. *Remote Sensing of Environment*, 113(7):1346–1356.

[Jong et al., 2012] Jong, R., Verbesselt, J., Schaepman, M. E., and Bruin, S. (2012). Trend changes in global greening and browning: contribution of shortterm trends to longerterm change. *Global Change Biology*, 18(2):642–655.

[Juffe-Bignoli et al., 2014] Juffe-Bignoli, D., Burgess, N. D., Belle, E., de Lima, M. G., Deguignet, M., Bertzky, B., Milam, A. N., Martinez-Lopez, J., Lewis, E., and Eassom, A. (2014). Protected planet report 2014. Report 9280734164.

[Kachelriess et al., 2014] Kachelriess, D., Wegmann, M., Gollock, M., and Pettorelli, N. (2014). The application of remote sensing for marine protected area management. *Ecological Indicators*, 36:169–177.

[Keeley, 2002] Keeley, J. E. (2002). Fire management of california shrubland landscapes. *Environmental Management*, 29(3):395–408.

[Keeley et al., 2008] Keeley, J. E., Brennan, T., and Pfaff, A. H. (2008). Fire severity and ecosytem responses following crown fires in california shrublands. *Ecological Applications*, 18(6):1530–1546.

[Key and Benson, 1999] Key, C. and Benson, N. (1999). Measuring and remote sensing of burn severity. In *Proceedings joint fire science conference and workshop*, volume 2, page 284.

[Kramer et al., 1997] Kramer, R., Schaik, C. v., and Johnson, J. (1997). *Last stand: protected areas and the defense of tropical biodiversity*. Oxford University Press.

[Krawchuk and Moritz, 2011] Krawchuk, M. A. and Moritz, M. A. (2011). Constraints on global fire activity vary across a resource gradient. *Ecology*, 92(1):121–132.

[Kutiel and Inbar, 1993] Kutiel, P. and Inbar, M. (1993). Fire impacts on soil nutrients and soil-erosion in a mediterranean pine forest plantation. *Catena*, 20(1-2):129–139.

[Leadley et al., 2010] Leadley, P. W., Krug, C. B., Alkemade, R., Pereira, H. M., Sumaila, U. R., Walpole, M., Marques, A., Newbold, T., Teh, L. S., and van Kolck, J. (2010). Progress towards the aichi biodiversity targets: An assessment of biodiversity trends, policy scenarios and key actions. In *Progress towards the Aichi Biodiversity Targets: An assessment of biodiversity trends, policy scenarios and key actions*. Secretariat of the Convention on Biological Diversity.

[Leon et al., 2012] Leon, J. R. R., van Leeuwen, W. J. D., and Casady, G. M. (2012). Using modis-ndvi for the modeling of post-wildfire vegetation response as a function of environmental conditions and pre-fire restoration treatments. *Remote Sensing*, 4(3):598–621.

[Levin et al., 2015] Levin, N., Kark, S., and Crandall, D. (2015). Where have all the people gone? enhancing global conservation using night lights and social media. *Ecological Applications*, 25(8):2153–2167.

[Li et al., 2005] Li, L., Ustin, S. L., and Lay, M. (2005). Application of multiple endmember spectral mixture analysis (mesma) to aviris imagery for coastal salt marsh mapping: a case study in china camp, ca, usa. *International Journal of Remote Sensing*, 26(23):5193–5207.

[Liu et al., 2012] Liu, Z. F., He, C. Y., Zhang, Q. F., Huang, Q. X., and Yang, Y. (2012). Extracting the dynamics of urban expansion in china using dmsp-ols nighttime light data from 1992 to 2008. *Landscape and Urban Planning*, 106(1):62–72.

[Liu and Wimberly, 2015] Liu, Z. H. and Wimberly, M. C. (2015). Climatic and landscape influences on fire regimes from 1984 to 2010 in the western united states. *Plos One*, 10(10).

[Lovejoy, 2006] Lovejoy, T. E. (2006). Protected areas: a prism for a changing world. *Trends in Ecology and Evolution*, 21(6):329–333.

[Lozano et al., 2007] Lozano, F. J., Suarez-Seoane, S., and de Luis, E. (2007). Assessment of several spectral indices derived from multi-temporal landsat data for fire occurrence probability modelling. *Remote Sensing of Environment*, 107(4):533–544.

[MacDonald, 2010] MacDonald, G. M. (2010). Water, climate change, and sustainability in the southwest. *Proceedings of the National Academy of Sciences of the United States of America*, 107(50):21256–21262.

[McDonald et al., 2009] McDonald, R. I., Fargione, J., Kiesecker, J., Miller, W. M., and Powell, J. (2009). Energy sprawl or energy efficiency: Climate policy impacts on natural habitat for the united states of america. *Plos One*, 4(8).

[Mcdonald et al., 2009a] Mcdonald, R. I., Forman, R. T. T., Kareiva, P., Neugarten, R., Salzer, D., and Fisher, J. (2009a). Urban effects, distance, and protected areas in an urbanizing world. *Landscape and Urban Planning*, 93(1):63–75.

[Mcdonald et al., 2009b] Mcdonald, R. I., Forman, R. T. T., Kareiva, P., Neugarten, R., Salzer, D., and Fisher, J. (2009b). Urban effects, distance, and protected areas in an urbanizing world. *Landscape and Urban Planning*, 93(1):63–75.

[Mcdonald et al., 2008] Mcdonald, R. I., Kareiva, P., and Formana, R. T. T. (2008). The implications of current and future urbanization for global protected areas and biodiversity conservation. *Biological Conservation*, 141(6):1695–1703.

[Meier and Brown, 2014] Meier, G. A. and Brown, J. F. (2014). Remote sensing of land surface phenology. Report 2014-3052.

[Mellander et al., 2015] Mellander, C., Lobo, J., Stolarick, K., and Matheson, Z. (2015). Night-time light data: A good proxy measure for economic activity? *Plos One*, 10(10).

[Milam et al., 2016] Milam, A., Kenney, S., Juffe-Bignoli, D., Bertzky, B., Corrigan, C., MacSharry, B., Burgess, N. D., and Kingston, N. (2016). *Maintaining a Global Data Set on Protected Areas*, book section Maintaining a Global Data Set on Protected Areas, pages 81–101. John Wiley & Sons, Ltd.

[Miller and Goodchild, 2014] Miller, H. J. and Goodchild, M. F. (2014). Data-driven geography. *GeoJournal*, pages 1–13.

[Miller et al., 2009] Miller, J. D., Knapp, E. E., Key, C. H., Skinner, C. N., Isbell, C. J., Creasy, R. M., and Sherlock, J. W. (2009). Calibration and validation of the relative differenced normalized burn ratio (rdnbr) to three measures of fire severity in the sierra nevada and klamath mountains, california, usa. *Remote Sensing of Environment*, 113(3):645–656.

[Miller et al., 2012] Miller, S. D., Mills, S. P., Elvidge, C. D., Lindsey, D. T., Lee, T. F., and Hawkins, J. D. (2012). Suomi satellite brings to light a unique frontier of nighttime environmental sensing capabilities. *Proceedings of the National Academy of Sciences of the United States of America*, 109(39):15706–15711.

[Mitchell, 2005] Mitchell, A. (2005). *The ESRI guide to GIS analysis, Volume 2: Spatial Measurements and Statistics. Redlands*. Esri Press, Redlands, California.

[Moritz, 2003] Moritz, M. A. (2003). Spatiotemporal analysis of controls on shrubland fire regimes: Age dependency and fire hazard. *Ecology*, 84(2):351–361.

[Moritz et al., 2014] Moritz, M. A., Batllori, E., Bradstock, R. A., Gill, M. A., Handmer, J., Hessburg, P. F., Leonard, J., McCaffrey, S., Odion, D. C., Schoennagel, T., and Syphard, A. D. (2014). Learning to coexist with wildfire. *Nature*, 515.

[Moritz et al., 2004] Moritz, M. A., Keeley, J. E., Johnson, E. A., and Schaffner, A. A. (2004). Testing a basic assumption of shrubland fire management: how important is fuel age? *Frontiers in Ecology and the Environment*, 2(2):67–72.

[Nagendra, 2008] Nagendra, H. (2008). Do parks work? impact of protected areas on land cover clearing. *AMBIO: A Journal of the Human Environment*, 37(5):330–337.

[NASA GES DISC, 2012] NASA GES DISC (2012). *Giovanni Online User's Manual*. NASA GES DISC.

[Natural Resources Conservation Service, 2015] Natural Resources Conservation Service (2015). *NRCS eVegGuide Version 2.33*. Natural Resources Conservation Service,.

[Nemani et al., 2009] Nemani, R., Hashimoto, H., Votava, P., Melton, F., Wang, W. L., Michaelis, A., Mutch, L., Milesi, C., Hiatt, S., and White, M. (2009). Monitoring and forecasting ecosystem dynamics using the terrestrial observation and prediction system (tops). *Remote Sensing of Environment*, 113(7):1497–1509.

[Odion et al., 2004] Odion, D. C., Frost, E. J., Strittholt, J. R., Jiang, H., Dellasala, D. A., and Moritz, M. A. (2004). Patterns of fire severity and forest conditions in the western klamath mountains, california. *Conservation Biology*, 18(4):927–936.

[Okin, 2007] Okin, G. S. (2007). Relative spectral mixture analysis - a multitemporal index of total vegetation cover. *Remote Sensing of Environment*, 106(4):467–479.

[Okin, 2010] Okin, G. S. (2010). The contribution of brown vegetation to vegetation dynamics. *Ecology*, 91(3):743–755.

[Okin et al., 2001] Okin, G. S., Murray, B., and Schlesinger, W. H. (2001). Degradation of sandy arid shrubland environments: observations, process modelling, and management implications. *Journal of Arid Environments*, 47(2):123–144.

[Omernik, 1987] Omernik, J. M. (1987). Ecoregions of the conterminous united states. *Annals of the Association of American geographers*, 77(1):118–125.

[Ornduff et al., 2004] Ornduff, R., Faber, P. M., and Keeler-Wolf, T. (2004). *Introduction to California plant life*. Univ. of California Press, Berkeley [u.a.

[Parks et al., 2016] Parks, S. A., Miller, C., Abatzoglou, J. T., Holsinger, L. M., Parisien, M.-A., and Dobrowski, S. Z. (2016). How will climate change affect wildland fire severity in the western us? *Environmental Research Letters*, 11(3):035002.

[Parks et al., 2014] Parks, S. A., Parisien, M. A., Miller, C., and Dobrowski, S. Z. (2014). Fire activity and severity in the western us vary along proxy gradients representing fuel amount and fuel moisture. *Plos One*, 9(6).

[Pausas, 2004] Pausas, J. G. (2004). Changes in fire and climate in the eastern iberian peninsula (mediterranean basin). *Climatic Change*, 63(3):337–350.

[Pausas and Fernandez-Munoz, 2012] Pausas, J. G. and Fernandez-Munoz, S. (2012). Fire regime changes in the western mediterranean basin: from fuel-limited to drought-driven fire regime. *Climatic Change*, 110(1-2):215–226.

[Pausas and Keeley, 2014] Pausas, J. G. and Keeley, J. E. (2014). Abrupt climate-independent fire regime changes. *Ecosystems*, 17(6):1109–1120.

[Pereira et al., 2013] Pereira, H. M., Ferrier, S., Walters, M., Geller, G. N., Jongman, R. H. G., Scholes, R. J., Bruford, M. W., Brummitt, N., Butchart, S. H. M., Cardoso, A. C., Coops, N. C., Dulloo, E., Faith, D. P., Freyhof, J., Gregory, R. D., Heip, C., Hoft, R., Hurtt, G., Jetz, W., Karp, D. S., McGeoch, M. A., Obura, D., Onoda, Y., Pettorelli, N., Reyers, B., Sayre, R., Scharlemann, J. P. W., Stuart, S. N., Turak, E., Walpole, M., and Wegmann, M. (2013). Essential biodiversity variables. *Science*, 339(6117):277–278.

[Pettorelli et al., 2014] Pettorelli, N., Safi, K., and Turner, W. (2014). Satellite remote sensing, biodiversity research and conservation of the future. *Philosophical Transactions of the Royal Society B-Biological Sciences*, 369(1643).

[Pettorelli et al., 2016] Pettorelli, N., Wegmann, M., Gurney, L., and Dubois, G. (2016). *Monitoring Protected Areas from Space*, book section Monitoring Protected Areas from Space, pages 242–259. John Wiley & Sons, Ltd.

[Pez et al., 2011] Pez, A., Farber, S., and Wheeler, D. (2011). A simulation-based study of geographically weighted regression as a method for investigating spatially varying relationships. *Environment and Planning A*, 43(12):2992–3010.

[Pfeifer et al., 2012] Pfeifer, M., Disney, M., Quaife, T., and Marchant, R. (2012). Terrestrial ecosystems from space: a review of earth observation products for macroecology applications. *Global Ecology and Biogeography*, 21(6):603–624.

[Pincetl and Hogue, 2015] Pincetl, S. and Hogue, T. S. (2015). Californias new normal? recurring drought: Addressing winners and losers. *Local Environment*, 20(7):850–854.

[Rocchini et al., 2010] Rocchini, D., Balkenhol, N., Carter, G. A., Foody, G. M., Gillespie, T. W., He, K. S., Kark, S., Levin, N., Lucas, K., Luoto, M., Nagendra, H., Oldeland, J., Ricotta, C., Southworth, J., and Neteler, M. (2010). Remotely sensed spectral heterogeneity as a proxy of species diversity: Recent advances and open challenges. *Ecological Informatics*, 5(5):318–329.

[Rybnikova and Portnov, 2014] Rybnikova, N. A. and Portnov, B. A. (2014). Mapping geographical concentrations of economic activities in europe using light at night (lan) satellite data. *International Journal of Remote Sensing*, 35(22):7706–7725.

[Sanderson et al., 2002] Sanderson, E. W., Jaiteh, M., Levy, M. A., Redford, K. H., Wannebo, A. V., and Woolmer, G. (2002). The human footprint and the last of the wild. *Bioscience*, 52(10):891–904.

[Sayre et al., 2014] Sayre, R., Dangermond, J., Frye, C., Vaughan, R., Aniello, P., Breyer, S., Cribbs, D., Hopkins, D., Nauman, R., and Derrenbacher, W. (2014). A new map of global ecological land unitsan ecophysiographic stratification approach. *Washington, DC: Association of American Geographers*.

[Schmidt and Karnieli, 2000] Schmidt, H. and Karnieli, A. (2000). Remote sensing of the seasonal variability of vegetation in a semi-arid environment. *Journal of Arid Environments*, 45(1):43–59.

[Serbin et al., 2013] Serbin, G., Hunt, E. Raymond, J., Daughtry, C. S. T., and McCarty, G. W. (2013). Assessment of spectral indices for cover estimation of senescent vegetation. *Remote Sensing Letters*, 4(6):552–560.

[Seto et al., 2011] Seto, K. C., Fragkias, M., Guneralp, B., and Reilly, M. K. (2011). A meta-analysis of global urban land expansion. *Plos One*, 6(8).

[Sleeter et al., 2012] Sleeter, B. M., Sohl, T. L., Wilson, T. S., Sleeter, R. R., Soulard, C. E., Bouchard, M. A., Sayler, K. L., Reker, R. R., and Griffith, G. E. (2012). *Projected land-use and land-cover change in the Western United States*, pages 65–86.

[Sleeter and Gould, 2007] Sleeter, R. and Gould, M. D. (2007). *Geographic information system software to remodel population data using dasymetric mapping methods*. US Department of the Interior, US Geological Survey.

[Somers et al., 2011] Somers, B., Asner, G. P., Tits, L., and Coppin, P. (2011). Endmember variability in spectral mixture analysis: A review. *Remote Sensing of Environment*, 115(7):1603–1616.

[Stevens et al., 2015] Stevens, J. T., Safford, H. D., Harrison, S., and Latimer, A. M. (2015). Forest disturbance accelerates thermophilization of understory plant communities. *Journal of Ecology*, 103(5):1253–1263.

[Sugihara, 2006] Sugihara, N. G. (2006). *Fire in California's ecosystems*. University of California Press, Berkeley.

[Syphard et al., 2007] Syphard, A. D., Radeloff, V. C., Keeley, J. E., Hawbaker, T. J., Clayton, M. K., Stewart, S. I., and Hammer, R. B. (2007). Human influence on california fire regimes. *Ecological Applications*, 17(5):1388–1402.

[Tanaka et al., 2006] Tanaka, S. K., Zhu, T. J., Lund, J. R., Howitt, R. E., Jenkins, M. W., Pulido, M. A., Tauber, M., Ritzema, R. S., and Ferreira, I. C. (2006). Climate warming and water management adaptation for california. *Climatic Change*, 76(3-4):361–387.

[Tiefelsdorf and Boots, 1995] Tiefelsdorf, M. and Boots, B. (1995). The exact distribution of moran's i. *Environment and Planning A*, 27(6):985–999.

[Tittensor et al., 2014] Tittensor, D. P., Walpole, M., Hill, S. L. L., Boyce, D. G., Britten, G. L., Burgess, N. D., Butchart, S. H. M., Leadley, P. W., Regan, E. C., Alkemade, R., Baumung, R., Bellard, C., Bouwman, L., Bowles-Newark, N. J., Chenery, A. M., Cheung, W. W. L., Christensen, V., Cooper, H. D., Crowther, A. R., Dixon, M. J. R., Galli, A., Gaveau, V., Gregory, R. D., Gutierrez, N. L., Hirsch, T. L., Hoft, R., Januchowski-Hartley, S. R., Karmann, M., Krug, C. B., Leverington, F. J., Loh, J., Lojenga, R. K., Malsch, K., Marques, A., Morgan, D. H. W., Mumby, P. J., Newbold, T., Noonan-Mooney, K., Pagad, S. N., Parks, B. C., Pereira, H. M., Robertson, T., Rondinini, C., Santini, L., Scharlemann, J. P. W., Schindler, S., Sumaila, U. R., Teh, L. S. L., van Kolck, J., Visconti, P., and Ye, Y. M. (2014). A mid-term analysis of progress toward international biodiversity targets. *Science*, 346(6206):241–244.

[Tobler, 1970] Tobler, W. R. (1970). A computer movie simulating urban growth in the detroit region. *Economic Geography*, pages 234–240.

[Urbieta et al., 2015] Urbieta, I. R., Zavala, G., Bedia, J., Gutierrez, J. M., San Miguel-Ayanz, J., Camia, A., Keeley, J. E., and Moreno, J. M. (2015). Fire activity as a function of fire-weather seasonal severity and antecedent climate across spatial scales in southern europe and pacific western usa. *Environmental Research Letters*, 10(11).

[USDA Office of Communications, 2016] USDA Office of Communications (2016). Forest service survey finds record 66 million dead trees in southern sierra nevada. techreport, United States Department of Agriculture, Vallejo, California.

[Veraverbeke et al., 2011] Veraverbeke, S., Harris, S., and Hook, S. (2011). Evaluating spectral indices for burned area discrimination using modis/aster (master) airborne simulator data. *Remote Sensing of Environment*, 115(10):2702–2709.

[Verbesselt et al., 2010a] Verbesselt, J., Hyndman, R., Newnham, G., and Culvenor, D. (2010a). Detecting trend and seasonal changes in satellite image time series. *Remote Sensing of Environment*, 114(1):106–115.

[Verbesselt et al., 2010b] Verbesselt, J., Hyndman, R., Zeileis, A., and Culvenor, D. (2010b). Phenological change detection while accounting for abrupt and gradual trends in satellite image time series. *Remote Sensing of Environment*, 114(12):2970–2980.

[Wickham et al., 2013] Wickham, J. D., Stehman, S. V., Gass, L., Dewitz, J., Fry, J. A., and Wade, T. G. (2013). Accuracy assessment of nlcd 2006 land cover and impervious surface. *Remote Sensing of Environment*, 130:294–304.

[Willis, 2015] Willis, K. S. (2015). Remote sensing change detection for ecological monitoring in united states protected areas. *Biological Conservation*, 182:233–242.

[Wilson et al., 2012] Wilson, T. S., Sleeter, B., Sohl, T. L., Griffith, G., Acevedo, W., Bennett, S., Bouchard, M., Reker, R., Ryan, C., and Sayler, K. L. (2012). Future scenarios of land-use and land-cover change in the united states: The marine west coast forests ecoregion. *US Geological Survey Open File Report*, 1252:14.

[Wilson et al., 2015a] Wilson, T. S., Sleeter, B. M., and Davis, A. W. (2015a). Potential future land use threats to california's protected areas. *Regional Environmental Change*, 15(6):1051–1064.

[Wilson et al., 2015b] Wilson, T. S., Sleeter, B. M., Sherba, J., and Cameron, D. (2015b). Land-use impacts on water resources and protected areas: applications of state-and-transition simulation modeling of future scenarios. *AIMS Environmental Science*, 2(2):282–301.

[Wilson et al., 2014] Wilson, T. S., Sleeter, B. M., Sleeter, R. R., and Soulard, C. E. (2014). Land-use threats and protected areas: a scenario-based, landscape level approach. *Land*, 3(2):362–389.

[Wittemyer et al., 2008] Wittemyer, G., Elsen, P., Bean, W. T., Burton, A. C. O., and Brashares, J. S. (2008). Accelerated human population growth at protected area edges. *Science*, 321(5885):123–126.

[Woodley et al., 2012] Woodley, S., Bertzky, B., Crawhall, N., Dudley, N., Londoo, J. M., MacKinnon, K., Redford, K., and Sandwith, T. (2012). Meeting aichi target 11: what does success look like for protected area systems. *Parks*, 18(1):23–36.

[Wu et al., 2013] Wu, J. S., He, S. B., Peng, J., Li, W. F., and Zhong, X. H. (2013). Intercalibration of dmsp-ols night-time light data by the invariant region method. *International Journal of Remote Sensing*, 34(20):7356–7368.

[Xian et al., 2012] Xian, G., Homer, C., and Aldridge, C. (2012). Assessing long-term variations in sagebrush habitat - characterization of spatial extents and distribution patterns using multi-temporal satellite remote-sensing data. *International Journal of Remote Sensing*, 33(7):2034–2058.

[Yin et al., 2013] Yin, S. J., Wu, C. Q., Wang, Q., Ma, W. D., Zhu, L., Yao, Y. J., Wang, X. L., and Wu, D. (2013). Review of change detection methods using multi-temporal remotely sensed images. *Spectroscopy and Spectral Analysis*, 33(12):3339–3342.

[Zhu et al., 2006] Zhu, Z., Key, C., Ohlen, D., and Benson, N. (2006). Evaluate sensitivities of burn severity mapping algorithms for different ecosystems and fire histories in the united states. final report jfsp 01-1-4-12. techreport, USGS.